NTIAC 95-01

Microwave Nondestructive Evaluation

State-of-the-Art Review

Prepared by

R. Zoughi and S. Ganchev
Applied Microwave Nondestructive Testing Laboratory
Electrical Engineering Department
Colorado State University
Ft. Collins, CO 80523

Prepared for

Nondestructive Testing Information Analysis Center (NTIAC)
Texas Research Institute Austin, Inc.
Austin, Texas

February 1995

This document was prepared by the Nondestructive Testing Information Analysis Center (NTIAC). TRI/Austin, Inc., 415 Crystal Creek Drive, Austin, TX 78746. NTIAC is a full service information analysis center sponsored by the U.S. Department of Defense, servicing the information needs of the Department of Defense, other U.S. Government agencies, and the private sector in the field of nondestructive testing.

NTIAC is operated under Contract DLA900-90-D-0123 with the Defense Technical Information Center. Technical aspects of NTIAC operations are monitored by the Office of the Director of Defense, Research, and Engineering (Advanced Technology).

Additional copies may be obtained from:

NTIAC
415 Crystal Creek Drive
Austin, TX 78746
(512) 263-2106

Unclassified
SECURITY CLASSIFICATION OF THIS PAGE

REPORT DOCUMENTATION PAGE

Form Approved
OMB No. 0704-0188
Exp. Date: Jun 30, 1986

1a. REPORT SECURITY CLASSIFICATION Unclassified	1b. RESTRICTIVE MARKINGS
2a. SECURITY CLASSIFICATION AUTHORITY	3. DISTRIBUTION/AVAILABILITY OF REPORT Approved for Public Release. Distribution Unlimited. Available only from NTIAC.
2b. DECLASSIFICATION/DOWNGRADING SCHEDULE	
4. PERFORMING ORGANIZATION REPORT NUMBER(S) NTIAC 95-01	5. MONITORING ORGANIZATION REPORT NUMBER(S)
6a. NAME OF PERFORMING ORGANIZATION NTIAC Texas Research Institute Austin, Inc. 6b. OFFICE SYMBOL (If applicable)	7a. NAME OF MONITORING ORGANIZATION ODDR&E(AT)
6c. ADDRESS (City, State, and ZIP Code) 415 Crystal Creek Dr. Austin, TX 78746	7b. ADDRESS (City, State, and ZIP Code) Rm. 3D1089 The Pentagon Washington, DC 20301-3080
8a. NAME OF FUNDING/SPONSORING ORGANIZATION DTIC 8b. OFFICE SYMBOL (If applicable) AI	9. PROCUREMENT INSTRUMENT IDENTIFICATION NUMBER Contract DLA900-90-D-0123
8c. ADDRESS (City, State, and ZIP Code) Defense Technical Information Center DTIC-AI Alexandria, VA 22304-6145	10. SOURCE OF FUNDING NUMBERS PROGRAM ELEMENT NO. / PROJECT NO. / TASK NO. / WORK UNIT ACCESSION NO.

11. TITLE (Include Security Classification)

Microwave Nondestructive Evaluation

12. PERSONAL AUTHOR(S)
R. Zoughi and S. Ganchev

13a. TYPE OF REPORT	13b. TIME COVERED	14. DATE OF REPORT (Year, Month, Day)	15. PAGE COUNT
Review	FROM _____ TO _____	February 1995	171

16. SUPPLEMENTARY NOTATION
A State-of-the-Art Review prepared under the auspices of the Nondestructive Testing Information Analysis Center (NTIAC); Available only from NTIAC.

17. COSATI CODES		
FIELD	GROUP	SUB-GROUP

18. SUBJECT TERMS (Continue on reverse if necessary and identify by block number)
nondestructive testing, nondestructive evaluation, microwaves, NDE, NDT, dielectric properties, composites

19. ABSTRACT (Continue on reverse if necessary and identify by block number)

This State-of-the-Art Review contains information on both the fundamental science and general applications of microwave nondestructive evaluation. Chapter contents include: introductory background on microwave and millimeter wave spectra, definition and scope of microwave NDE, dielectric properties of materials, material characterization using microwaves, thickness and disbond measurements, microwave techniques for surface cracks, defect detection in thick composites, and concluding remarks and the future of microwave NDE. The publication contains 553 references to microwave NDE-related papres in the public literature.

20. DISTRIBUTION/AVAILABILITY OF ABSTRACT	21. ABSTRACT SECURITY CLASSIFICATION
☒ UNCLASSIFIED/UNLIMITED ☐ SAME AS RPT. ☐ DTIC USERS	Unclassified
22a. NAME OF RESPONSIBLE INDIVIDUAL Mr. Jerome Persh	22b. TELEPHONE (Include Area Code) (703) 695-0005
	22c. OFFICE SYMBOL ODDR&E(AT)

DD FORM 1473, 84 MAR 83 APR edition may be used until exhausted. All other editions are obsolete.

SECURITY CLASSIFICATION OF THIS PAGE
Unclassified

NTIAC 95-01

Microwave Nondestructive Evaluation

State-of-the-Art Review

Prepared by

R. Zoughi and S. Ganchev
Applied Microwave Nondestructive Testing Laboratory
Electrical Engineering Department
Colorado State University
Ft. Collins, CO 80523

Prepared for

Nondestructive Testing Information Analysis Center (NTIAC)
Texas Research Institute Austin, Inc.
Austin, Texas

February 1995

Table of Contents

CHAPTER 1

INTRODUCTION

Microwave nondestructive techniques have a long history dating from the early 1950s, with a strong flurry of activities in the 1960s and 1990s. However, these techniques are still not widely known in the nondestructive testing (NDT) community and are often referred to as "emerging techniques" or "others". It is only during the last two or three years that some NDT conferences have allocated a whole session or two solely to the topic of microwave NDT. For those involved in the research and development of microwave and millimeter-wave NDT techniques who have long appreciated the advantages of such techniques, this increased visibility is a welcome and encouraging change.

It appears that unlike the NDT community, the microwave community is generally more aware of the applications of microwaves for non-intrusively inspecting materials and structures. However, articles published in microwave oriented journals (not NDT) do not always receive the attention of NDT practitioners. Furthermore, most of these scientific investigations may not always attack an NDT problem directly, but the approaches developed by them can be modified and expanded to include practical NDT problems. The theoretical development of an antenna admittance variations in layered plasma is a good example of this. Although most of such problems have dealt with understanding of the characteristics of an antenna on a spacecraft during re-entry into the atmosphere, a layered plasma is very similar to a layered dielectric composite. There are also new microwave and millimeter wave theoretical and experimental developments specifically for NDT purposes that have taken place in the last few years (in addition to research in the 1970s and early 1980s). The inspection of new dielectric materials such as composites represents an example of an important new potential application area for microwave and millimeter wave NDT.

The ever expanding materials technology, by which lighter, stiffer, stronger and more durable electrically insulating composites are replacing metals in many applications, demands alternative inspection techniques to the existing NDT methods. This is due to the fact that the

existing standard and well established NDT techniques may not always be capable of inspecting these composites.

Microwave signals penetrate inside dielectric (electrically insulating) media easily. The depth of penetration is dictated by the loss factor of the dielectric material (ability to absorb microwave energy) and the frequency of operation. Measurements can be conducted on a contact or non-contact fashion while operating on one side of a material or using its both sides (reflection or transmission techniques). Microwave NDT techniques are sensitive to geometrical and dimensional variations of a medium or a defect. Polarization properties of microwave signals can be used to increase measurement sensitivity to defects of a certain orientation. The evaluation of the properties and composition of mixtures including the effect of curing in chemically produced composites is also possible. It is not necessarily true that because microwave signals have wavelengths in the centimeter range, the resolution obtained using these signals cannot be better than a *large* fraction of the operating wavelength. For instance, in monitoring thickness variation in dielectric slabs and coatings, if resolution is considered to be the smallest thickness variation that is possible to be detected, then microwave NDT techniques have shown measurement resolutions of a few microns at 10 GHz (wavelength of 3 cm in free-space). If resolution, in a given application, is considered to be the smallest spatial distance between two defects so that they can be individually detected, then near-field microwave and millimeter wave techniques have provided resolutions of better than a tenth of a wavelength. It has also been shown that an increase in frequency does not necessarily render better measurement resolution in all cases. Also, at around 12 GHz fatigue cracks on metal surfaces with widths in the range of a few microns have been detected. In addition, spatial resolution is a function of the microwave sensor used (e.g. open-ended waveguides, open-ended coaxial lines, cavity resonators, etc.). Statements made in conjunction with radar resolutions do not always apply to microwave NDT techniques even though both use microwaves since most of NDT applications are conducted in the near-field of a probe as opposed to its far-field. Furthermore, changes in the reflection coefficient properties for a given microwave sensor and defect are very different in the near-field compared to the far-field.

Hardware systems for microwave NDT applications need not be expensive. It is true that if laboratory test equipment is used to conduct measurements, the cost will be high. However, hardware for a specific application can be developed and built to be relatively inexpensive, simple in design, hand-held, battery operated, operator friendly and operate on an on-line basis. In a majority of microwave NDT applications where detection is the primary objective, there is very little

to no need for complicated post signal processing. Capability of providing real-time information makes these techniques suitable for on-line industrial applications. The operator need not be a microwave expert to conduct microwave NDT measurements once a system has become operational. Since, the required operating power for most NDT applications (excluding ground probing radars and microwave heating sources) are in the few milliwatts range, and the majority of these techniques are conducted in near-field with a high degree of frequency selectivity (narrow band CW measurements), they do not cause any EMI and are not affected by EMI. There are no environmentally hazardous or undesirable byproducts associated with these techniques.

Large scan areas can be accommodated with an array of sensors. Microwave signals do not penetrate inside conductors and graphite composites. However, this is not always a limitation since surface features such as cracks on metal surfaces and impact damage on graphite composites can be inspected along with the properties of dielectric coatings (thickness and material composition) on top of metals and graphite composites. One of the most attractive aspects of microwave NDT techniques is the availability of many different probes/sensors. Some of these may render better results than the others for a specific application. In addition, optimization of system parameters for obtaining more sensitive results makes microwave NDT techniques very powerful.

Once the underlying theoretical foundation of the interaction of microwaves with a given medium is understood and modelled, one may develop electromagnetic codes to predict the outcome of a measurement in order to optimize it for obtaining the highest possible measurement sensitivity. It is argued here that unless one has a sound and clear understanding of the fundamental steps in the interaction of microwaves with various media and a thorough understanding of how to manipulate various microwave sensors for measurements purposes, the so-called tinkering with microwave sensors may not render acceptable results.

Areas that may (some already have) benefit from using microwaves NDT techniques are:

- accurate thickness measurement of coatings, single dielectric slabs, layered dielectric composites made of plastics, ceramics and any other type of dielectric materials
- minute thickness variation of each layer in these dielectric media
- disbond, delamination and void detection and thickness evaluation in stratified media

- inspection of thick plastics and glass reinforced composites for detection of interior flaws, fiber bundle orientation and breakage, moisture content, etc.
- detection and estimation of porosity in dielectrics
- impact damage detection and evaluation in reinforced composite structures including graphite composites
- accurate material/constituent characterization in dielectric mixtures
- detection and evaluation of curing in chemically reactive media
- relating electrical properties of materials such as dielectric characteristics to physical and mechanical properties such as compressive strength of concrete members
- detection of surface cracks (stress and fatigue) in metals including sizing of the three dimensions of a crack. This feature extends to filled and cracks covered with various dielectric coatings. As a matter of fact, covered cracks have been shown to be detected easier than exposed cracks which allows for crack detection under various coatings without the need for the coating removal prior to testing
- optimization capability for all of these measurements to obtain higher measurement sensitivity
- production of defect images
- using microwaves as heat sources in thermography
- finally, new applications are continuously being discovered

The time is right for renewed vigor in applying microwave NDT techniques to new inspection problems. A fresh sustained effort in this area should bare many fruits. Many investigators believe that, given the same level of effort enjoyed by other NDT techniques during their development, microwave NDT will find a prominent place in a wide realm of applications. In some cases it will prove to be the technique of choice. In other cases it will prove to be a useful complement when used in conjunction with other methods. A comprehensive reference list is provided here for further inquiry by the reader [1-260].

MICROWAVE & MILLIMETER WAVE FREQUENCY SPECTRUM

There is no firm definition for microwave spectrum, however the frequency range between about 300 MHz to 300 GHz (1 m to 1 mm in wavelength) is known as the microwave frequency region (giga = 10^9). Frequency range below 40 GHz is known as the microwave region and above it is known as the millimeter wave region (although some consider above 30 GHz to be the millimeter wave region). There are numerous schemes for designating letters to different frequency bands

in the microwave range. The following is the IEEE (Institute of Electrical and Electronics Engineers) letter band designation (frequency and wavelength shown) [261].

P	band	0.23 - 1	GHz	130 - 30	cm
L	band	1 - 2	GHz	30 - 15	cm
S	band	2 - 4	GHz	15 - 7.5	cm
C	band	4 - 8	GHz	7.5 - 3.75	cm
X	band	8 - 12.5	GHz	3.75 - 2.4	cm
Ku	band	12.5 - 18	GHz	2.4 - 1.67	cm
K	band	18 - 26.5	GHz	1.67 - 1.13	cm
Ka	band	26.5 - 40	GHz	1.13 - 0.74	cm
mm	Waves	40 - 300	GHz	7.5 - 1	mm

The millimeter wave band is subdivided into Q, V and W bands (old DoD designation).

DEFINITION AND SCOPE OF THE MICROWAVE NDT/E

Microwave NDT/E includes non-intrusive techniques using different kinds of sensors operating in the above frequency ranges. These techniques are based on the interaction of radiated electromagnetic energy with material media. Not only microwave (millimeter wave) techniques are based on this principle but also other frequencies have been used for NDT purposes such as low frequencies (for capacitive sensors), optical frequencies (including infrared and ultraviolet), X-rays, and gamma rays. It is obvious, that although the underlaying principle is the same, the scope of possible applications, the equipment and technology used may be quite different.

Microwave NDT methods may be considered as part of broader area of industrial applications of microwaves. Medical applications of microwaves is another area which is usually considered separate from industrial applications.

Some of the established areas of industrial applications for microwaves include:

Microwave drying:
- paper and printing industries (paper, printing ink, glued products)
- leather and textile industries
- construction (wood, plaster, tiles, ceramics)
- foundries
- pharmaceutical industry
- tobacco industry

Microwave vulcanization and polymerization in:
- rubber industry
- chemical industry

Food industry applications:
- cooking
- thawing and tempering
- drying
- preservation (sterilization)

Other miscellaneous applications:
- disinfection
- soil treatment (use of microwaves instead of herbicides for destruction of unwanted seeds)
- germination
- crop protection
- wine making by carbolic fermentation

Microwave NDT methods may be tentatively divided into the following categories, most of which are the subject of this report in the upcoming chapters:

- measuring and control of distance (near-field and far-field)
- measuring and control of geometrical dimensions of dielectric objects
- measuring of the properties of the materials (including moisture measurements)
- detection and sizing of cracks in metals
- microwave imaging and holography

DIELECTRIC PROPERTIES OF MATERIALS

Propagation of an electromagnetic wave inside a dielectric medium is dependent upon the dielectric properties and the geometry of the material (e.g. thickness) and the operating wavelength. Therefore, it is of utmost importance to have a clear knowledge of the dielectric properties of materials when using microwave NDE techniques. Dielectric properties of a material is a complex quantity, and is denoted by $\varepsilon = \varepsilon' - j\varepsilon''$, where ε is called the absolute complex dielectric constant of the medium, ε' is known as the *permittivity* (indicating the ability of the material to store electromagnetic energy) and ε'' is known as the dielectric *loss factor* (indicating the ability of the material to absorb electromagnetic energy). Once normalized with respect to the

permittivity of free-space, $\varepsilon_o = (1/36\pi)\text{x}10^{-9}$ (F/m), the relative complex dielectric constant of the medium, $\varepsilon_r = \varepsilon/\varepsilon_o = \varepsilon'_r - j\varepsilon''_r$ is obtained. It must be noted that although ε_r is referred to as the dielectric *constant*, it is indeed a *function* of frequency and thus is not a constant in this respect. The degree to which this parameter is a function of the operating frequency depends on the molecular structure a medium. The ratio of $(\varepsilon''_r/\varepsilon'_r)$ is known as the *loss tangent* $(\tan\delta)$ of the medium indicating its ability to absorb electromagnetic energy [262]. The absolute dielectric constant is also related to the conductivity of a material, σ, through $\varepsilon = \varepsilon' - j\sigma/\omega$, where $\omega = 2\pi f$ where f is the operating frequency [263]. From the loss point of view, materials may be divided into two categories of low loss and high loss dielectrics. A lossless medium is one whose dielectric constant is purely real ($\varepsilon''_r = 0$). The only example of this type of a dielectric is vacuum, however many low loss materials such as Teflon, glass, Styrofoam are often considered to be lossless.

For a plane wave propagating in the z-direction and polarized along the x-axis inside a medium with a relative dielectric constant of $\varepsilon_r = \varepsilon'_r - j\varepsilon''_r$, the propagation constant, γ, determines the magnitude and the phase of the wave at any point z inside the medium. The electric field intensity at any point is given by:

$$\overline{E}(z) = E_o e^{-\gamma z}\hat{a}_x \qquad (1)$$

E_o is the electric field intensity at z = 0 and $\gamma = \alpha + j\beta$, where α and β are the absorption and phase constants of the medium, respectively. They are related to ε_r by:

$$\alpha = k_o\left|\text{Im}\left\{\sqrt{\varepsilon_r}\right\}\right| \qquad (Np/m) \qquad (2)$$

$$\beta = k_o\,\text{Re}\left\{\sqrt{\varepsilon_r}\right\} \qquad (rad/m) \qquad (3)$$

where $k_o = 2\pi/\lambda_o$ is the wavenumber in free-space and λ_o is the wavelength in free-space. Thus, if a plane wave travels through a thickness, d, of a material, (γd) determines the amount of attenuation and phase shift that the wave experiences. This quantity is known as the electrical thickness. The power absorption coefficient (assuming a non-scattering medium) is given by:

$$\kappa_a(dB/m) = 8.68\alpha(Np/m) \qquad (4)$$

The depth of penetration, which is the depth at which the power density reaches (1/e) of its value at the surface of the medium is then given by:

$$\delta_p = \frac{1}{\kappa_a} \qquad (m)$$

Therefore, the penetration depth is a function of the operating wavelength (frequency) and the dielectric properties of the medium [262].

A low-loss medium is assumed to have ($\omega\varepsilon' \gg \sigma$). For such a medium $\alpha = \eta\sigma/2$ and $\beta = \omega(\mu\varepsilon)^{1/2}$, where η is the intrinsic impedance of the medium and μ is its permeability. For a high-loss medium ($\sigma \gg \omega\varepsilon'$), and $\alpha = \beta = (\omega\mu\sigma/2)^{1/2}$ [263].

The knowledge of the dielectric properties of materials is an important issue in microwave NDE from two primary stand points:

- when dealing with the interaction of electromagnetic waves with material media
- when dealing with the material composition of a medium

The latter is known as *material characterization* using microwaves. Using various techniques (on- and off-line) the dielectric properties of many mixtures can be measured and related back to the mixture constituent dielectric properties and their volume contents. Microwave material characterization can also provide information about chemical reactions (curing) associated with the production of a dielectric mixture. This issue will be discussed in detail in the following chapter.

REFERENCES

[1] Kashyap, S.C, J.E. Lewis and M.H.Steves, "A Surface-Wave Method for Moisture Content of Sheet Materials," J. Microwave Power, vol. 9, no. 1, pp.14-21,1974.

[2] Kraszewski, A.,"Microwave Instrumentation for Moisture Content Measurement," J. Microwave Power, vol. 8, no. 3/4, pp. 323-35, 1973.

[3] Bahr, A.J., "Microwave Nondestructive Testing Methods," Gordon and Breach Science Publishers, New York, 1982.

[4] Jose, K.A, P. Venugopalan, K.G. Nair, V.R.Ravindran and P.K.Chaturvedi, "Microwave Method for Monitoring the Curing Conditions of a Solid Rocket Propellant," NDT International, pp. 398-400, Dec.1986.

[5] Bahr, A.J., "Nondestructive Microwave Evaluation of Ceramics," IEEE Trans. on Microwave Theory Tech, vol. MTT-26, no. 9, pp. 676-683, Sept. 1978.

[6] Hochschild, R., "Microwave Nondestructive Testing in One (Not-So-Easy) Lesson," Materials Evaluation, pp.35A-42A, Jan. 1968.

[7] Botsco, R.J., "Nondestructive Testing of Plastics with Microwaves," Materials Evaluation, pp. 25A-32A, June 1969.

[8] Rollwitz, W., "Microwave Inspection," Metals Handbook, vol. II, pp. 244-253,1976.

[9] Dean, D.S., L.A. Kerridge,"Microwave Techniques," Chapter 13, in Research Techniques in Nondestructive Testing, vol. I, Ed.R.S.Sharpe, pp.417-441, Academic Press, 1970.

[10] Tiuri, M., and P. Liimatainen, "A Microwave Method for Measurement of Fiber Orientation in Paper," J. Microwave Power, vol. 10, pp. 142-145, no.2, 1975.

[11] Leppin, J., "Thermal Design of Ferrite Isolators for Industrial Microwave Equipment," J. Microwave Power, vol. 9, no. 3, pp. 250-261, 1974.

[12] Kent, M., "The Use of Strip-Line Configuration in Microwave Moisture Measurements," J. Microwave Power, vol. 7, no. 3, pp. 185-193, 1972; Part II, J. Microwave Power, vol. 8, no. 2, pp. 189-194, 1973.

[13] Bibliography I: "Microwave Non-Contact Measurement," Prepared by Institute Members, J. Microwave Power, vol. 4, no. 3, 1969..

[14] Geoffrey Voss, W. A., "Microwave Instruments for Material Control Part 1: A Review," J. Microwave Power, vol. 4, no. 3, pp. 200-215, 1969.

[15] Brady, M.M., "Tables of Constants for ISM Waveguides," J. Microwave Power, vol. 5, no. 3, pp. 175-182, 1970.

[16] Rudge, A.W., "An Electromagnetic Radiation Probe for Near Field Measurements at Microwave Frequencies," J. Microwave Power, vol. 5, no. 3, pp. 155-174, 1970.

[17] Soga, H., "A New Microwave Thickness Gauge," J. of Microwave Power, vol. 8, no. 3, pp. 253-266, 1973.

[18] Dalton, B.L., "Microwave Non-Contact Measurement and Instrumentation in the Steel Industry," J. Microwave Power, vol. 8, no. 3, pp. 235-244, 1973.

[19] Kardicali, "A Portable Microwave Phase Detector," J. Microwave Power, vol. 10. no. 1, pp. 49-58, 1975.

[20] Metaxas, A.C., "Design of a TM-010 Resonant Cavity as a Heating Device at 2.45 GHz," J. Microwave Power, vol. 9, no. 2, pp. 123-127, 1974.

[21] Tiuri, M., and P. Liimatainen, "A Microwave Instrument for Measurement of Small Inhomogeneities in Supercalendar Rollers and Other Dielectric Cylinders," J. Microwave Power, vol. 9, no. 2, pp. 118-121, 1974.

[22] Lavelle, T.M., "Microwaves in Nondestructive Testing," Materials Evaluation, vol. XXI, pp. 254-725, Nov. 1967.

[23] Thuery, J., Microwaves: Industrial, Scientific, and Medical Applications," Artech House, Boston, 1992.

[24] Botso, R.J., "Nondestructive Testing of Plastics with Microwaves," Materials Evaluation, vol. XXVII, pp. 25A-32A, Dec. 1969.

[25] Rolwitz, W.L., "Microwave Inspection," in Metals Handbook, vol. II Nondestructive inspection and quality control, pp. 244-253, 8 th Edit., 1976.

[27] Lord, W., "Applications of Numerical Field Modeling to Electromagnetic Methods of Nondestructive Testing," IEEE Trans. on Magnetics, vol. MAG-19, no. 6, pp. 2437-2442, Nov. 1983.

[28] Dean, D.S., and D.T. Green, "The Use of Microwaves for the Detection of Flaws and Measurement of Erosion Rates in Materials," J. Sci. Instrum., vol. 44, pp. 699-701, 1967.

[29] Nyfors, E., and P. Vainikainen, "Industrial Microwave Sensors," Artech House, Norwood MA, 1989

[30] Schilz, W., and B. Schiek, "Microwave Systems for Industrial Measurements,"in Advances in Electronics and Electron Physics, pp.309-381, vol. 55.

[31] Whetton, C.P., "Industrial and Scientific Applications of Doppler Radar," Microwave Jour., pp. 39-42, Nov. 1975.

[32] Bramanti, M., and E. Salerno, "Experiments on Some Particular Permittivity Sensors in Nondestructive Testing of Dielectric Materials," J. Microwave Power and Electromagnetic Energy, vol. 27, no. 4, pp. 209-216, 1992.

[33] Hruby, R.J., and L. Feinstein, "A Novel Nondestructive, Noncontacting Method of Measuring the Depth of Thin Slits and Cracks in Metal," The Rev. Sci. Instr., vol. 41, pp. 679-683, May 1970.

[34] Rzepecka, M.A., and S.S. Stuchly, "A Microwave System for Measurement of the Diameter of Thin Dielectric Fibers," IEEE Trans. on Inst. Meas, vol. IM-23, pp. 100-101, March 1974.

[35] Bosisio, R.G., M. Giroux and D. Couderc, "Paper Sheet Moisture Measurement by Microwave Phase Perturbation Techniques," J. Microwave Power, vol. 5, no. 1, 25-34,1970.

[36] Bosisio, G., L. Nappert and H. Hua Quoc, "The Regenerative Digital Transducer (RDT): A New Active Microwave Field Sensor for Industrial Measurements and Control," Proc. 4th European Microwave Conf., (EuMC'74), pp. 141-145, 1974.

[37] Forssell, B., "Non-Destructive Measurements of the Glass-Fibre Content in Reinforced Plastics by Means of Microwaves," Proc. 4th European Microwave Conf., (EuMC'74), pp. 132-136, 1974.

[38] Tiuri, M., and P. Liimatainen, "Microwave Method for Measurement of Fiber Orientation of Paper," Proc. 4th European Microwave Conf., (EuMC'74), pp. 137-140, 1974.

[39] Ramachandraiah, M., "A Survey of the Applications of Microwaves in Non-Communication Areas," Proc. 3rd European Microwave Conference, (EuMC'73), 1973.

[40] Griffin, D.W., "Microwave Oscillator Transducer Design for Industrial Applications," Proc. 3rd European Microwave Conf., (EuMC'73), 1973.

[41] Ash, E.A., and A. Husain, "Surface Examination Using a Superresolution Scanning Microwave Microscope," Proc. 3rd European Microwave Conf., (EuMC'73), 1973.

[42] Stuchly, S.S., M.A. Rzepecka and M.A.K. Hamid, "Microwave Void Fraction Monitor for Organic Coolants in Nuclear Reactors," Proc. 3rd European Microwave Conf., (EuMC'73), 1973.

[43] Kraszewski, A.W., "Microwave Aquametry - Needs and Perspectives," IEEE Trans. on Microwave Theory Tech., vol. 39, no. 5, pp. 828-835, May 1991.

[44] Kraszewski, A.W., S.O. Nelson and T.-S. You, "Use of a Microwave Cavity for Sensing Dielectric Properties of Arbitrary Shaped Biological Objects," IEEE Trans. on Microwave Theory Tech., vol. 38, no. 7, pp. 858-63, July 1990.

[45] Kurian, J., K. Jose, K. Balakrishnan and K. Nair, "Microwave Non-Destructive Flaw/Defect Detection System for Non-Metallic Media Supported by Microprocessor-Based Instrumentation," J. Microwave Power and Electromagnetic Energy, vol. 24, no. 2,pp. 74-78,1989.

[46] Kashyap, S.C., J.E. Lewis and M.H. Steeves, "A Surface-Wave Method for Measuring Moisture Content of Sheet Materials," J. Microwave Power, vol. 9, pp. 13-21, no. 1,1974.

[47] Cutmore, N., D. Abernethy and T. Evans, "Microwave Technique for the On-Line Determination of Moisture in Coal," J. Microwave Power and Electromagnetic Energy, vol. 24, no. 2, pp. 79-90,1989.

[48] Bramanti, M., and G. de Michele, "A Microwave Method to Measure Unburnt Coal Content in Ashes," IEEE Trans. on Inst. Meas., vol. 39, no. 5, pp. 804-806, Oct. 1990.

[49] Nelson, S.O., "Measurements and Applications of Dielectric Properties of Agricultural Products," IEEE Trans. on Inst. Meas., vol. 41, no. 1, pp. 116-122, Feb. 1992.

[50] King, R.J., K.V. King and K. Woo, "Microwave Moisture Measurement of Grains," IEEE Trans. on Inst. Meas., vol. 41, no. 1, pp. 111-115, Feb. 1992.

[51] Nelson, S.O., Comments on "Permittivity Measurements of Granular Food Products Suitable for Computer Simulations of Microwave Cooking Processes," IEEE Trans. on Inst. Meas., vol. 40, no. 6, pp. 1048-1049, Dec. 1991.

[52] Botros, A.Z., A.D. Olver, L.G. Cuthbert and G. Farmer, "Microwave Detection of Hidden Objects in Walls," Electronic Letters, pp. 379-380, 27 Feb. 1984.

[53] Bramanti, M., and E. Salerno, "Electromagnetic Techniques for Nondestructive Testing of Dielectric Materials: Diffraction Tomography," J. Microwave Power and Electromagnetic Energy, vol. 27, no. 4, pp. 233-240, 1992.

[54] Fu, W., and A. Metaxas, "A Mathematical Derivation of Power Penetration Depth for *Thin* Lossy Materials," J. Microwave Power and Electromagnetic Energy, vol. 27, no. 4, pp. 217-222, 1992.

[55] Ou, W., C. G. Gardner and S.A. Long, Nondestructive Measured of a Dielectric Layer Using Surface Electromagnetic Waves," IEEE Trans. on Microwave Theory Tech., vol. MTT-31, no. 3, pp. 255-260, March 1983.

[56] Stuchly, S.S., M.A. Rzepecka and M. Hamid, "A Microwave Open-Ended Cavity as a Void Fraction Monitor for Organic Coolants," IEEE Trans on Industrial Electronics and Control Instrumentation, vol. IECI-21, no. 2, pp. 78-80, May 1974

[57] Prachomchuk, P., W. Wallender and R. King, "Calibration of a Waveguide Sensor for Measuring Soil Moisture, " IEEE Trans. on Geoscience and Remote Sensing, vol. 28, no. 5, pp. 873-877, 1990.

[58] Root, L., and I. Kaufman, "Microwave-Based Low-Cost Instrument for Film Thickness Measurement," IEEE MTT-S Digest, pp. 1553-1556, 1992.

[59] Khan, S., J. Farmer, R. Gutmann and J. Borrego, "In Situ Monitor for Conducting Films," IEEE MTT-S Digest, pp. 1561-1564, 1992.

[60] Kaiser, J.H., "Millimeter Wave Heating for Thermographic Inspection of Carbon Fiber-Reinforced Composites," Materials Evaluation, pp. 597-599, May 1993.

[61] Su, W., O.A. Hasim, I.L. Al-Qadi and S.M. Raid, "Permittivity of Portland Cement Concrete at Low RF Frequencies," Materials Evaluation, pp. 496-502, October 1993.

[62] d'Ambrosio, G., R. Massa, M.D. Migliore and C. Sabatino, "Microwave Defect Detection on Low-Loss Composites," Materials Evaluation, pp. 285-289, February 1993

[63] Aaron, M., E. Grant, S. Young, "The Dielectric Properties of some Amino-Acids. Peptides and Proteines at Decimetre Wavelengths" In: Molecular Relaxation Processes, Proceeding of the Chemical Society Symposium, pp. 77-82, Aberistwyth, Academic Press, London, 1966.

[64] Buchanan, T., "The Dielectric Properties of Some Long -Chain Fatty Acids and Their Methyl Esters in the Microwave Region," J. Chem. Phys., vol. 22, no. 4, p. 578, 1954.

[65] Chahine, R., T. Bose, C. Akyel and R. Bosisio, "Computer-Based Permittivity Measurements and Analysis of Microwave Power Absorption Instabilities," J. Microwave Power, vol. 19, no.2, pp. 127-134, 1984.

[66] Chamberlain, J., M. Afsar, G. Davies, J. Hasted and M. Zafar, "High-Frequency Dielectric Processes in Liquids," IEEE Trans. on Microwave Theory Tech, vol. MTT-22, no. 12, pp. 1028-1032, Dec. 1974.

[67] Kent, M., "Complex Permittivity of Protein Powders at 9.4 GHz as a Function of Temperature and Hydration," J. Phys. D: Appl. Phys., vol. 5, pp. 394-409, 1972.

[68] Kraszewski, A., "Prediction of the Dielectric Properties of Two-Phase Mixtures," J. Microwave Power, vol. 12, no. 3 pp. 215-222, 1977.

[69] Kraszewski, A., "A Model of the Dielectric Properties of Wheat at 9.4 GHz," J. Microwave Power, vol. 13, no. 4, pp. 293-296, 1978.

[70] Amato, J.C., "Design of Partial Dielectric Cavities for Wide-Band Microwave Measurements," Rev. Sci. Instrum., vol. 51, no. 9, pp. 1231-1233, 1980.

[71] Backhouse, P., N. Apsley and A. Smart, "Measurement of Dielectric Loss in Thin Parallel-Sided Samples Using an Untuned Cavity," IEE Proc., vol. 132, Pt. A, no 5, pp. 280-284, Sept. 1985.

[72] Berteaud, A.J., F. Hoffman and J. F. Mayalut, "Complex Frequency Perturbation of a Microwave Cavity Containing a Lossy Liquid," J. Microwave Power, vol. 10, no. 3, pp. 301-313, 1975.

[73] Birchak, J.R., L.G. Gardner, J.W. Hipp and J.M. Victor, "High Dielectric Constant Microwave Probes for Sensing Soil Moisture," Proc. IEEE, vol. 62, no. 1, pp. 93-98, Jan, 1974.

[74] Chan, W.F.P., and B. Chambers, "Measurement of Nonplanar Dielectric Samples Using an Open Resonator," IEEE Trans. on Microwave Theory Tech, vol. MTT-35, no. 12, pp. 1429-1432, Dec. 1987.

[75] Khalid, K.B., T.S.M. Maclean, M. Razaz and P.W. Webb, "Analysis and Optimal Design of Microstrip Sensors," IEE Proc., vol. 135, Pt. H, no. 3, pp. 187-195, June 1988.

[76] Kent, M., and W. Meyer, "A Density-Independent Microwave Moisture Meter for Heterogeneous Food-Stuffs," J. Food Engineering, No 1, pp. 31-42, 1982.

[77] Klein, A., "Microwave Determination of Moisture Compared with Capacitive, Infrared and Conductive Measurement Methods. Comparison of On-Line Measurements at Coal Preparation Plants," Proc. 14th European Microwave Conf., (EuMC'84), pp. 661-666, 1984.

[78] Rzepecka, M.A., "A Cavity Perturbation Method for Routine Permittivity Measurements," J. Microwave Power, vol. 8, no. 1, pp. 3-12, 1973.

[79] Sihvola, A., and M. Tiuri, "Snow Fork for Field Determination of the Density and Wetness Profiles of a Snow Pack," IEEE Trans. Geosci. Remote Sensing, vol. GE-24. No 5, pp. 717-721, 1986.

[80] Wang, M.S., and J.M. Borrego, "High-Resolution Scanning Microwave Electric-Field Probe for Dielectric Constant Uniformity Measurement," Materials Evaluation, pp. 1106-1109, Sept. 1990.

[81] Stuchly, S.S., Dielectric Properties of Granular Solids Containing Water," J. Microwave Power, vol. 5, no. 2, pp. 62-68, 1970.

[82] Stuchly, S.S., M.A. Stuchly and B. Carraro, "Permittivity Measurements in a Resonator Terminated by an Infinite Sample," IEEE Trans. on Inst. Meas., vol. 27, no. 4 pp. 436-439, Dec. 1978,.

[83] Thomson, M.C., F.E. Frethey and D.M. Waters, "End Plate Modification of X-Band TE011 Cavity Resonators," IRE Trans. on Microwave Theory Tech, vol. MTT-7, pp. 388-389, 1959.

[84] Tinga, W.R., and E.M. Edwards, "Dielectric Measurements Using Swept Frequency Techniques," J. Microwave Power, vol. 3, no.3, pp. 114-125, 1968.

[85] Toropainen, A.P., P.V. Vainikainen and E.G. Nyfors, "Microwave Humidity Sensor for Difficult Environmental Conditions," Proc. 14th European Microwave Conf., (EuMC'87), pp. 887-891, 1987.

[86] Vainikainen, P.V., E.G. Nyfors and M.T. Fischer, "Radiowave Sensor for Measuring the Properties of Dielectric Sheets: Application for Veneer Moisture Content and Mass per Unit Area Measurement," IEEE Trans. on Inst. Meas., vol. 36, no. 4, pp. 1036-1039, Dec. 1987.

[87] Weiss, J.A., and D.A. Hawks, "Dielectric Constant Evaluation of Insulating Materials: An Accurate Practical Measurement Device," IEEE MTT-S Digest, vol. I, pp. 456-460, 1987.

[88] Wenger, N.C., "Resonant Frequency for Open-Ended Cylindrical Cavity," IEEE Trans. on Microwave Theory Tech, vol. MTT-15, no. 6, pp. 334-340, June 1967.

[89] Baumann, S.B., W.T. Joines and E. Berman, "Feasibility Study of Batteryless Temperature Transponders Using Miniature Microwave Cavity Resonators," IEEE Trans. Biomed. Eng., vol. BME-34, no. 9, pp. 754-757, Sept. 1987.

[90] Bennet, P.G., "The Use of a Microwave Moisture Meter for Processing Investigations," Appita, vol. 26. No 4, pp. 267-272, 1973.

[91] Besada, J.L., M. Elices, J. Planas, J. Sanchez Minana and J.A. Garcia Cachero, "A New Technique of Deformation Measurements Based on Microwave Resonant Cavities," Proc. 10th European Microwave Conf., (EuMC'80), pp. 288-292, Sept. 1980.

[92] Clapeau, M., P. Guillon and Y. Garault, "Resonant Frequencies of Superposed Dielectric Resonators: Application to the Determination of the Local Dielectric Permittivity of MIC substrates," Proc. 7th European Microwave Conf., (EuMC'77), pp. 545-549, Sept. 1977.

[93] Doughty, D.A., "The Measurement of Water in Oil Emulsions by a Microwave Resonance Procedure," Analytical Chemistry, vol. 49, No 6, pp. 690-694, May 1977.

[94] Fisher, M., P. Vainikainen, E. Nyfors and M. Kara, "Fast Moisture Profile Mapping of a Wet Paper Web with Dual-Mode Resonator Array," Proc. 18h European Microwave Conf., (EuMC'88), pp. 607-612, Sept. 1988.

[95] Hoppe, W., W. Mayer and W.M. Schilz, "Density-Independent Moisture Metering in Fibrous Materials Using a Double-Cut-Off Gunn Oscillator," IEEE Trans. on Microwave Theory Tech, vol. MTT-28, no. 12, pp. 1449-1452, Dec. 1980.

[96] King, R.J., and P. Stiles, "Microwave Nondestructive Evaluation of Composites," Review of Progress in Quantitive Nondestructive Evaluation, vol. 3, Proc. 10th Annual Review, Santa Cruz, CA, pp. 1073-1081, Aug. 1983.

[97] Kobayashi, S., and S. Miyahara, "A Particulate Flow Meter Using Microwaves," Proc. IMECO, Prague, pp. 112-119, 1985.

[98] Konopka, J., and J.J. Majewski, "A New Microwave Method for Testing Nonlinear Effects in Solids," Proc. 10th European Microwave Conf., (EuMC'80), pp. 246-250, Sept. 1980.

[99] Korneta, A., and A. Milewski, "The Application of Two- and Three-Layer Dielectric Resonators to the Investigation of Liquids in the Microwave Region," IEEE Trans. on Inst. Meas., vol. IM-37, no. 1, March. 1988, pp. 106-109

[100] Laksminarayana, M.R., L.D. Partain and W.A. Cook, "Simple Microwave Technique for Independent Measurement of Sample Size and Dielectric Constant with Results for a Gunn Oscillator System," IEEE Trans. on Microwave Theory Tech, vol. MTT-27, no. 7, pp. 661-665, July 1979.

[101] Linzer M., and D.P. Stokesberry, "A Frequency-Lock Method for the Measuremnt of Q-Factors of Reflection and Transmission Resonators," IEEE Trans. on Inst. Meas., vol. IM-22, no. 1, pp. 61-77, March. 1973.

[102] Markowski, J., A.D. MacDonald and S.S. Stuchly, "The Dynamic Responce of a Resonant Frequency Tracking System," IEEE Trans. on Inst. Meas., vol. IM-26, no. 3, pp. 231-237, Sept. 1977.

[103] Merlo, A.L., "Combustion Chamber Investigations by Microwave Resonances," IEEE Trans. Ind. Electron. Contr. Instrum., vol. IECI-17, no. 2, pp.60-66, April 1970.

[104] Miyahara, S., and S. Kobayashi, "A Thickness Meter Using the Resonance of Microwaves," Trans. IECE of Japan, vol. E-68, no. 4, pp. 227-232, April 1985.

[105] Ney, M., and F.E. Gardiol, "Automatic Monitor of Microwave Resonators," IEEE Trans. on Inst. Meas., vol. IM-26, no. 1, pp. 10-13, March 1977.

[106] Nyfors, E., and P. Vainikainen, "Sensor for Measuring the Mass per Unit Area of a Dielectric Layer," Proc. 14th European Microwave Conf., (EuMC'84) pp. 667-672, Sept. 1984,.

[107] Pandrangi, R.K., S.S. Stuchly and M. Barski, "A Digital System for Measurement of Resonant Frequency and Q Factor," IEEE Trans. on Inst. Meas., vol. IM-31, no. 1, pp. 18-21, March 1982.

[108] Rzepecka, M.A., S.S. Stuchly and M.A.K. Hamid, "High-Frequency Monitoring of Residual and Bound Water in Nonconductive Fluids," IEEE Trans. on Inst. Meas., vol. IM-24, no. 3, pp. 205-210, Sept. 1975.

[109] Sihvola A., "Note on Frequency Dependence of Quality Factor of Cavity Resonators," Electron. Lett., vol. 21, no. 17, pp. 736-737, 1985.

[110] Sihvola, A., and M. Tiuri, "Snow Fork for Field Determination of the Density and Wetness Profiles of a Snow Pack," IEEE Trans. Geoscience and Remote Sensing, vol. GE-24, no. 5, pp. 717-721, Sept. 1986.

[111] Tiuri M., P. Liimatainen and S. Reinamo, "A Microwave Instrument for Measurement of Small Inhomogeniuities in Supercalendar Rollers and Other Dielectric Cylinders," J. Microwave Power, vol. 9, no.2, pp. 117-121, 1974.

[112] Williams, R.V., "Application of Microwave Techniques in the Iron and Steel Industry," ISA Proc. Nat. Conf. Inst. for Iron and Steel, 1967

[113] Yamanaka, T., M. Esaki and M. Kinoshita, "Measurement of TDC in Engine by Microwave Technique," IEEE Trans. on Microwave Theory Tech, vol. MTT-33, pp. 1489-1494, no. 12 Dec. 1985.

[114] Zurcher, J.F., and F.E. Gardiol, "Nondestructive Microwave Measurements of materials' Moisture in Building Walls," Proc. IMEKO Congress Int. Measurement Confederation, pp. 393-398, Moscow, May 1979.

[115] Brodwin, M., and J. Benway, "Experimental Evaluation of a Microwave Transmission Moisture Sensor," J. Microwave Power, vol. 15, pp. 261-265, no. 4, Dec. 1980.

[116] Chudobiak, W.J., M.R. Beshir and J.S. Wight, "An Open Transmission Line UHF CW Phase Technique for Thickness/Dielectric Constant Measurements," IEEE Trans. Inst. Meas., vol. IM-28, no. 1, pp. 18-25, March 1979.

[117] Jacobsen, R., W. Meyer and B. Schrage, "Density Independent Moisture Meter at X-Band," Proc. 10th European Microwave Conf., (EuMC'80), pp. 216-220, Sept. 1980.

[118] Jakkula, P., " Method and Apparatus for Measurement the Moisture Content or Dry-Matter Content of Materials Using a Microwave Dielectric Waveguide," U.S. Patent no. 4,755,743, July 5, 1988.

[119] Kalinski, J., "A Chopped Subcarrier Methods of Simultaneous Attenuation and Phase-Shift Measurement under Industrial Conditions," IEEE Trans. Ind. Electron. Contr. Instrum., vol. IECI-28, no. 3, pp. 201-209, Aug. 1981.

[120] Khalid, K.B., T.S.M. Maclean, M. Razaz and P.W. Webb, "Analysis and Optimal Design of Microstrip Sensors," IEE Proc., vol. 135, Pt. H, no.3, pp. 187-195, June 1988.

[121] Kent, M., J. Kohler, "Broadband Measurement of Stripline Moisture Sensors," J. Microwave Power, vol. 19, no. 3, pp. 173-179, Sept. 1984.

[122] Klein, A., "Microwave Determination of Moisture in Coal: Comparison of Attenuation and Phase Measurement," J. Microwave Power, vol. 16, no. 3-4, pp. 289-304, 1981.

[123] Kraszewski, A., S. Kulinski, J. Madziar and K. Zielkowski, "Microwave On-Line Moisture content Monitoring in Low-Hydrated Organic Materials," J. Microwave Power, vol. 15, no. 4, pp. 267-275, Dec. 1980.

[124] Okamura, S., "High-Moisture Content Measurement of Grain by Microwaves," J. Microwave Power, vol. 16, no. 3-4, pp. 253-256, 1981.

[125] Ozamiz, J.M., and S.J. Hewitt, "Microwave Moisture Measurement System,"Proc. 9h European Microwave Conf., (EuMC'79), pp. 340-344, Sept. 1979.

[126] Shafer, G.E., "A Modulated Subcarrier Technique of Measuring Microwave Phase Shift," IRE Trans. Instrum., vol. I-9, 217-219, 1960.

[127] Shiraiwa, T., S. Kobayashi, A. Koyama, M. Tokuda and S. Koizumi, "Microwave Moisture Gauge for Limestone," J. Microwave Power, vol. 15, no. 4, pp. 255-260, Dec. 1980.

[128] Wyslouzil, W., and A.L. VanKoughnett, "An Attenuation Based Microwave Moisture Gauge for Sheet Materials," J. Microwave Power, vol. 9, no. 2, pp. 91-98, June 1974.

[129] Heikkila, S., P. Jakkula and M. Tiuri, "Microwave Methods for Strength Grading of Timber and for Automatic Edging of Bonds," Proc. 12th European Microwave Conf., (EuMC'82), pp. 599-603, Sept. 1982.

[130] Jakkula, P., "Method and Apparatus for Knot Detection in Sawn Timber," U.S. Patent no 4,607,212.

[131] Ou, W., C.G. Gardner and S.A. Long, "Nondestructive Measurements of a Dielectric Layer Using Surface Electromagnetic Waves," IEEE Trans. on Microwave Theory Tech, vol. MTT-31, no. 3, pp. 255-261, March 1983.

[132] Reinschlussel, R., and B. Schiek, "A Sensitive Cavity-Based Gas-Spectrometer for Broadband Operation at 26-40 GHz," Proc. 15th European Microwave Conf., (EuMC'85), pp. 895-900, Sept. 1985.

[133] Schiek, B., T. Paukner and W. Schilz, "A Microwave Spectrometer - Suitable for Gas Analysis in Industrial Applications," Proc. 7th European Microwave Conf., (EuMC'77), pp. 251-255, Sept. 1977.

[134] Tiuri, M., K. Jokeda and S. Heikkila, "Microwave Instrument for Accurate Moisture and Density Measurement of Timber," J. Microwave Power, vol. 15, no. 4, pp. 251-254, June 1980.

[135] Akhmetsin, A.M., "Determining Parameters of Laminated Dielectrics Near Minima of Absolute Reflection Coefficients," Sov. J. Nondest. Test. (US), vol. 22, no. 3 pp. 213-219, March 1986,.

[136] Akhmetsin, A.M., and A.Y. Kurin, "Determining Parameters of Laminated Materials Having Dielectrics Losses by Measurements in a Range of Frequencies," Sov. J. Nondest. Test. (US), vol. 22, no. 3, pp. 205-213, March 1986.

[137] Arai, I., and T. Suzuki, "A Microwave Interferometer System for the Displacement Measurements of Biological Subject," Electronics and Communications in Japan, vol. 67-C, no. 10, pp. 108-118, 1984.

[138] Atek, K.A., S.A. Mawjoud and A.S. Jabber, "The Effect of Humidity and Bulk Density on Flow Rate Measurements of Rice, Salt and Sugar," J. Inst. Electron., and Telecommun. Eng. (India), vol. 30, no. 5, pp. 124-128, Sept. 1984.

[139] Bailey, S.J., "Level Sensor'80: A Key Partner in Productivity," Control Eng. (US), vol. 27, no. 10, pp. 75-79, Oct. 1980.

[140] Bartashevskii, E.L., V.F. Borul'ko, O.O. Drobakhin and I.V. Slavin, "Effectiveness of Data Processing in Determining Parameters of Dielectrics by the Multifrequency Method," Sov. J. Nondest. Test. (US), vol. 22, no. 6, pp. 372-374, June 1986.

[141] Bastida, E.M., N. Fanelli and E. Marelli, "Microwave Instruments for Moisture Measurements of Soils, Sands and Cements," 14th Microwave Power Symp., Monaco, pp. 147-149, June 1979.

[142] Hobson, G.S., R.C. Tozer, J.M. Rees, P.L. Judd and R. Devayya, "Microprobe - Microwave Measurement of Furnace Wall Thickness," Proc. 17th European Microwave Conf., (EuMC'87), pp. 881-886, Sept. 1987.

[143] Kobayashi, S., and S. Miahara, "Applications of Microwave Displacement Meter Using a Five-Port Device," Proc. IECON'84, pp. 633-636, Tokyo, Oct. 1984.

[144] Konev, V.A., S.A. Tikhanovich and M.I. Zhigalko, "Error in Determination of the Dielectric Properties and Thickness of Surface Layers by the Method of Radiometric Ellipsometry," Sov. J. Nondest. Test. (US), vol. 22, no. 6, pp. 363-366, June 1986.

[145] Martinson, T., T. Sphicopoulos and F.E. Gardiol, "Nondestructive Measurement of Materials Using a Waveguide-Fed Series Slot Array," IEEE Trans. Inst. Meas., vol. IM-34, no. 3, pp. 422-426, Sept. 1985.

[146] Shiraiwa, T., and S. Kobayashi, "The Applications of Microwave Techniques for Measurement in the Steel Industry," Proc. SIMAK'74 Conf., pp. P16/1-12, Sheffield, UK, Oct. 1974.

[147] Sphicopoulos, T., V. Teodoridis and F.E. Gardiol, "Simple Nondestructive Method for the Measurement of Material Permittivity," J. Microwave Power, vol. 20, no. 3, pp. 165-172, Sept. 1985

[148] Stuchly, S.S., M.S. Sabir and A. Hamid, "Advances in Monitoring of Velocities and Densities of Particulates Using Microwave Doppler Effect," IEEE Trans. Inst. Meas., vol. IM-26, no. 1, pp. 21-24, March 1977.

[149] Tsansandote, A., S.S. Stuchly and J.S. Wight, Microwave Interferometer for Measurements of Small Displacements," IEEE Trans. Inst. Meas., vol. IM-31, no. 4, pp. 227-232, Dec. 1982.

[150] Lin, J.C., "Microwave Sensing of Physiological Movement and Volume Change: A Review," Bioelectromagnetics, vol. 13, no. 6, pp. 557-565, 1992.

[151] Detlefsen, J., "Industrial Applications of Microwave Imaging," Conference Proc. Military Microwaves MM'92, p. 96, 1992.

[152] Chufo, R.L., "Noncontact Coal and Rock Thickness Measurement with a Vector Network Analyzer," Proc. RF Expo East, p. 488, Tampa FL, 22-24 Sept. 1992.

[153] Woods, G.S., D. Maskell, C. Kikkert, J. Cutmore, "Microwave Height Measurement Systems for Industrial Applications," IREECON'91, Australia's Electronic Convention Proceedings, vol. 1, pp. 377-380, Sydney, 16-20 Sept. 1991.

[154] Al Zoubi, A.Y., and A.S. Al Dmour, "Automatic Measurements of Resonator Characteristics for the Determination of the Electronic and Magnetic Properties of Materials," Measurement Science and Technology, vol. 4, pp. 12-15, Jan. 1993.

[155] King, R.J., "Microwave Sensors for Process Control. I Transmission Sensors," Sensors, vol. 9, pp. 68-74, Oct. 1992

[156] King, R.J., "Microwave Sensors for Process Control. II Open Resonator Sensors," Sensors, vol. 9, pp. 25-30, Oct. 1992

[157] Tran V.N., and Y. Shen, "A Flexible Microwave Moisture Meter," IREECON'91, Australia's Electronic Convention Proceedings, vol. 2, pp. 654-657, Sydney, 16-20 Sept. 1991.

[158] Moreo J.M., and R. Aziz, "Dielectric Study of Granular Media According to the Type of Measurement Device: Coaxial Cell or Open-Ended Probe," Measurement Science and Technology, vol. 4, pp. 124-129, Jan. 1993

[159] Ida N., "Microwave NDT," Electrosoft, vol. 2, pp. 215-237, June-Sept. 1991

[160] Ulaby, F.T., M.C. Dobson and D. Brunfeld, "Microwave Probe for In Situ Observation of Vegetation Dielectric Constant," IEEE Instrumentation and Measurement Technology Conference, Atlanta, GA., pp. 631-635, May. 14-16, 1991.

[161] Kraszewski, A.W., and S.O. Nelson, "Sorting Biological Objects with Microwave Resonant Cavities,"IEEE Instrumentation and Measurement Technology Conference, Atlanta, GA., pp. 40-43, May. 14-16, 1991.

[162] Cutmore, N., T. Evans and A. McEwan, "On Conveyor Determination of Moisture in Coal," J. Microwave Power and Electromagnetic Energy, vol. 26, no.4, pp. 237-242, 1991.

[163] Tiuri, M., "Microwave Sensor Applications in Industry," 17th European Microwave Conference (EuMC), pp. 25-32, 1987.

[164] Carlini, C., P.A. Rolla and E. Tombari, "Measurement Method and Apparatus for Monitoring the Kinetics of Polymerization and Crosslinking Reactions by Microwave Dielectrometry," Journal of Applied Polymer Science, vol. 41, no. 3-4, pp. 805-818, 1990

[165] Davis, R.L., "Use of Microwave Distance Measuring Instruments in Industrial Plant Control Systems," Colloquium on Industrial Uses of Microwaves, London, (IEE Coloquium Digest), 1990.

[166] Delmotte, M., H. Jullien and M. Ollivon, "Variation of the Dielectric Properties of Epoxy Resins During Microwave Curing," European Polymer Journal, vol. 27, pp. 371-376, no. 4-5 1991.

[167] Anon, "Three-Probe Microstrip Measuring System for S-Parameters Measurements," Electronics Letters, vol. 27, no. 10, pp. 836-837, 1991.

[168] Bramanti, M., "Slot Line Microwave Dielectric Permittivity Sensor for Measure and Control of Laminated Materials," J. Microwave Power and Electromagnetic Energy, vol. 26, no.2, pp. 67-71, 1991.

[169] Binstock, D.A., P.M. Grohse, A. Gaskill and C. Sellers, "Validation of a Microwave Digestion Method for Solid Wastes," Waste Testing and Quality Assurance Symposium, pp. 245-254, Washington DC, ASTM Special Technical Publication, no. 1075.

[170] Bolomey, J.-C., and C. Pishot, "Microwave Tomography: From Theory to Practical Imaging Systems," International Journal of Imaging Systems and Technology, vol. 2, pp. 144-156, 1990.

[171] Anderson, A.P.and S. Sali, "New Possibilities for Phaseless Microwave Diagnostics. Part 1: Error Reduction Techniques," IEE Proc., vol. 132, Pt.H, pp. 291-298, No 5, Aug. 1985.

[172] Sali, S., "New Possibilities for Phaseless Microwave.Diagnostics. Part 2: "The Uniqueness Problem and Half Plane Imaging," IEE Proc, vol. 132, Pt.H, pp. 299-306, No 5, Aug. 1985.

[173] Caldecott, R., M.Poirier, D.Scofea, D.E.Svoboda and A.Terzuoli, "Underground Mapping of Utilities Lines Using Impulse Radar" IEE Proc.,vol. 135, Pt.F, pp. 343-353, No 4, Aug. 1988.

[174] Bardati, F., M. Monqiardo, D. Solimini and P. Tognolatti, "Biological Temperature Retrieval by Scanning Radiometry" 1986 IEEE MTT-S Digest, pp. 763-766, 1986.

[175] Schultz,K.I., and D.L. Jaggard, "Novel Microwave Projection Imaging for Determination of Internal Structure," Electronics Letters, vol. 23, pp. 267-269, No 6, 12th March 1987.

[176] Lin, J.C., "Frequency Optimization for Microwave Imaging of Biological Tissues" Proc. of the IEEE, vol. 73, no. 2, pp. 374-375, Feb. 1985.

[177] Yamani, A., and J.C. Bennett, "Depth-Of-Field Improvements and Removal of Distortion in Long Wavelength Imaging Systems" IEE Proc., vol. 132, Pt.F, pp. 149-152, no 3, June 1985.

[178] Bolomey, J.-C., "Recent European Developments in Active Microwave Imaging for Industrial, Scientific, and Medical Applications" IEEE Trans. Microwave Theory Tech, vol. 37, pp. 2109-2117, no 12, Dec. 1989.

[179] Chu, T.-H.and N. Farhat, "Frequency-Swept Microwave Imaging of Dielectric Objects" , IEEE Trans. Microwave Theory Tech., vol. 36, pp.489-493, March 1988.

[180] Chu, T.-H., "Polarization Effects on Microwave Imaging of Dielectric Cylinder" IEEE Trans. Microwave Theory Tech., vol. 36, pp. 1366-1369, no 9, Sept.1988.

[181] Chommeloux, L., C. Pichot and J.-C. Bolomey "Electromagnetic Modeling for Microwave Imaging of Cylindrical Buried Inhomogenuties" IEEE Trans. Microwave Theory Tech., vol. MTT-34, pp. 1064-1076, no 10, Oct. 1986.

[182] Pichot, C., L Jofre, G. Peronnet and J.-C. Bolomey "Active Microwave Imaging of Inhomogeneous Bodies" IEEE Trans.Antennas Propagat.,vol. AP-33, pp. 416-425, no 4, 1985.

[183] Osumi, N., and K. Ueno, "Microwave Holographic Imaging of Underground Objects" ., IEEE Trans.Antennas Propagat, vol. AP-33, pp. 152-159, no 2, Feb. 1985.

[184] Guo, T., and W. Guo "Generation of acoustic waves at dielectric interface by microwave pulses,"Diel. Mat. Meas. and Appl., IEE: Conf.Publ. no 281, pp.348-351, 27-30 June 1988.

[185] Chan, W., and B. Chambers, "Open Resonator Permittivity of Curved Dielectric Samples,"Diel. Mat. Meas. and Appl., IEE: Conf.Publ. No 289, pp. 336-339, 27-30 June 1988.

[186] Sigfrid Yngversson, K., J.Johanson and E. Kollberg, "A New Integrated Array for Multi-Beam Systems with Application to Millimeter Imaging" IEEE - AP-S, vol. 2, pp.895-898,1985.

[187] Osumi, N., and K. Ueno "Resolution Improvement and Clutter Reduction in Underground Object Imaging," IEEE-AP-S-1985, vol.1,2, pp. 753-756, 1985.

[188] Schaller, G., "Microwave and Infrared Thermograms of Hot Spots in Tissue," 1984 IEEE MTT-S Digest, 6-6, pp. 148-149, 1984.

[189] Sakamoto, Y., K. Tajiri, T. Sawai and Y. Aoki "Detection of Objects Buried in Snow Using Microwave Holography," IEE, ICAP'87, Conf.Publ. No 274, pp. 364-367, 1987.

[190] Aoki, Y. , Y. Sakamoto, K. Tajiri and T. Sawai, "Signal Processing of Holographic Under-Snow Radar with a Displaying Systems of Three-Dimensional Information" 1986 ICASSP, pp. 2883-2886, 1986.

[191] Detlefsen, J., "Application of Multistatic Radar Principles to Short-Range Imaging," IEE Proc., vol. 133, Pt.F, no 7, pp. 658-663, Dec.1986.

[192] Osumi, N., and K. Ueno, "Detecton of Buried Plant," IEE Proc., vol. 135, Pt. F, pp.330-342, no 4, Aug. 1988.

[193] Yue, O.-C., E.L. Rope and G. Tricoles, "Two Reconstruction Methods for Microwave Imaging of Buried Dielectric Anomalies," IEEE Trans. on Computers, vol. C-24. nno.o 4, pp. 381-390, Apr. 1975.

[194] Caorsi, S., G.L. Gragnani, S. Medicina, M. Pastorino and G. Zunino, "Microwave Imaging Based on a Markov Random Field Model," IEEE Trans. on Antennas and Propagation, vol. 42, pp.293-303, March 1994.

[195] Bianco, B., G.P. Drago, M. Marchesi, C. Martini, G.S. Mela and S. Ridella, "Measurements of Complex Dielectric constant of Human Sera and Erythrocytes," IEEE Trans. on Inst. Meas., vol. 28, pp. 290-295, no.4, Dec. 1979.

[196] Mahony, J.D., "A Low-Frequency Investigation Into the Discontinuity Capaciatance Of a Coaxial Line Terminated in a Lossless, Dielectric-Loaded Circular Waveguide," IEEE Trans. on Microwave Theory Tech., vol. 35, pp. 344-346, March 1987.

[197] Taherian,M., D. Yuen, T. Habashy and J. Kong, "A Coaxial-Circular Waveguide for Dielectic Measurement," IEEE Trans. on Geosci., and Remote Sensing, vol. GE-29, pp. 321-330, March. 1991.

[198] Makphie, R.H., M. Opi and C. Ries, "Input Impedance of a Coaxial Line Probe Feeding a Circular Wavegide in the TM01 Mode," IEEE Trans. on Microwave Theory Tech., vol. 38, pp. 334-337, March.. 1990.

[199] Bussey, H., "Dielectric Measurements in Shielded Open Circuit Coaxial Line," IEEE Trans. on Inst. Meas., vol. 29, pp. 120-124, No. 2, June 1980

[200] Marcuvitz, N., Waveguide Handbook, McGraw-Hill, N.Y. 1951.

[201] Levine, H., and C. Papas, "Theory of Circular Diffraction Antenna," J. Appl. Phys., vol. 22, pp. 29-43, 1951.

[202] Epstein, B.R., M.A. Gealt and K.R. Foster, "The Use of Coaxial Probes for Precise Dielectric Measurements: A Reevaluation," IEE MTT-S Int. Microwave Symp. Digest, Las Vegas, pp. 255-258, June 1987.

[203] Misra, D., "A Quasi-Static Analysis of Open-Ended Coaxial Lines," IEEE Trans. on Microwave Theory Tech., vol. MTT-35, pp. 925-928, Oct. 1987.

[204] Stuchly, M., and S. Stuchly, "Coaxial Line Reflection Methods for Measuring Dielectric Properties of Biological Substances at Radio and Microwave Frequencies - A Review," IEEE Trans. Instr. Meas., vol. IM-29, pp. 176-183, Sept. 1980.

[205] Mosig, J., J.-C. Besson, M. Gex-Farby and F. Gardiol, "Reflection of an Open-Ended Coaxial Line and Application to Nondestructive Measurement of Materials," IEEE Trans. Instr. Meas., vol. IM-30, pp. 46-51, March. 1981.

[206] Fan, S., K. Staebel and D. Misra, "Static Analysis of an Open-Ended Coaxial Line Terminated by Layered Media," IEEE Trans. Instr. Meas., vol. 39, pp. 435-437, Apr. 1990.

[207] Anderson, L., G. Gajda, and S. Stuchly, "Analysis of an Open-Ended Coaxial Line Sensor in Layered Dielectrics," IEEE Trans. Instr. Meas., vol. IM-35, pp. 13-18, March. 1986.

[208] Swift, C., "Input Admittance of a Coaxial Transmission Line Opening onto a Flat, Dielectric-Covered Ground Plane," NASA Technical Note D-4158, Sept. 1967.

[209] Kraszewski, A., M. Stuchly, and S. Stuchly, "ANA Calibration Method for Measurements of Dielectric Properties,"IEEE Trans. Instr. Meas., vol. IM-32, pp.385-387, June. 1983.

[210] Nyshadham, A., C. Sibbald and S. Stuchly, "Permittivity Measurements Using Open-Ended Sensors and Reference Liquid Calibration - An Uncertainty Analysis," IEEE Trans. on Microwave Theory Tech., vol. 40, pp. 305-313, Feb. 1992.

[211] Marsland, T., and S. Evans, "Dielectric Measurements With an Open-Ended Coaxial Probe,"IEE Proc., Pt.H, vol. 134, pp.341-349, Aug.1987.

[212] Misra, D., M. Chabra, B. Epstein, M. Mirotznik and K. Foster, "Noninvasive Electrical Characterization of Materials at Microwave Frequencies Using an Open-Ended Coaxial Line: Test of an Improved Calibration Technique," IEEE Trans. on Microwave Theory Tech., vol. MTT-38, pp. 8-14, Jan. 1990.

[213] Staebel, K., and D. Misra, "An Experimental Technique for I*n Vivo* Permittivity Measurement of Materials at Microwave Frequencies," IEEE Trans. on Microwave Theory Tech., vol. MTT-38, pp. 337-339, March. 1990.

[214] Burdette, E., F. Cain and J. Seals, "*In Vivo* Probe Measurement Technique for Determining Dielectric Properties at VHF Through Microwave Frequencies," IEEE Trans. \on Microwave Theory Tech., vol. MTT-28, pp. 414-426, Apr 1980.

[215] El-Rayes, M., and F. Ulaby, "Microwave Spectrum of vegetation - Part I: Experimental Observations," IEEE Trans. on Geosci. and Remote Sensing, vol. GE-25, pp. 541-549, Sept. 1987.

[216] Otto, G., and W. Chew, "Improved Calibration of a Large Open-Ended Coaxial Probe for Dielectric Measurements," IEEE Trans. Instr. Meas., vol. 40, pp. 742-746, Aug. 1991.

[217] Gajda, G., and S. Stuchly, "Numerical Analysis of Open-Ended Coaxial Lines," IEEE Trans. on Microwave Theory Tech., vol. MTT-31, pp. 380-384, May 1983.

[218] Gardiol, F., "Open-Ended Waveguides: Principles and Applications," Advances in Electronics and Electron Physics, vol. 63, pp. 139-187, 1985.

[219] Kraszewski, A., and S. Stuchly, "Capacitance of Open-Ended Dielectric Filled Coaxial Lines - Experimental Results," IEEE Trans. Instr. Meas., vol. IM-32, pp. 517-519, Dec. 1983.

[220] Xu, Y., R. Bosisio and T. Bose, "Some Calculation Methods an Universal Diagrams for Measurement of Dielectric Constants Using Open-Ended Coaxial Probes," IEE Proc., Pt H, vol. 138, pp. 356-360, Aug. 1991.

[221] Athey, T., M. Stuchly and S. Stuchly, "Measurement of Radio Frequency Permittivity of Biological Tissues with an Open-Ended Coaxial-Line: Part I," IEEE Trans. on Microwave Theory Tech., vol. MTT-30, pp. 82-86, Jan. 1982.

[222] Athey, T., M. Stuchly and S. Stuchly, "Measurement of Radio Frequency Permittivity of Biological Tissues with an Open-Ended Coaxial-Line: Part II - Experimental Results," IEEE Trans. on Microwave Theory Tech., vol. MTT-30, pp. 87-92, Jan. 1982.

[223] Stuchly, M., M. Brady, S. Stuchly and G. Gajda, "Equivalent Circuit of an Open-Ended Coaxial Line in a Lossy Dielectric," IEEE Trans. Instr. Meas., vol. IM-31, pp. 116-119, June. 1982.

[224] Kraszewski, A., S. Stuchly, M. Stuchly and S. Symons, "On the Measurement Accuracy of the Tissue Permittivity *In Vivo*," IEEE Trans. Instr. Meas., vol. IM-32, pp. 37-42, March. 1983.

[225] Gajda, G., and S. Stuchly, "An Equivalent Circuit of an Open-Ended Coaxial Line," IEEE Trans. Instr. Meas., vol. IM-32, pp. 506-508, Dec. 1983.

[226] Seaman, R., E. Burdette and R. Dehaan, "Open-Ended Coaxial Exposure Device for Applying RF/Microwave Fields to Very Small Biological Preparations," IEEE Trans. on Microwave Theory Tech., vol. MTT-37, pp. 102-111, Jan. 1989.

[227] Belhadj-Tahar, N.-E., A. Fourrier-Lamer and H de Chanterac, "Broad-Band Simultaneous Measurement of Complex Permittivity and Permeability Using a Coaxial Discontinuity," IEEE Trans. on Microwave Theory Tech., vol. MTT-38, pp. 1-7, Jan. 1990.

[229] Zheng, H., and C. Smith, "Permittivity Measurements Using a Short Open-Ended Coaxial Probe," IEEE Microwave and Guided Wave Let.., vol. 1, pp. 337-339, Nov. 1991.

[230] Liping, L., X. Deming, and J. Zhiyan, "Improvement in Dielectric Measurement Technique of Open-Ended Coaxial Line Resonator Method," Electronics Letters, vol. 22, pp. 373-375, no 7, 27 March 1986.

[231] Bliot, F., A. Castelain and B. Dujardin, "Numerical Simulation and Models for Microcoaxial Probes Application to 'In Vivo' Measurements of Dielectric Parameters of Biological Media in the Microwave Band (1-12 GHz)," Proc. 10th European Microwave Conf., pp. 531-535, Sept. 1980.

[232] Smith, G., and J. Nordgard, "Measurement of the Electrical Parameters of Materials Using Antennas," IEEE Trans. on Antennas Propagat., vol. AP-33, pp. 783-792, no 7, July 1985.

[233] Grant, J., R. Clarke, G. Symm and N. Spyrou, "A Critical Study of the Open-Ended Coaxial Line Sensor Technique for RF and Microwave Complex Permittivity Measurements," J. Phys. E., Sci. Instrum., vol. 22, pp.757-770, 1989

[234] Jenkins, S., T. Hodgetts, R. Clarke and A. Preece, "Dielectric Measurements of Reference Liquids Using Automatic Network Analysers and Calculable Geometries," Meas. Sci. Technol., vol. 1, pp. 691-702, 1990.

[235] Jenkins, S., A. Warham, and R. Clarke, "Use of Open-Ended Coaxial Line Sensor with a Laminar or Liquid Dielectric Backed by a Conducting Plane," IEE Proc., Pt H, vol. 139, pp. 179-182, no. 2, Apr. 1992.

[236] Kent, M., " A simple Flowthrough Cell for Microwave Dielectric Measurements," J. Phys.E., Sci. Instrum., vol. 22, pp.269-271, 1989.

[237] Anderson, L., S.S. Stuchly and G.B. Gajda, "Parallel-Plate Coaxial Sensor for Dielectric Measurements - Further Analysis," IEEE Trans. on Inst. Meas., vol. IM-35, pp. 89-91, no. 1, March 1986.

[238] Olson, S.C., and and M.F. Iskander, "A New In Situ Procedure for Measuring the Dielectric Prperties of Low Permittivity Materials," IEEE Trans. on Inst. Meas., vol. IM-35, pp. 2-6, no. 1, March 1986.

[239] Colpitts, B.G., "Temperature Sensitivity of Coaxial Probe Complex Permittivity Measuerements: Experimental Approach," IEEE Trans. on Microwave Theory Tech., vol. MTT-41, pp. 229-233, Feb. 1993.

[240] Xu, Y., and R.G. Bosisio, "Nondestructive Measurements of Resistivity of Thin Conductive Films and the Dielectric Constant of Thin Substrates Using an Open-Ended Coaxial Line," IEE Proc., Pt H, vol. 139, pp. 500-506, no. 6, Dec. 1992.

[241] Nishikata, A., and Y. Shimizu, "Analysis for Reflection from Coaxial End Attached to Lossy Sheet and Its Application to Nondestructive Measurement," Electron.Commun. Jpn., Part 2, vol. 71, pp. 95-107, No. 6, 1988.

[242] Roussy, G., K. K. Agbossou and J.-M. Thiebaut,"Improved Modeling of Permittivity Measurement Cells," IEEE Trans. on Inst. Meas., vol. 41, pp. 366-369 No. 3, June 1992

[243] Swicord M.L., and C.C. Davis, "Energy Absorption from Small Radiating Coaxial Probes in Lossy Media, "IEEE Trans. on Microwave Theory Tech., vol. MTT-29, pp. 1202-1209, Nov. 1981.

[244] Nevels, R.D., C.M. Butler and W. Yablon, "The Annular Slot Antenna In a Lossy Biological Medium," IEEE Trans. on Microwave Theory Tech., vol. MTT-33, pp. 314-319, Apr. 1985.

[245] Gabriel, C., E.H. Grant and I.R. Young, "Use of Time Domain Specroscopy for Measuring Dielectric Properties with a Coaxial Probe," J. Phys. E., Sci. Instrum., vol. 19, pp.843-846, 1986.

[246] Wei, Y.-Z., and S. Sridhar, "Radiation Correction Open-Ended Coax Line Technique for Dielectric Measurements of Liquids up to 20 GHz," IEEE Trans. on Microwave Theory Tech., vol. 39, pp. 526-531, March. 1985.

[247] Thansandote, A., and J. Ponukkha, "Shielded-Open-Coaxial-Line and Short-Monopole Reflection Techniques for Measuring Moisture Content of Grain and Peanuts," J. Microwave Power and Electromagnetic Energy , vol. 25,pp. 195-201, no. 4, 1990.

[248] Nishikata, A., and Y. Shimizu, "Effectivnes of Gaps for Lossy Dielectric Sheet Measurement by Coaxial Electrode," Electron.Commun. Jpn., Part 2, Vol. 73, pp. 14-21, No. 7, 1990.

[249] Nevels, R.D., and J.E. Wheeler, "Near Field Radiation from Four Coaxial Line Fed Structures," Microwave Opt. Technology Letters , vol. 3, pp.90-95, March 1990.

[250] Durney, C.H., "Antennas and Other Electromagnetic Applicators in Biology and Medicine," Proc. IEEE, vol. 80, pp. 194-199, Jan. 1992.

[251] Bianco, B., A. Corana, L. Gogioso, S. Ridella, M. Parodi, "Open-Circuited Coaxial Lines as Standards for Microwave Measurements," Electronics Letters, vol. 16, pp. 373-374, no 10, 8 May 1980.

[252] Xu, Y., F. Ghannouchi and R. Bosisio, "Theoretical and Experimental Study of Measurement of Microwave Permittivity Using Open Ended Elliptical Coaxial Probes," IEEE Trans. on Microwave Theory Tech., vol. 40, pp. 143-150, Jan. 1992.

[253] Olp, K., G. Otto, W.C. Chew and J.F. Young, "Electromagnetic Properties of Mortars over a Broad Frequency Range and Different Curing Times," J. Materials Science, vol. 26, pp. 2978-2984, 1991.

[254] Chew, W., K. Olp and G. Otto, "Design and Callibration of a Large Broadband Dielectric Measurement Cell," IEEE Trans. on Geosci. and Remote Sensing, vol. GE-29, pp. 42-47, Jan. 1991.

[255] Vaitkus, R.L., "Wide-Band De-Embedding with a Short, an Open, and Through Line," Proc. IEEE, vol. 74, pp. 71-74, Jan. 1992.

[256] Gajda, G.B., "A Method for the Measurement of Permittivity at Radio and Microwave Frequencies," Proc IEEC&E, pp.160-161, 1979.

[257] Zurcher, J., L. Hoppie, R. Lade, S. Srinivasan and D. Misra, "Measurement of the Complex Permittivity, of Bread Dough by an Open-Ended Coaxial Line Method at Ultrahigh Frequencies," J. Microwave Power and Electromagnetic Energy , vol. 25, pp. 161-167, no. 3, 1990

[258] Pournaropoulos, C., and D. Misra, "An Integral Equation Procedure for Electrical Characterization of Materials Using a Coaxial Microwave Sensor," Proc. of 3rd Int. Symp. on Recent Advances in Microwave Technology (ISRAMT '91), pp. 157-160, 1991.

[259] Tanguay, L., and R. Vaillancourt, "Numerical Solution of the Dielectric Equation for a Coaxial Line," IEEE Trans. on Inst. Meas., vol. 33, pp. 366-369 No. 2, June 1984

[260] Chang, D.C., "Input Admittance and Complete Near-Field Distribution of an Annular Aperture Antenna Driven by a Coaxial Line," IEEE Trans. on Antennas Propagat., vol. AP-18, pp. 610-616, no. 5, Sept. 1970.

[261] Liao, S.Y., Engineering Applications of Electromagnetic Theory, pp. 3-4, West Publishing Co., St. Paul, MN, 1988.

[262] Ulaby, F.T., R. K. Moore, and A.K. Fung, "Microwave Remote Sensing, Passive and Active," Vol. III, pp. 2017-2020, Artech House, Dedham, MA, 1986.

[263] Ulaby, F.T., R. K. Moore, and A.K. Fung, "Microwave Remote Sensing, Passive and Active," Vol. I, pp. 61-67, Artech House, Dedham, MA, 1986.

CHAPTER 2

MATERIAL CHARACTERIZATION

The dielectric properties of a material made of several constituents (dielectric mixture) are dependent upon the dielectric properties of each constituent, their volume contents, the operating frequency and any polymerization (e.g. molecular bonding and curing) that may have occured during the production of the mixture. It is also possible to use microwaves as a heat source to promote and facilitate curing in various composite materials. Potentially, the following pieces of information may be obtained when interrogating the dielectric properties of a composite material (mixture):

- dielectric properties of any given constituent comprising a mixture
- volume content of any given constituent
- cure state
- physical and mechanical properties which are dictated by the cure state and condition (i.e. compressive strength in concrete)

There are various empirical dielectric mixing models that have also been developed in conjunction with this issue. These models which generally have an electromagnetic basis can be used to predict the dielectric properties of a mixture as a function varying type and amount of constituents and the operating frequency. They usually consider a dielectric mixture to consist of a host medium (the most prominent constituent) and several types of inclusions. Appendix E of reference [1] provides a fairly detailed discussion of these models as they relate to earth matters such as water, soils, snow, etc. However, it must be noted that similar approaches may be used to develop models for dielectric composite mixtures, as will be seen later in this chapter. A partial list of references is provided here which deals with mixing models and some microwave dielectric property measurements of materials [2-53].

There are numerous methods for dielectric property measurement of materials. These techniques differ as a function of the following considerations:

- type of material to be measured (i.e. liquids, solids, gases, etc.)
- on-line or off-line requirements of the measurements
- required measurement accuracy
- type of measurement apparatus such as open-ended transmission lines (e.g. waveguide, coax, open-resonators, etc.), cavity resonators, microstrip patches and filled (completely or partially) transmission lines
- loss tangent of the material (i.e. low loss vs. high loss)
- destructive or nondestructive requirements of the measurement
- contact or noncontact requirements of a measurement
- geometry of the material under test (i.e. cylindrical fibers, sheets, etc.)
- particular piece of information that may be sought such a volume content or the dielectric properties of the host or any given inclusion

In addition to some of the references given above (dealing with dielectric property measurements) an extensive list of references are provided here which deals primarily with various aspects of dielectric property measurement [54-153].

The authors of this report have used several of these techniques to study the properties of various dielectric mixtures the recent years. One of these studies has focused on detecting the presence of curatives in carbon black rubber compounds, the other two deal with porosity determination in low permittivity and low loss dielectric mixtures (i.e. plastics or glass composites) and correlation of the reflection properties of cement paste to its compressive strength, respectively [154-155].

MICROWAVE DIAGNOSIS OF CARBON BLACK RUBBER COMPOUNDS

Dielectric properties of rubber have been investigated during microwave curing process [132,133]. The objectives of these studies have been to choose the optimum rubber composition as a function of microwave absorption (heating), and to show that microwave curing produces rubber compounds with similar properties as those produced by the standard curing process. These measurements were conducted using cavity techniques. Other investigators have reported tensor microwave dielectric constant measurement of anisotropic rubber samples as it pertains to microwave shielding [74,78].

Recently, microwave techniques have been used as diagnostic tools for investigation of chemically reacting materials (i.e. epoxy) and studying polymerization process [134,135]. These studies show the potential of

microwaves for monitoring chemical reactions associated with the forming of cross-linked molecular networks.

Very little is known about rubber dielectric properties as a function of microwave frequency. Also there is a lack of information about the behavior of rubber compound constituents (ethylene propylene diene rubbers or EPDM, oil, mineral filler, etc.) as a function of microwave frequency. Furthermore, there is very little to none reported on the influence of constituent volume fraction variation and chemical reactions among these constituents on the rubber relative dielectric constant. These types of information may lead to important practical applications such as controlling rubber mixing process and introduction of new materials with predictable properties (i.e. microwave absorbers).

In this section we discuss the results of a study of the dielectric properties of various rubber stocks as a function of microwave frequency [154]. To perform this task, first we studied the dielectric properties of rubber constituents namely: EPDM, mineral filler, oil, zinc oxide and curatives. Subsequently, the influence of carbon black volume percentage on the dielectric properties of rubber was investigated. The ability of microwaves to detect the presence of curatives in uncured rubber, and the role of frequency in this detection is presented. The impact of chemical reactions on the dielectric constant is also discussed.

MEASUREMENT PROCEDURE

There are various well established techniques available for dielectric constant measurement of materials [18]. However, we had to consider a technique that possessed the following characteristics

- be able to measure low and high loss dielectric materials such as EPDM and carbon black loaded rubber with good accuracy
- be inexpensive and simple so that it could be reproduced easily and be operated by those who are not trained in this area
- be suitable for measuring powders, fluids and bulk materials

Initially a dual arm waveguide bridge [25] and partially filled waveguide techniques were considered [157]. These were soon abandoned as the former technique requires quite a few microwave components which must posses very good frequency characteristics, and the latter technique is only suitable for sheet type materials. Finally, the well known completely filled short circuited waveguide technique was used [66,136], which was the best compromise considering the measurement

requirements. This method is based on the measurement of the complex reflection coefficient whose magnitude and phase are used to extract dielectric properties of the samples.

Fig. 1 shows the measurement apparatus that was used to measure the dielectric properties of rubber samples and their constituents. Five different waveguide set-ups operating in 3.95 - 5.85 GHz (R-48), 5.85 - 8.2 GHz (R-70), 8.2 - 12.4 GHz (R-100), 12.4 - 18 GHz (R-140), and 18 - 26.5 GHz (R-220) were used. The oscillator generates a microwave signal at the desired frequency. This signal is then fed through a precision attenuator followed by an isolator into a slotted waveguide. The standing wave characteristics inside the waveguide are measured via a detector and a sensitive voltmeter. The measurements were performed using precisely machined sample holders to accommodate samples of different thicknesses. For liquid and powdered constituents the sample holder was filled completely and a piece of clear tape was used to hold them in place.

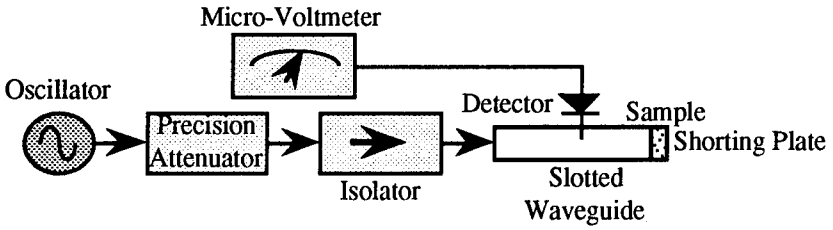

Fig. 1: Measurement apparatus for completely filled waveguide method, [154].

The relationship between the measured complex reflection coefficient, Γ, and the complex dielectric constant $\varepsilon_r = \varepsilon'_r - j\varepsilon''_r$ is given by

$$\varepsilon_r = \frac{\left(\frac{x}{kL}\right)^2 + \left(\frac{\lambda_g}{2a}\right)^2}{1 + \left(\frac{\lambda_g}{2a}\right)^2} \qquad (1)$$

where x is a solution of the following transcendental equation

$$\frac{\tan x}{x} = \frac{1-\Gamma}{jkL(1+\Gamma)} \qquad (2)$$

and k is the wavenumber inside the waveguide given by $2\pi/\lambda_g$. λ_g is the waveguide wavelength, L is the sample thickness and a is the broad dimension of the waveguide. It is known that Equation (1) has an infinite set of complex roots [136]. Thus, to find the correct root we either must have some idea of the dielectric constant value, or make two or more measurements for different sample thicknesses. Hence, not only for obtaining the correct root, but also for increased measurement confidence, Γ was measured for several samples with different thicknesses. Γ as a function of dielectric constant and sample thickness can be expressed as

$$\Gamma(\varepsilon_r, L) = \frac{\sqrt{Y} - j\tanh\left(kL\sqrt{Y}\right)}{\sqrt{Y} + j\tanh\left(kL\sqrt{Y}\right)} \qquad (3)$$

where Y is given by

$$Y = \left[1 + \left(\frac{\lambda_g}{2a}\right)^2\right]\varepsilon_r - \left(\frac{\lambda_g}{2a}\right)^2 \qquad (4)$$

From the measurements we obtained an array of values, $\Gamma(\varepsilon_r, L_n)$, where n is the number of samples with different thicknesses. The unknown dielectric constant, ε_r, is then determined by finding the best fit to Equation (3). The two measured parameters are

$$SWR = 20\log(VSWR) = 20\log\left(\frac{1+|\Gamma|}{1-|\Gamma|}\right) \qquad (5)$$

and the position of the standing wave null (which is related to the phase of Γ) in the slotted waveguide. The discrete points shown in Figs. 2 and 3 represent typical results for two rubber samples (the type of the materials used to obtain these figures will be discussed later) of various thicknesses at 5 GHz. These values were used to calculate the dielectric constant of the rubber samples using the best fit Equation (3). The lines represent the results obtained from Equation (3) using the calculated value of the dielectric constant. It is important to note that more sample thicknesses render results with higher level of confidence. Additional improvements in the measurement accuracy can be obtained by using samples whose thicknesses are around the phase transition (minimum *SWR*) as shown in Figs. 2 and 3. The position of the phase transition may be calculated either from prior approximate knowledge of the

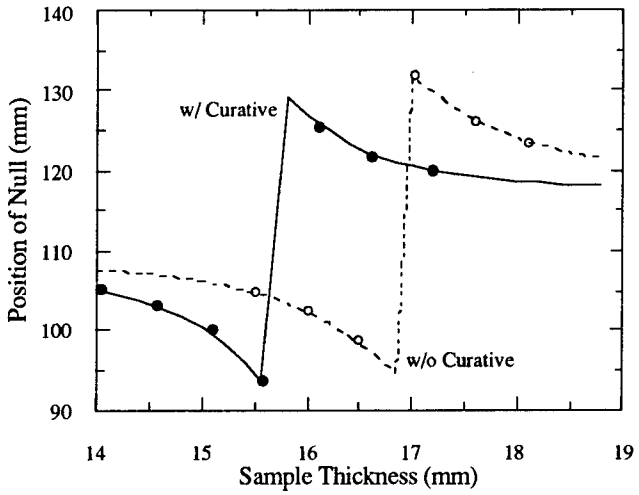

Fig. 2: Null position in the slotted waveguide as a function of sample thickness at 5 GHz. Solid and dashed lines pertain to uncured samples with and without curative, respectively, [154].

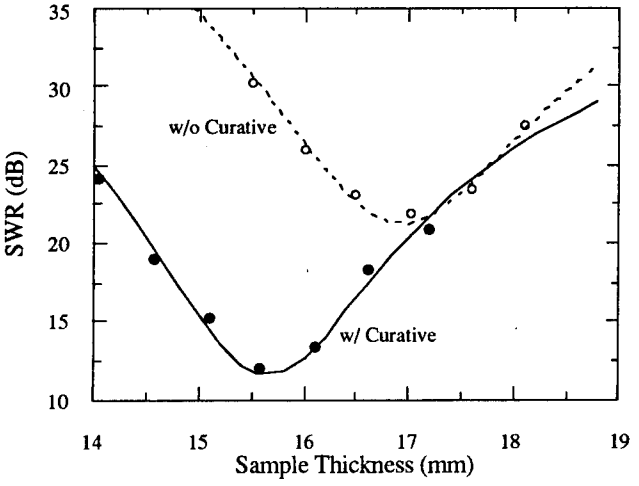

Fig. 3: The *SWR* (dB) as a function of sample thickness at 5 GHz. Solid and dashed lines pertain to uncured samples with and without curative, respectively, [154].

dielectric constant or preliminary measurement with random thicknesses.

DIELECTRIC PROPERTIES OF RUBBER COMPOUND CONSTITUENTS

To fully understand the dielectric properties of various rubber compounds, one must first have a complete knowledge of the dielectric characteristics of each individual rubber compound constituent, namely EPDM, mineral filler, zinc oxide, oil and curatives. Table I lists the volume content (by percentage) and dielectric properties of main constituents for the rubber compound which we consider our *basic* sample throughout this investigation. Due to the very high conductivity of the carbon black, its dielectric properties were not measured. This table shows the mean value of ε_r' and loss tangent ($tan\delta = \varepsilon''_r/\varepsilon'_r$) of the constituents measured at several frequencies in X-band (8.2 - 12.4 GHz), using the technique described earlier. Measurements in other frequency bands resulted in similar values of dielectric constant for these constituents. The accuracy of these measurements is relatively less (about 5% for ε_r' and 10% for $tan\delta$) compared to all other measurements of rubber compounds reported later, since only two random thicknesses of the material were used. The measurement accuracy is discussed in detail later. The results indicate that the dielectric constants of EPDM, oil and mineral filler are for all practical purposes equal. Zinc oxide and curatives have slightly higher dielectric constants but they have small volume percentages in the total composition of a typical rubber compound. Through only physical mixing (not considering any chemical reaction), the contribution of curatives to the rubber compound dielectric constant should be negligible. However, in the course of our investigations it was discovered that the chemical reaction triggered by curatives in uncured rubber samples causes a detectable change in the dielectric properties of rubber at ambient temperature. This particular issue will be discussed separately later.

CURED RUBBER DIELECTRIC CONSTANT DEPENDENCE ON CARBON BLACK

Our primary objective was to investigate the influence of carbon black volume content (%) on the dielectric properties of rubber compound. Consequently, measurements were performed on fourteen rubber samples with varying degrees of carbon black concentration. The rubber compounds were prepared by carefully measuring the ingredients in a precision laboratory scale. They were loaded in a laboratory Banbury mixer by upside down method and mixed for five minutes at maximum temperature of 130° C. Then the compounds were mixed for

another five minutes at ambient temperature in an open two-roll mill. The rubber sheets were vulcanized in molds at 150°C for a predetermined time.

Table I: Basic rubber sample constituents volume content (%) and their X-band dielectric properties, [154].

Constituent	Volume %	ε_r'	$tan\delta$
EPDM	45.50	2.1	0.008
Oil	25.85	2.2	0.014
Carbon Black	17.00		
Mineral Filler	9.30	2.3	0.017
Curatives	1.80	3.1	0.032
Zinc Oxide	0.360	3.9	0.280

The carbon blacks used for this study were aggregates of particles ranging in diameter from 5 to 125 nanometers . During the mixing process the aggregates are usually broken in smaller sizes and distributed uniformly throughout the mass. The rubber samples were prepared starting from the basic formulation given in Table I. Then, the volume percentage of carbon black was varied between 8.4% to 35.6%. This was done in such a way that any change in the amount of carbon black percentage was at the expense of EPDM, and the percentages of all other constituents were kept constant (same percentages as shown in Table I). The goal was to isolate the influence of carbon black on rubber compound dielectric constant. Table II lists the carbon black volume content for the measured rubber samples (sample #5 is the *basic* sample).

These samples were prepared in sheet forms with thicknesses of 0.5, 1, 2, 3 and 5 mm to accommodate the completely filled waveguide technique, and their dielectric constants were measured at 5, 7, 10, 16 and 24 GHz. Figs. 4 and 5 show the results of these measurements for the real part and loss tangent at 5 and 24 GHz, respectively (results for other frequencies fall in between these two extremes). The results show that the dielectric constant of rubber increases as the carbon black volume percentage increases. Clearly, dielectric constant variations are more pronounced at 5 GHz which renders this frequency (or lower) useful for dielectric constant variation measurement.

Table II: Carbon black volume % for measured samples, [154].

Sample no.	Carbon Black Volume Percentage
1	8.40
2	10.13
3	12.13
4	14.41
5 (basic)	17.00
6	18.02
7	19.07
8	20.14
9	21.23
10	22.34
11	25.29
12	28.58
13	32.05
14	35.61

It has been reported [78] that the rolling effect associated with rubber sheet production process of rubber sheets causes anisotropy. To alleviate this problem, our samples were prepared in such a way that rolling effect was minimized by performing the rolling process in many different directions. To check the success of this manipulation, we measured the dielectric constant of several samples for several arbitrarily oriented (with respect to the electric field vector in the waveguide) pieces. Two open-ended rectangular waveguide measurement techniques were used: "infinite" sample method [158] and short-circuited sample method [159]. The results indicated no systematic deviations in dielectric constant values (i.e. within the measurement errors) which shows the absence of anisotropy in our samples.

DETECTION OF CURATIVES IN UNCURED RUBBER

The presence of curatives was checked for two types of rubber, namely carbon black filled and mineral filler rubber. The goal of these experiments was to investigate the possibility of using microwaves to detect the presence (or absence) of curatives prior to product preforming stage and curing. All of the following measurements were performed at ambient temperature.

Curatives in Carbon Black Filled Rubber

Uncured version of samples #4, 5, 7, 9, 11 and 14 (referring to Table II) were prepared with and without curatives. These samples were

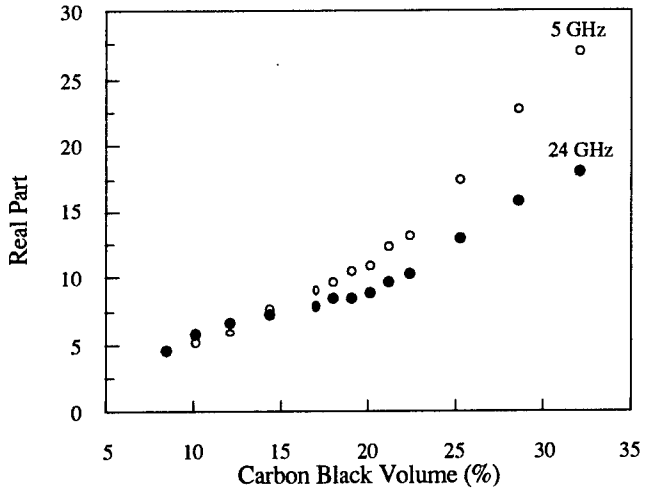

Fig. 4: ε'_r for all cured rubber compounds at 5 and 24 GHz, [154].

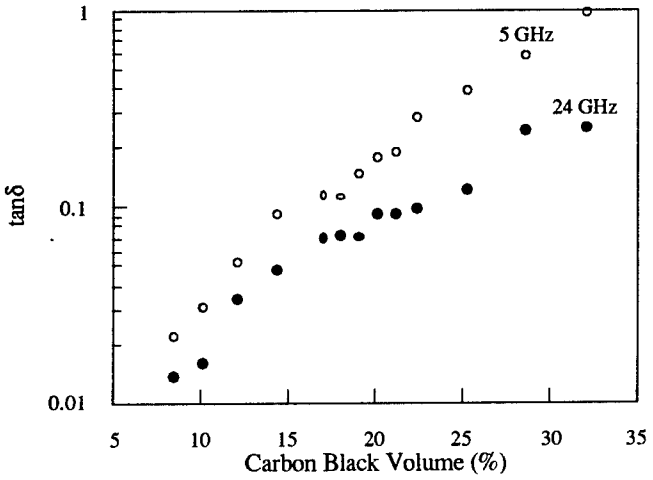

Fig. 5: $tan\delta$ for all cured rubber compounds at 5 and 24 GHz, [154].

chosen to represent the entire range of carbon black percentages used in practical applications. It was soon determined that the dielectric constant variations for these samples were most pronounced at 5 GHz (as anticipated based on the previous results). We also learned that the dielectric constant difference between these two types of rubber samples was usually small. Therefore, as already discussed, the sample thicknesses are best to be around the phase transition regions. Figs. 2 and 3 show typical results of such measurement (sample #5 at 5 GHz). It is obvious that for sample thickness between 15 mm and 16 mm a difference of more than 10 dB is measured for *SWR* values. The opposite is true for measurements between 17 mm and 18 mm. These examples illustrate the importance of choosing optimum sample thicknesses to detect this difference for a given frequency.

Figs. 6 and 7 show the real part of dielectric constant and the loss tangent of uncured samples with and without curative at 5 GHz as a function of carbon black volume percentage. From Fig. 6 it is apparent that the addition of curatives does not affect the real part of the dielectric constant in a uniform fashion for all carbon black volume percentages. However, in spite of the low losses exhibited by curatives themselves (Table I), the imaginary part of the dielectric constant of these samples tends to increase with the addition of curatives for all carbon black volume percentages. Furthermore, in the presence and absence of curatives, the difference in $tan\delta$ is consistently detected as shown in Fig. 7. The detected difference is attributed to a chemical reaction triggered by the curatives at room temperature. It is well known in the rubber industry that a rubber compound containing curatives will cross link (cure) in due time even at room temperature. The rate of curing will depend upon the type and the amount of curatives, the polymer and the carbon black. It is apparent from these measurements that the initial stage of curing can be detected. As it was discussed earlier, the difference in the dielectric properties of rubber compound in the presence of curatives can not be described by a simple physical mixing effect (curatives occupy only 1.8% of the total rubber volume with dielectric properties close to those of EPDM). Another observation is that after the carbon black percentage increases beyond 25%, the difference between the samples with and without curatives becomes smaller. It may be hypothesized that at these carbon black percentages the effect of the chemical reaction caused by the presence of the curatives is masked by the overwhelming presence of unlinked carbon black.

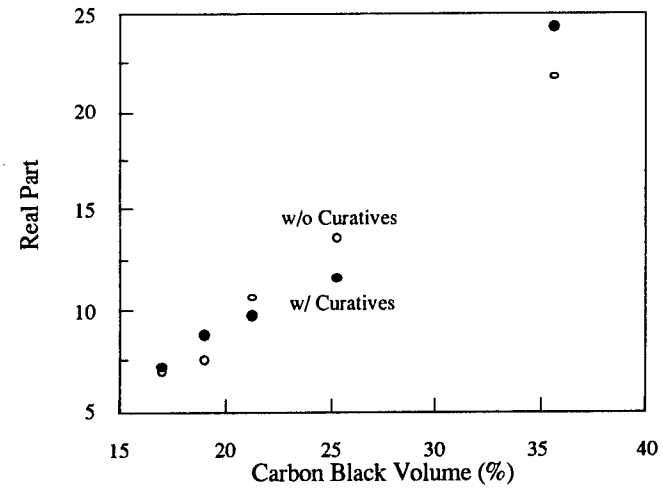

Fig. 6: ε'_r for uncured rubber compounds with and without curatives at 5 GHz, [154].

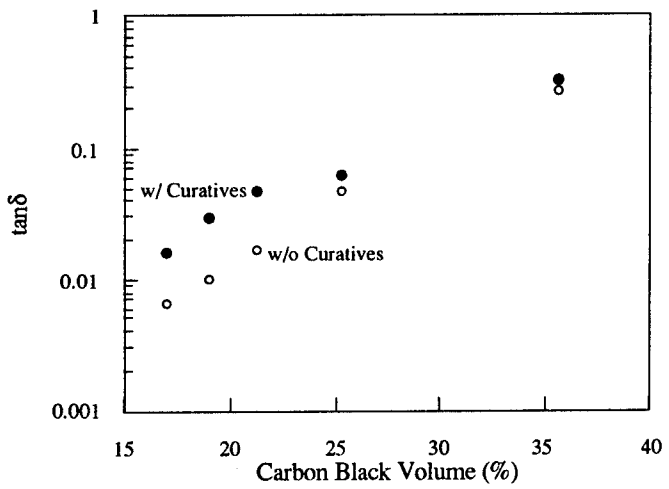

Fig. 7: $tan\delta$ for uncured rubber compounds with and without curatives at 5 GHz, [154].

Relationship Among EPDM, Carbon Black and Curatives

The measurements performed thus far involved a constant percentage of curatives while the ratio of carbon black to EPDM was changed. This may not reflect the composition of a real rubber product. Subsequently, having noticed the effect of curatives on dielectric constant, a new sample (named sample #15) was prepared. The dielectric properties of this sample when cured and not cured (with and without curatives) were then measured. Based on the cured results it was predicted that the carbon black content was close to that of sample #11 (25%). The measured dielectric properties of both samples are listed in Table III. However, a glance at the uncured compound compositions, listed in Table IV, indicates that samples #15 and #11 are not similar which may suggest the following. It is apparent that the volume percentage of carbon black in sample #15 is higher than that in sample #11. This is confirmed only if we focus on the dielectric constant of the uncured samples. Then, if the uncured dielectric constant values for sample #15 and Figs. 6 and 7 are used, we may closely predict the carbon black percentage.

Table III: Measured dielectric properties of rubber samples #15 and #11 for cured and uncured with and without curatives, [154].

	Sample #15		Sample #11	
	ε'_r	$tan\delta$	ε'_r	$tan\delta$
Cured	18.8	0.400	17.4	0.385
Uncured without	17.6	0.099	13.6	0.046
Uncured with	16.0	0.056	11.6	0.062

Table IV: Constituent formulation of samples #15 and #11, [154].

Constituent	#15 Volume %	#11 Volume %
EPDM	22	34.84
Carbon Black	33.8	25.3
Oil	32.4	27.5
Mineral Filler	7.53	9.85
Curatives	0.85	1.91
Zinc Oxide	0.29	0.28

Thus, for the samples without curatives only a physical mixing process may be considered. However, once cured, the chemical reaction will have changed the properties of the rubber sample and hence its dielectric properties.

The volume percentages of EPDM and curatives are considerably higher in sample #11 than in sample #15. Therefore, we may hypothesize that similarity of the dielectric constants of the cured samples is due to the fact that the lack of carbon black in sample #11 is compensated by the increased reaction involving EPDM. What was not expected is the importance of this reaction (cross-linking) which in this case is compensating for the influence of carbon black on the dielectric constant. There still remains a question regarding the reduction in uncured with and without curatives loss tangent in the opposite directions between sample #15 and sample #11. Obviously, here we encounter some phenomenon which decreases the losses, and may be due to formation of cross-linked molecular network in such a way that dipoles rotate less freely [134]. Most likely there are two opposite mechanisms influencing the dielectric constant of uncured material when curatives are added depending on the carbon black, EPDM and curatives volume percentages. Clearly, further studies are needed to fully understand the impact of these mechanisms on dielectric constant.

Effect of Curatives in Mineral Filled Rubber

Similar measurements were also performed on uncured samples with and without curatives in which carbon black was replaced by mineral filler. As expected, this sample exhibits different dielectric properties than its carbon black counterpart. The results for this measurement are presented in Table V. From this table one may conclude that for such a low-loss rubber, the presence of curatives is difficult to be detected. The difference between the two samples is comparable with the accuracy we report in the next paragraph. However, we believe that this difference may still be detected if samples with optimum thicknesses are used. For thicknesses just after the second phase transition (between 29 mm and 32 mm) at 5 GHz a repeatable difference of about 3 dB in the value of *SWR* was detected. This difference will be more pronounced for thicknesses after the third phase transition. This part of the study confirms that the effect of curatives on carbon black loaded rubber dielectric constant may not be limited to a chemical interaction involving EPDM (cross linking), but carbon also plays a significant role in this chemical process.

Table V: Dielectric properties of uncured mineral filled rubber with and without curatives, [154].

Uncured Sample	ε'_r	$tan\delta$
w/o Curatives	3.00	0.0090
with Curatives	2.91	0.0107

MEASUREMENT ACCURACY

The accuracy of the measurement technique used in this study is well established. However, our accuracy and sensitivity have been improved by measuring multiple sample thicknesses around the phase transition region and direct fitting of the measurement results to obtain the dielectric constant. We believe this was the reason for the consistent ability to detect curatives in uncured rubber samples particularly for low-loss materials.

The measurement technique reported here consisted of determining two parameters (*SWR* and relative null position) for various sample thicknesses. The accuracy of these measurements is increased if we use a rotary-vane attenuator and a precision slotted line. For high *SWR* cases we used the following correction factor

$$SWR_c = -20\log(10^{\frac{-SWR}{20}} - 10^{\frac{-SWR_o}{20}}) \qquad (dB) \qquad (6)$$

where SWR_c is the corrected value of the parameter shown in Equation (5). *SWR* in *dB*, is the measured value, and SWR_o in *dB*, is the value for the short circuited waveguide. The use of this correction factor is justified because a lossless waveguide and perfect short circuit termination were assumed. Equation (6) shows that there is a limitation in the measurement of low-loss materials (*SWR* approximately equal to SWR_o). However, the use of thicker samples of low-loss materials can reduce this problem.

Specific precautions must be considered for low and high-loss materials. For low-loss materials the real part of the dielectric constant may be precisely obtained from the multiple thickness null location information, but the imaginary part may not be deduced with reasonable accuracy. Thus, for this case the *SWR* measurement is very important as this is the sole indication of losses. For high-loss materials a different problem exists. The null location curve quickly degenerates to a line with certain slope as a function of sample thickness. This is why

the precise value of dielectric constant can not be extracted from the null location measurements alone. In this case the *SWR* measurement plays a crucial role as well. Thus, for high-loss materials, measurements should be performed close to the first *SWR* minimum, because beyond that the *SWR* oscillates negligibly as a function of sample thickness.

It is difficult to estimate our measurement accuracy directly, because we do not use a straightforward approach in determining the dielectric constant of each sample (see Equation (3)). However, from the repeatability of our results, especially when detecting small changes in losses due to the presence of curatives, it is clear that the accuracy is better than the usually accepted for a waveguide method [137,160]. A numerical approach was used to estimate our apparatus measurement error. The following sources of error were considered: uncertainties due to the resolution error of the rotary-vane attenuator (±0.25 dB), the position of the standing-wave minimum (±0.05 mm), and the thickness of the sample (±0.1 mm). The error due to the frequency instability was neglected as a very stable oscillator was used. The analysis consisted of the following steps. The uncertainty associated to measured quantities for all sample thickness was added (or subtracted). Then dielectric constant, and subsequently the percentage difference for the real part and the loss tangent were calculated. Finally, the maximum error (worst case) for a given measurement was chosen. This procedure was performed for all the measurements reported in previous section. The results in all cases was less than 1% for the real part of dielectric constant and less than 3.5% for the loss tangent. This accuracy is worse if measurement points are not in the vicinity of the phase transition.

CARBON BLACK RUBBER DIELECTRIC MIXING MODEL

It was also intended to develop a dielectric mixing model for cured carbon black loaded rubber based on the measured results depicted in Figs. 6 and 7 without considering the influence of any chemical reaction. The intention was to show that a simple model can be developed to predict carbon black percentage in a cured rubber sample. Clearly, for accurate prediction one must eventually bring into this model the influence of the curatives and EPDM percentages as well. There are various types of dielectric mixing models available. A two phase mixing model considers a dielectric medium (rubber) as a combination of a host medium (EPDM) and an inclusion (carbon black). Multi-phase dielectric mixing models allow for more than one type of inclusion in the host medium. These models are usually for heterogeneous media in which the dielectric constants of the constituents are not very different. In the present case carbon black has very high conductivity and hence a high dielectric constant. Knowing that the

dielectric properties of all rubber constituents are similar, we modeled rubber as a two-phase dielectric medium with EPDM as the host medium and carbon black as the inclusion.

Upon the conclusion of this study a semi-empirical dielectric mixing formula which showed to be well suited for cured carbon black loaded rubber was developed similar to mixing models for soil moisture. Equation (7) expresses the relationship between rubber compound mixture dielectric constant, ε_m, dielectric constants of EPDM, ε_h, and carbon black, ε_c ,and their volume fractions.

$$\varepsilon_m(x,y,z,V) = z\left[V^y \varepsilon_c^x + (1-V)\varepsilon_h^x\right]^{\frac{1}{x}} \qquad (7)$$

where

V is the volume fraction of carbon black,
x, y, z are unknown coefficients.

The unknown coefficients x, y and z are calculated by setting Equation (7) equal to the measured value of dielectric constant of rubber compound with different carbon black contents. Figs. 8 and 9 show the results of Equation (7) and the measured real and imaginary parts of rubber compound dielectric constant for all carbon black volume fractions at 5 GHz. The good agreement between the model and the measurement results indicates that the properties of the cured rubber may be predicted using comparatively simple mixing model. Upon extracting more data about chemical reaction this model may be improved and generalized.

POROSITY DETERMINATION IN POLYMERS

Determining porosity level (or the amount of air content) in cured polymers, ceramics and composite materials is an important practical issue. In cured polymers, the presence of porosity causes lowered mechanical performance due to stress concentrations. Localized porosity can be particularly damaging to the joint strength of adhesively bonded components. In ceramics, the relative density is an important processing parameter, and again the ceramic is extremely sensitive to stress concentration (lowered density). If not fully densified, a ceramic is weak and has low stiffness. In composites, the porosity can be within the matrix material which will affect the performance in a similar fashion to those in bulk materials. However, porosity often concentrates at specific locations in composite materials (either between plies or at the fiber/matrix interface), and can dramatically lower flexural and shear performance. Increases in porosity during operation (material

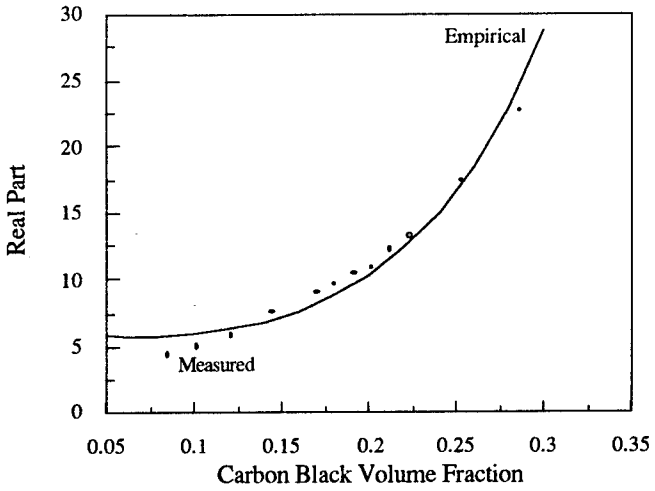

Fig. 8: Real part of the dielectric constant of rubber as a function of carbon black volume percentage; empirical and measured results at 5 GHz.

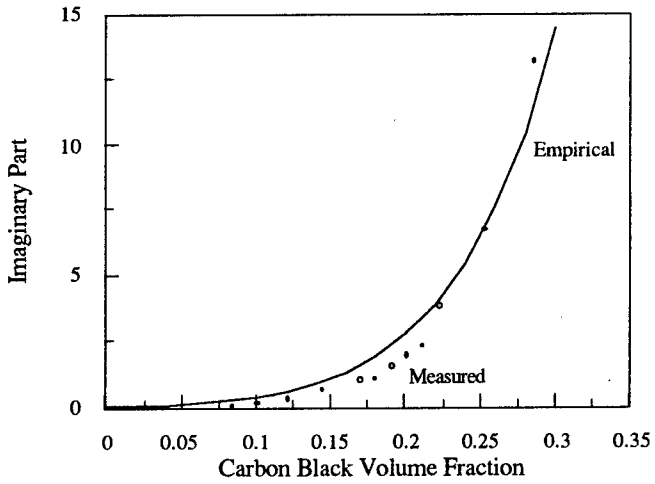

Fig. 9: Imaginary part of the dielectric constant of rubber as a function of carbon black volume percentage; empirical and measured results at 5 GHz.

under loading) may precede macroscopic damage and possibly indicate the presence of delamination. Hence, a nondestructive inspection (NDI) technique capable of detecting and accurately determining porosity level in materials is desirable.

Microwave NDI techniques are well suited for inspecting polymers and ceramics. This is partially due to the fact that microwaves easily penetrate inside dielectric material and the reflected or transmitted signal can be related to the dielectric properties of the material, and subsequently to its physical and mechanical characteristics [154,156].

In this section we demonstrate the potential of microwaves for porosity determination in low permittivity and low loss composites samples. We used a similar technique to that discussed in the previous sections (Fig. 1) to determine the dielectric properties of these composite samples [155].

SAMPLE PREPARATION AND MEASUREMENT PROCEDURE

Samples of polymer microballoon-filled epoxy resin with 0%, 48.9%, 58.7% and 68.5% air volume fractions were carefully prepared. The uniformly distributed air-filled microballoon sizes ranged, in diameter, between 15 to 200 micrometers with a bulk density of 0.009 gm/cm^3. These microballoons created the porosity levels in these samples. The samples were shaped to fit inside rectangular waveguides covering frequencies of 8.2, 10, 12, 14, 16 and 18 GHz. The goal of these measurements is to study the sensitivity of microwaves to small changes in porosity level (as it relates to changes in dielectric properties).

Fig. 1 shows the apparatus used to measure the dielectric properties of the porous samples. Two different waveguide set-ups were utilized, operating in 8.2 - 12.4 GHz (R-100) and 12.4 - 18 GHz (R-140) bands. Dielectric measurements were conducted at the frequencies of 8.2, 10, 12, 14, 16 and 18 GHz. Table VI and VII show the results of the permittivity and loss factor for these samples. The results show little variation of ε'_r and ε''_r as a function of frequency, which is expected since these samples have low permittivities and loss factors. However, there is a clear distinction among different air volume contents. ε'_r and ε''_r for the 0% porosity samples indicate the dielectric properties of the basic sample (i.e. not porous). The difference in porosity level of about 10% among the other three samples causes a nearly linear change in the values of ε'_r and ε''_r. However, one must be careful not to generalize this trend for composites with different dielectric properties than those used here. For example, in ceramics with higher permittivities (ε'_r = 6-

10) one would expect a larger change in the dielectric properties for linear changes in porosity levels.

Table VI: ε'_r results fro 0%, 48.9%, 58.7% and 68.5% air content in polymer microballoon-filled epoxy, [155].

	0%	48.9%	58.7%	68.5%
8.2 GHz	2.80	1.87	1.69	1.48
10	2.87	1.84	1.63	1.46
12	2.83	1.88	1.70	1.47
14	2.87	1.83	1.70	1.50
16	2.84	1.82	1.68	1.47
18	2.84	1.84	1.67	1.47

Table VII: ε''_r results fro 0%, 48.9%, 58.7% and 68.5% air content in polymer microballoon-filled epoxy, [155].

	0%	48.9%	58.7%	68.5%
8.2 GHz	0.086	0.032	0.020	0.013
10	0.086	0.034	0.023	0.015
12	0.082	0.033	0.022	0.014
14	0.083	0.033	0.027	0.022
16	0.077	0.026	0.021	0.019
18	0.068	0.027	0.025	0.014

Using our measurements at 10 GHz, one percent change in porosity level translates to 1.1% change in ε'_r and 3% change in ε''_r, respectively. This means that if we can measure the permittivity and the loss factor within these percentages, then it is possible to detect 1% change in porosity for this dielectric material. As already mentioned, there are several nondestructive microwave techniques for dielectric properties monitoring, and each technique has its own specific range of measurement accuracy (yielding different sensitivity to porosity variation). The following section discusses the accuracy associated with our technique which is then used to determine the percentage of porosity variation that is possible to detect.

The measurement accuracy was calculated using the same procedure used for rubber for the measured dielectric properties at 10 and 16 GHz. The results for these two frequencies showed the measurement accuracy to be less than 1.2% for the permittivity and less than 5% for the loss

factor. Thus, using the change in the dielectric constant as an indicator of porosity level change, it is possible to determine porosity changes of slightly more than 1% (when using ε'_r) and about 2% (when using ε''_r). Since there is little variation in ε'_r and ε''_r as a function of frequency, we assume the same measurement accuracy for the other frequencies.

AIR-FILLED POLYMER MIXING MODEL

Since the polymer microballoons and the epoxy resin have very similar dielectric properties, these samples were considered to be made of only two constituents, air and polymer (a two-phase mixture). The air inclusions are in the form of microballoons, hence they are considered to be spherical in shape. For these reasons, the following well known two-phase spherical mixing model was used to predict the dielectric properties as a function of porosity level or air volume fraction [1].

$$\varepsilon_m = \varepsilon_h + 3V_i\varepsilon_m\left(\frac{\varepsilon_i - \varepsilon_h}{\varepsilon_i + 2\varepsilon_m}\right) \qquad (8)$$

where ε_m, ε_i and ε_h are the dielectric constants of the composite mixture, inclusion (air), and the host medium (the dielectric properties of the sample with 0% porosity), respectively. V_i is the volume fraction of the air inclusion (porosity).

Figs. 10 and 11 show the real and imaginary parts of the model (solid line), along with the measured values (diamonds) at frequency of 10 GHz. The agreement between the results of this two-phase dielectric mixing model and the measurements is good (other frequencies rendered similar results). Thus, it is possible to either predict the dielectric properties of this composite as a function of porosity level, or more importantly by measuring the dielectric properties of a sample one is able to determine the level of porosity in it.

MICROWAVE CHARACTERIZATION OF CEMENT PASTE

A nondestructive, real-time, reliable and inexpensive technique for the in-situ evaluation of compressive strength of existing concrete structures would be very beneficial to the construction industry. Until recently, the in-place strength of concrete members was found by drilling a core and testing it in a laboratory. This destructive technique takes several days and is relatively expensive. Some nondestructive techniques have been developed for detecting the strength of concrete. These include: pulse velocity method, surface hardness, penetration, pullout, breakoff and maturity techniques [161]. Some of these techniques are not truly

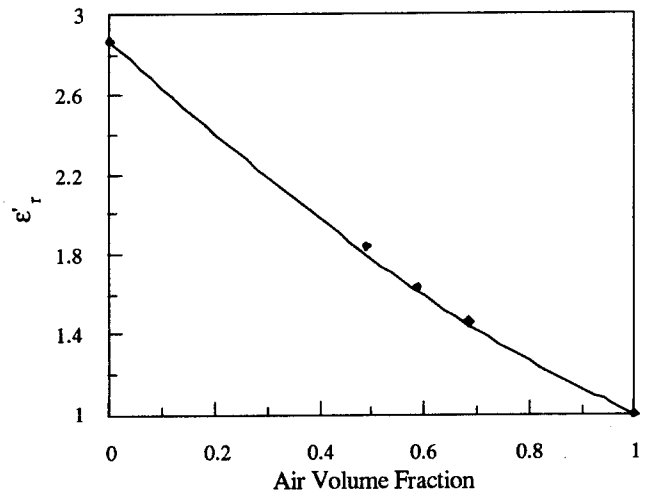

Fig. 10: Empirical and measured results of ε'_r as a function of air volume fraction, [155].

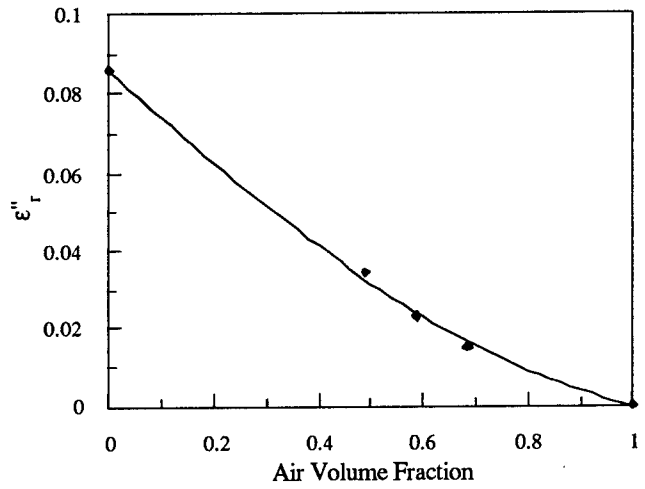

Fig. 11: Empirical and measured results of ε''_r as a function of air volume fraction, [155].

nondestructive since they cause some damage to the concrete. The use of these methods is limited because the accuracy and reliability of their results are not well established.

The authors have previously investigated the nondestructive use of microwaves for interrogating common construction materials. Zoughi et al., used a simple microwave nondestructive technique, to detect the location of reinforcing steel in a concrete slab [162]. They showed the ability to manipulate the polarization properties of microwaves to enhance the rebar image. In that experiment they also detected the presence of a separation in the steel bar. Their experiments also showed the sensitivity of microwaves to various aggregate size distributions. Subsequently, Zoughi et al., showed the potential of microwaves for detecting aggregate size distribution by manipulating the frequency of a microwave signal [163]. They also showed a possible correlation between the magnitude of the reflection coefficient of the microwave signal and concrete water/cement (w/c) ratio. Other investigators have also attempted to study the curing process in concrete using microwaves [164].

Concrete compressive strength, f'_c, is strongly dependent on the w/c ratio [165,166]. If microwaves demonstrate the ability to estimate w/c ratio in a concrete specimen, their use can be a basis for a direct or an indirect approach to measure its compressive strength nondestructively.The following sections discuss the results of an extensive set of experiments on several cement paste blocks with different w/c ratios. The primary goal of these experiments was to establish a correlation between microwave reflection properties of these blocks and their w/c ratios, and subsequently to their compressive strengths.

APPROACH

The dielectric properties of a material are dependent on the physical as well as the chemical composition of the material including the effects of chemical processes such as curing. To establish a relation between the dielectric constant and curing, an extensive study of the characteristics of ε_r at various microwave frequencies for several cement paste blocks with different w/c ratios was conducted to see whether an indication of concrete strength is possible.

Four cement paste blocks with dimensions of 15 cm x 15 cm x 15 cm were prepared with w/c ratios of 0.31, 0.40, 0.50 and 0.60, respectively using ASTM type II cement [156]. These blocks were moist cured for three days and the remaining curing occurred in air at room temperature with approximate relative humidity of less than 25%.

The dielectric properties of each block was measured daily, for 27 days (time period for concrete design strength to be reached) at frequencies of 5, 9, 13 and 17 GHz. Each dielectric measurement reported here is an average of four measurements conduced on four sides of each block. These measurements were also conduced at day 39 to see if further curing had occurred. The density of these blocks were also measured periodically, to see whether the results of the testing was an indication of density change rather than an indication of curing (compressive strength) [156]. The dielectric measurements were conducted using an open-ended rectangular slotted waveguide radiating into the cement paste sample. Fig. 12 shows the experimental setup. The sweep oscillator produces the microwave signal which is fed into the slotted waveguide via a calibrated attenuator. The crystal detector output voltage, measured with a voltmeter, is proportional to the properties of the standing wave inside the waveguide. These properties were compared to those of a short circuited waveguide, yielding the dielectric properties of the sample [158].

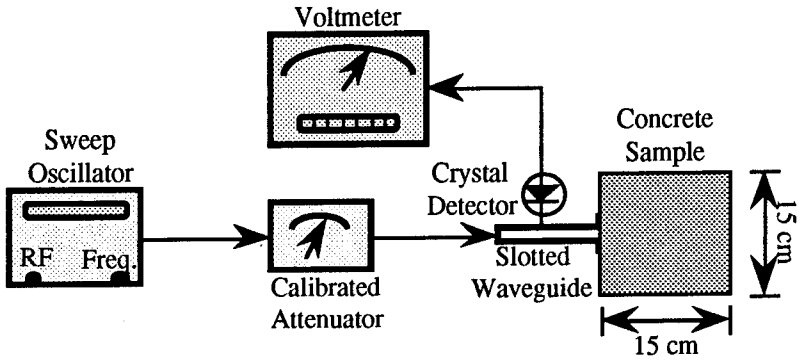

Fig. 12: The experimental apparatus, [156].

RESULTS

For brevity, only the results of daily measurements of ε'_r and ε''_r for the four blocks at 5 GHz are presented here as shown in Figs. 13 and 14. The results at other frequencies follow similar trends as those of 5 GHz. The results indicate a rapid decrease in the value of ε'_r and ε''_r during the first five days particularly for the higher w/c ratios. This is attributed to the bleeding and subsequent evaporation of the free water from the surface of the cement paste blocks. Beyond the fifth day, ε'_r and ε''_r for the 0.31 w/c ratio sample remained consistently higher than ε'_r and ε''_r for 0.60 w/c ratio. After the fifth day most of the free water in the air dried samples is bound [167]. This would indicate that any

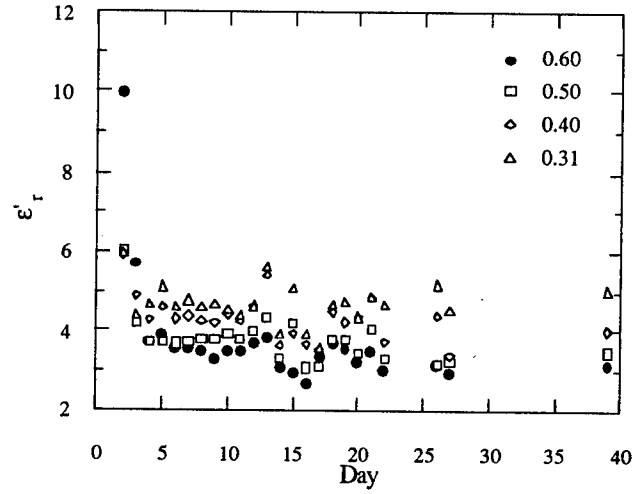

Fig. 13: Permittivity variation at 5 GHz, [156].

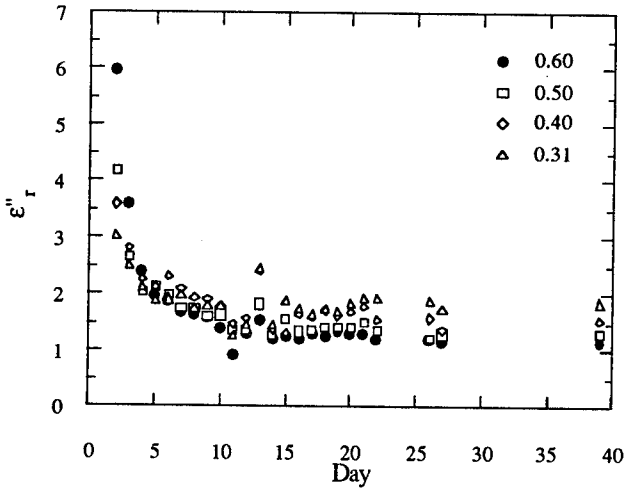

Fig. 14: Loss factor variation at 5 GHz, [156].

measurements of water taken after day five are an indication of hydration, and thus, strength.

After day seventeen, one can clearly observe a trend of increasing ε'_r and ε''_r as a function of decreasing w/c ratio. ε'_r and ε''_r for a mixture consisting of a relatively low dielectric constituent (cement) and a high dielectric constituent (water) are expected to increase as a function of increasing water content. This expectation is valid under the assumption that only physical mixing is present (before the hydration process begins), as is the behavior for the first few days. However, the results shown in Figs. 13 and 14, after day 5 do not indicate this. They indicate the presence of curing (a chemical reaction, hydration) in the cement paste samples. Curing seems to increase ε'_r and ε''_r, which has been noticed in carbon black rubber mixtures as well.

The measurement accuracies for ε'_r and ε''_r, using the approach followed here, are approximately 5% and 10%, respectively. Tables VIII-X show the dielectric properties of the cement paste samples, averaged over the last four days the measurements were made, as a function of w/c ratio at frequencies of 9, 13 and 17 GHz, respectively. These results indicate the potential of using dielectric constant measurements as an indication of w/c ratio in a concrete structure.

Table VIII: Dielectric properties of samples at 9 GHz, [156].

w/c Ratio	ε'_r	ε''_r
0.31	4.54	0.5
0.40	4.22	0.59
0.50	3.71	0.48
0.60	3.51	0.40

Table IX: Dielectric properties of samples at 13 GHz, [156].

w/c Ratio	ε'_r	ε''_r
0.31	4.89	0.38
0.40	4.28	0.35
0.50	3.73	0.26
0.60	3.54	0.16

Table X: Dielectric properties of samples at 17 GHz, [156].

w/c Ratio	ε'_r	ε''_r
0.31	7.11	0.78
0.40	6.22	0.31
0.50	5.74	0.47
0.60	5.44	0.48

In microwave measurements, it is common to measure the reflection coefficient associated with a medium. Unlike the dielectric constant measurement, the measurement of the magnitude of the reflection coefficient does not require any phase measurement. Therefore, it is a much simpler type of measurement and one that is of interest here. The reflection coefficient, Γ, is the ratio of the reflected wave from a medium to the incident wave. Subsequently, the variation of the magnitude of reflection coefficient, $|\Gamma|$, as a function of time for all samples and for all frequencies were studied. The behavior of ϕ was not monitored since it does not provide any useful information for these tests. Fig. 15 shows the variation of $|\Gamma|$ at 9 GHz (other frequencies follow a similar trend). Similar to the case of ε'_r and ε''_r, $|\Gamma|$ decreases as w/c ratio increases. The reflection coefficient of the cement paste blocks (average of the last four measurements) are listed in Table XI for all w/c ratios and frequencies.

Table XI: $|\Gamma|$ of samples for various w/c ratios and frequencies, [156].

Frequency	w/c ratio			
(GHz)	0.31	0.40	0.50	0.60
5	0.53	0.49	0.45	0.40
9	0.52	0.50	0.48	0.47
13	0.53	0.51	0.48	0.48
17	0.51	0.48	0.47	0.46

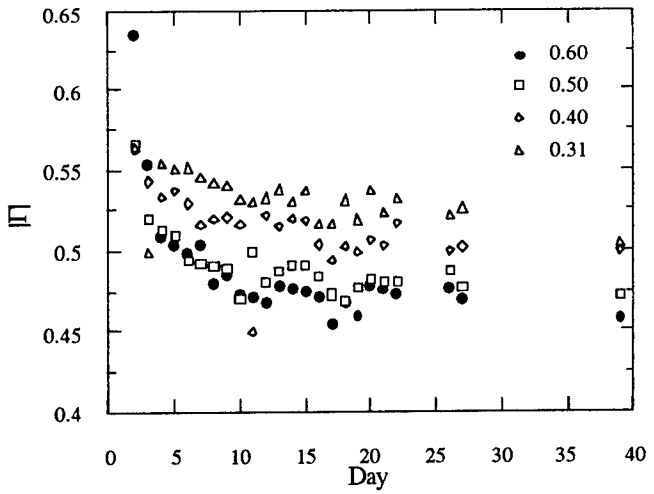

Fig. 15: Variation of $|\Gamma|$ at 9 GHz, [156].

COMPRESSIVE STRENGTH ESTIMATION

Compressive strength of cured concrete is known to be directly related to its w/c ratio (165,166). The compressive strengths of the samples were measured on the fortieth day using a Forney Hydraulic 300 kip cylinder testing machine. The blocks in this experiment were rectangular and moist cured only for three days. There is a loss of strength to approximately 75% to 80% for specimens that are moist cured for three days compared to those that are continuously moist cured. On the other hand, rectangular test specimens have an increase in strength to 125% when compared to strength of cylindrical test specimens.

The results from Table XI were used, for each frequency, to calculate the percentage change (increase) in $|\Gamma|$ for w/c ratios of 0.50, 0.40 and 0.31 with respect to $|\Gamma|$ obtained for w/c ratio of 0.60, namely

$$\Delta|\Gamma(f)| = \frac{\left\| \Gamma_{0.6}(f) \right| - \left| \Gamma_{w/c}(f) \right\|}{\left| \Gamma_{0.6}(f) \right|} \times 100 \qquad (8)$$

where f is the frequency in GHz ($f \in \{5, 9, 13, 17\}$). Fig. 16 illustrates the results of Equation (8) in which the solid lines are a

logarithmic fit to each respective data set (correlation coefficient R > 0.995) and are given by

$$\Delta|\Gamma(f)| = 32.78 - 19.16\log(f) \quad for \quad w/c = 0.31 \qquad (9)$$

$$\Delta|\Gamma(f)| = 24.55 - 16.50\log(f) \quad for \quad w/c = 0.40 \qquad (10)$$

$$\Delta|\Gamma(f)| = 10.88 - 9.21\log(f) \quad for \quad w/c = 0.50 \qquad (11)$$

Subsequently, $\Delta\Gamma(\%)$ for each sample was calculated for 5 and 9 GHz with respect to Γ for the sample with w/c ratio equal to 0.60, namely

$$\Delta|\Gamma(w/c)| = \frac{\left\|\Gamma_f(0.6)\right| - \left|\Gamma_f(w/c)\right\|}{\left|\Gamma_f(0.6)\right|} \times 100 \qquad (12)$$

Again a logarithmic fit was applied to the data and the following equations were obtained (R > 0.995, for both equations)

$$\Delta|\Gamma(w/c)| = -16.93 - 74.48\log(w/c) \quad f = 5GHz \qquad (13)$$

$$\Delta|\Gamma(w/c)| = -11.07 - 47.49\log(w/c) \quad f = 9GHz \qquad (14)$$

Fig. 16 shows, once again, the ability of lower microwave frequencies to better estimate w/c ratios in cement paste members. Furthermore, Equations (13) and/or (14) may be used to determine w/c ratio given D|Γ|, which can easily be measured. The coefficients in the above equations may be determined more precisely provided additional data for intermediate w/c ratio values are available. Consequently, in a similar fashion a relationship between the change in compressive strength, $\Delta f'_c$, as a function of $\Delta|\Gamma|$ (which is a measurable) is found [156]. These results are shown in Fig. 17. Therefore, one may conclude that compressive strength may be *directly* estimated using a set of curves, similar to those shown in Fig. 17, at various frequencies. The above results indicate a good degree of correlation between $\Delta|\Gamma|$ and $\Delta f'_c$.

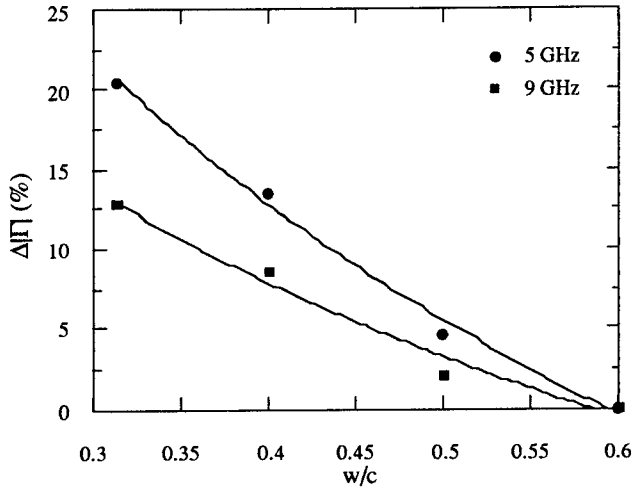

Fig. 16: Percentage change in $|\Gamma|$ vs. w/c ratio for 5 and 9 GHz, [156].

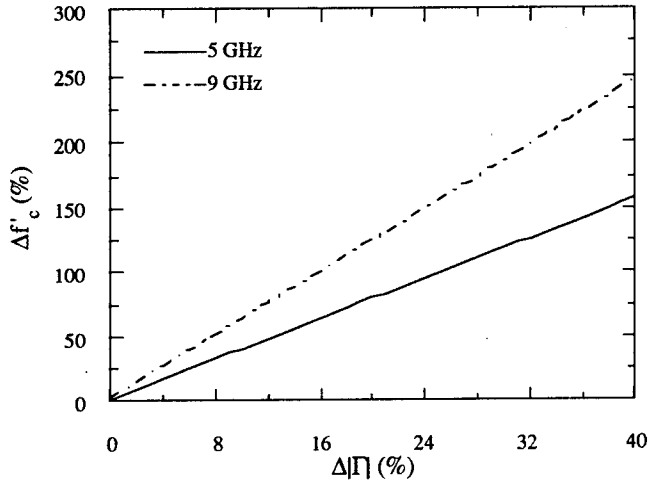

Fig. 17: Percentage change in the measured compressive strength vs. percentage change in $|\Gamma|$, [156].

SUMMARY

Microwave dielectric characterization is a powerful approach for inspecting material properties of various media and mixtures. The results of these inspections can be used to determine the contribution of a constituent to a mixture, curing state and even a correlation to some mechanical properties. There are a variety of measurement techniques that may be utilized to determine the dielectric properties of liquids, powders, solids, gases, etc. Some of these techniques are suitable for on-line measurements as well.

To summarize this chapter, a completely filled waveguide approach was used to conduct extensive dielectric constant measurement of rubber compounds. The measurement apparatus was comparatively simple, inexpensive and may be put together for a large range of frequency bands. Moreover, this technique offered very good repeatability and measurement accuracy characteristics particularly after some refinements of the measurement procedure. Subsequently, the dielectric constant of individual rubber compound constituents, namely EPDM, oil, mineral filler, zinc oxide and curatives were measured. The results showed that all of these constituents have similar dielectric properties.

The dielectric constants of many rubber compounds with different carbon black volume percentages were measured at 5, 7, 10, 16 and 24 GHz. These samples were carefully prepared such that an increase in carbon black volume percentage was compensated by a reduction in the volume percentage of EPDM, while the volume percentage of all other constituents were kept constant. The results showed that the real and imaginary parts of rubber dielectric constant increase as a function of increasing carbon black percentage. An empirical dielectric mixing model was also developed with which the carbon black volume percentage could be predicted.

The influence of curatives in uncured rubber compounds with different carbon black volume percentages was also investigated. The goal was to establish whether the presence of curatives which is very small in volume content causes any detectable changes in the dielectric constant of the rubber compounds. The results of measurements showed that the presence of curatives can be detected. The sensitivity of detection increases with decreasing frequency.

The results of an extensive study of the potential of microwaves for detecting changes in porosity were also presented. Using the completely filled short circuited waveguide technique several specially prepared samples with different levels of air-filled microballoon inclusions are investigated. This multi length measurement procedure

results in estimated measurement accuracy of 1.2% (for ε'_r) and less than 5% (for ε''_r) which translates to detectable porosity changes of around 2%. The good agreement between the two-phase spherical mixing model and the measurement results allows for accurate prediction of porosity level in a sample from its measured dielectric properties. The knowledge of the dielectric properties may be utilized for optimization of other microwave nondestructive techniques used in particular industrial applications.

Microwave dielectric properties of four cement paste samples with w/c ratios of 0.31, 0.40, 0.50 and 0.60 were measured daily for 27 days (also at the the 39th day) at frequencies of 5, 9, 13 and 17 GHz. The results of these measurements were used to calculate the microwave reflection properties of these samples. The results showed the presence of curing (a chemical reaction involving hydration) in the samples. This curing increased the dielectric properties of the samples inversely as a function of increasing w/c ratio. Normally, in a physical mixing process, where no chemical reaction occurs, higher water content results in higher dielectric properties. This finding demonstrates the sensitivity of microwaves to curing (hydration), and to possibly the potential to monitor the curing state in concrete structures.

Results of lower frequency measurements were found to be more sensitive to changes in the reflection coefficient. It was shown that a swept microwave frequency technique may be used to estimate w/c ratio using $\Delta\Gamma$, and then *indirectly* estimate cement paste compressive strength using standard tables for compressive strength. Additionally it was shown that the change in the reflection coefficient is related to the w/c ratio. From this a correlation in the change in reflection coefficient to change in compressive strength was obtained. This provides for a *direct* and *in situ* microwave nondestructive estimation of compressive strength of an unknown cement paste sample.

These preliminary results are encouraging for the use of microwaves as a practical nondestructive tool for cement paste compressive strength estimation using relatively simple and inexpensive equipment. The extension of this work for nondestructively estimating concrete compressive strength is also encouraging and requires additional work.

REFERENCES

[1] Ulaby, F.T, R. K. Moore and A.K. Fung, "Microwave Remote Sensing, Passive and Active," Vol. III, Appendix E, Artech House, Dedham, MA, 1986.

[2] Kline, L.A., and C.T. Swift, "An Improved Model for the Dielectric Constant of Sea Water at Microwave Frequencies," IEEE Trans. on Antennas and Propagation, vol. AP-25, pp. 104-111, 1977.

[3] Stogryn, A., "Equations for Calculating the Dielectric Constant of Saline Water," IEEE Trans. on Microwave Theory and Tech., vol. MTT-19, pp. 733-736, 1971.

[4] Hasted, J.B., "Liquid Water: Dielectric Properties, Ch. 7 in Water-A Comprehensive Treatise," (F. Franks, ed.), vol. I, The Physics and Chemistry of Water, Plenum Press, New York, 1972.

[5] Auty, R., and R. Cole, "Dielectric Properties of Ice and Solid D_2O," J. Chem. Phys., vol. 20, pp. 1309-1314, 1952.

[6] Cumming, W., "The dielectric Properties of Ice and Snow at 3.2 cm," J. Appl. Phys., vol. 23, pp. 768-773, 1952.

[7] Korneenko, I.A., "Mean Values of the Parameters in Inhomogenous Media," Soviet Phys.-Tech. Soc.., vol. 5, p. 40, 1978.

[8] Taylor, L.S., "Dielectric Properties of Mixtures," IEEE Trans. on Antennas and Propagation, vol. AP-13, pp. 943-947, 1965.

[9] Taylor, L.S., "Dielectric Loaded with Anisotropic Materials," IEEE Trans. on Antennas and Propagation, vol. AP-14, pp. 669-670, 1966.

[10] Haste, J.B., "Aqueous Dielectrics," Chapman and Hall, London, 1973.

[11] Tinga, W.R., W.A.G. Voss and D.F. Blossey, "Generalized Approach to Multiphase Dielectric Mixture Theory," J. Appl. Phys., vol. 44, pp. 3897-3902, 1973.

[12] de Loor, G.P., "Dielectric Prperties of Heterogenous Mixtures Contating Water," J. Microwave Power, vol. 3, pp. 67-73, 1968.

[13] Bottcher, C.J.F., "Theory of Electric Polarization," Elsevier, Amsterdam, 1952.

[14] van Beek, L.K.H., "Dielectric Behavior of Heterogenous Systems," Ch. 7, in Progress in Dielectrics, (J. Birks, ed.) Heywood Books, London, 1967.

[15] von Hippel, A.R., "Dielectrics and Waves," John Wiley and Sons, New York, NY, 1954.

[16] Landau, L.D., and E.M. Lifshitz, "Electrodynamics of Continuous Media," Pergamon, Oxford, 1975.

[17] Polder, D., and J.H. Van Santen, "The Effective Pearmiability of Mixtures of Solids," Phisica, vol. 12, p. 257, 1946.

[18] Bussey, H.E., "Measurement of RF Properties Materials: A Survey," Proc. IEEE, vol. 55, pp. 1046-1053, 1967.

[19] Campbell, C.K., "Free-Space Permittivity Measurements on Dielectric Materials at Millimeter Wavelengths," IEEE Trans. on Inst. and Meas., vol. IM-27, pp. 54-58, 1978.

[20] Cihlar, J., and F.T. Ulaby, "Dielectric Properties of Soils as a Function of Moisture Content," RSL Tech. Rep. 177-47, Remote Sensing Lab., The University of Kansas, Lawrence, KS, 66045, 1974.

[21] Frankenstein, G., and R. Garner, "Equations for Detremining the Brine Volume of Sea Ice from -0.5°C to 22.9°C," J. Glaciol., vol. 6, pp. 943-947, 1967.

[22] Geiger, F.E., and D. Williams, "Dielectric Constants of Soils at Microwave Frequencies," NASA TMS-65987, Washington, D.C., 1972.

[23] Gloersen, P., and J.K. Larabee, "An Optical Model for the Microwave Properties of Sea Ice," NASA TM-83865, Goddard Space Flight Center, Greenbelt, MD, 1981.

[24] Hallikainen, M., F.T. Ulaby and M. Abdelrazik, "Modeling of Dielectric of Wet Snow in the 4-18 GHz Range," IEEE Int. Geosci. Remote Sensing Symp. (IGARSS'83) Digest, San Francisco, CA, 31 Aug.-2 Sept., 1983.

[25] Hallikainen, M., F.T. Ulaby, M.C. Dobson, M. El-Rayes and L.K. Wu, "Microwave Dielectric Behavior of Wet Soil - Part I: Empirical Models and Experimental Observations," IEEE Trans. on Geosci. and Remote Sensing, vol. GE-23, pp. 25-34, 1985.

[26] Hipp, J.E., "Soil Electromagnetic Parameters as a Function of Frequency, Soil Density and Moisture," Proc. IEEE, vol.62, pp. 98-103, 1974.

[27] Jones, R.G., "Precise Dielectric Measurements at 35 GHz Using an Open Microwave Resonator," Proc. IEE, vol. 123, pp. 285-290, London, 1976.

[28] Kraszewski, A., "A Model of the Dielectric Prperties of Wheat at 9.4 GHz," J. Microwave Power, vol. 13, pp. 293,296, 1978.

[29] Lane, J., and J. Saxton, "Dielectric Dispersion in Pure Polar Liquids at Very High Radio Frequencies, III. The Effect of Electrolytes in Solutions," Proc. Roy. Soc., vol. 214A, pp. 531-545, 1952.

[30] Nelson, S.O., "Microwave Dielectric Properties of Insects and Grain Kernels," J. Microwave Power, vol. 11, pp. 299-303, 1976.

[31] Nicolson, A.M., and G.F. Ross, "Measurement of the Intrinsic Properties of Materials by Time-Domain Techniques," IEEE Trans. on Inst. and Meas., vol. IM-19, pp. 377-382, 1970.

[32] Rayleigh, Lord (J.W. Strutt), "On the Influence of Obstacles Arranged in Rectangular Order on the Properties of a Medium," Phil. Mag., vol. 34, pp. 482-502, 1892.

[33] Saxton, J., "Dielectric Dispersion in Pure Polar Liquids at Very High Radio Frequenies, II, Relation of Experimental Results to Theory," Proc. Roy. Soc., vol. 213A, pp. 473-492, 1952.

[34] Shutko, A.M., and E.M. Reutov, "Mixture Formulas Applied in Estimation of Dielectric and Radiative Characteristics of Soils and Grounds at Microwave Frequencies," IEEE Trans. on Geosci. and Remote Sensing, vol. GE-20, pp. 29-32, 1982.

[35] Stuchly, M.A., and S.S. Stuchly, "Coaxial Line Reflection Method for Measuring Dielectric Properties of Biological Substances at Radio and Microwave Frequencies - A Review," IEEE Trans. on Inst. and Meas., vol. IM-29, pp. 176-183, 1980.

[36] Tan, H.S., "Microwave Measurements and Modelling of the Permeability of Tropical Vegetation Samples," Appl. Phys., vol. 25, pp. 351-355, 1981.

[37] von Hippel, A.R., "Dielectric Materials and Applications," MIT Press, Cambridge, MA, 1954.

[38] Wabg, J.R., and T.J. Schmugge, "An Empirical Model for the Compex Dielectric Permittivity of Soils as a Function of Water Content," IEEE Trans. on Geosci. and Remote Sensing, vol. GE-18, pp. 288-295, 1980.

[39] Tinga, W.R., "Fundamentals of Microwave-Material Interactions and Sintering," Materials Research Society Symposium Proceedings, vol. 124, pp. 33-43, Symposium Microwave Processing of Materials, Apr. 5-8, Reno, Nevada, 1998.

[40] Varadan, V.K., Y. Ma, A. Lakhtakia and V.V. Varadan, "Microwave Sintering of Ceramics," Materials Research Society Symposium Proceedings, vol. 124, pp. 45-57, Symposium Microwave Processing of Materials, Apr. 5-8, Reno, Nevada, 1988.

[41] Nelson, S.O.,"Estimating the Permittivity of Solids from Measurements on Granular or Pulverized Materials" Materials Research Society Symposium Proceedings, vol. 124, pp. 149-54, Symposium Microwave Processing of Materials, Apr. 5-8, Reno, Nevada, 1988.

[42] Shou Ho, Y., and J.J. Kramer, "Microwave Dielectric Properties of Metal Filled Particulate Composites," Materials Research Society Symposium Proceedings, vol. 124, pp. 161-66, Symposium Microwave Processing of Materials, Apr. 5-8, Reno, Nevada, 1988.

[43] Bruce, R.W., and M.W. McCurdy, "Dielectric Measurements of Particulate Organic Polymers," Materials Research Society Symposium Proceedings, vol. 124, pp. 167-72, Symposium Microwave Processing of Materials, Apr. 5-8, Reno, Nevada, 1988.

[44] Bruce, R.W., and R.A. Quarles, "Measurement of the Absorption of Microwave Power by Corroded Metals," Materials Research Society Symposium Proceedings, vol. 124, pp. 173-178, Symposium Microwave Processing of Materials, Apr. 5-8, Reno, Nevada, 1988.

[45] Edgar, R.H., "Advanced Microwave Technology," Materials Research Society Symposium Proceedings, vol. 124, pp. 379-91, Symposium Microwave Processing of Materials, Apr. 5-8, Reno, Nevada, 1988.

[46] Sutton, W.H., "Microwave Processing of Materials (editorial)," MRS (Materials Research Society) Bulletin, pp. 22-4, Nov. 1993.

[47] Iskander, M.F., "Computer Modelling and Numerical Simulation of Microwave Heating Systems," MRS (Materials Research Society) Bulletin, pp. 30-6, Nov. 1993.

[48] Lewis, D.A., and J.M. Shaw, "Recent Developments in the Microwave Developing of Polymers," MRS (Materials Research Society) Bulletin, pp. 37-40, Nov. 1993.

[49] Clarck, D.E., D.C. Folz, R.L. Schulz, Z. Fathi and A.A. Cozzi, "Recent Developments in the Microwave Processing of Ceramics," MRS (Materials Research Society) Bulletin, pp. 41-46, Nov. 1993.

[50] Silberglitt, R., I. Ahmad, W.M. Black and J.D. Katz, "Recent Developments in Microwave Joining," MRS (Materials Research Society) Bulletin, pp. 47-50, Nov. 1993.

[51] Willert-Porada, M., "Microwave Processing of Metalorganics to form Powders, Compacts, and Functional Gradient Materials," MRS (Materials Research Society) Bulletin, pp. 51-7, Nov. 1993.

[52] Paton, B.E., V.E. Sklyarevich and M.G. Slusarczuk, "Gyrotron Processing of Materials," MRS (Materials Research Society) Bulletin, pp. 58-63, Nov. 1993.

[53] Binner, J.G.P., "Applications of Microwaves in the Sintering of Ceramics," Colloquium on Industrial Uses of Microwaves, London, (IEE Coloquium Digest), 1990.

[54] Nelson, S.O., C.W. Schlaphoff and L.E.Stetson, "A Computer Program for Short-Circuited Waveguide Dielectric-Properties Measurements on High- or Low-Loss Materials", Journal of Microwave Power, v8(1), pp. 14-22, 1973.

[55] Nelson, S.O., C.W. Schlaphoff and L.E.Stetson, "Computation of Dielectric-Properties from Short-Circuited Waveguide Measurements of High- or Low-Loss Materials"(Computer Program Description), IEEE Trans. on Microwave Theory Tech., vol. MTT-21, no. 3, pp. 342-343, March 1974.

[56] Risman, P.O., and Th. Ohlsson, Brief communication: "Dielectric Constants for High Loss Materials a Comment on Earlier Measurements", Journal of Microwave Power, 8(2), pp.186-188, 1973.

[57] Tinga, W.R., and S.O.Nelson, "Dielectric Properties of Materials for Microwave Processing-Tabulated," Jour. of Microwave Power, 8(1), pp. 23-63, 1973.

[58] Misra, D.K., "Permittivity Measurement of Modified Infinite Samples by a Directional Coupler and a Sliding Load," IEEE Trans. on Microwave Theory Tech., vol. MTT-29, no. 1, pp. 65-67, Jan. 1981.

[59] Walter Barry, "A Broad-Band, Automated, Stripline Technique for the Simultaneous Measurement of Complex Permittivity and Permeability," IEEE Trans. on Microwave Theory Tech., vol. MTT-34, no. 1, pp. 80-84, Jan. 1986.

[60] Li, S., C.Akyel, and R.G.Bosisio, "Precise Calculations and Measurements on the Complex Dielectric Constant of Lossy Materials Using TM-010 Cavity Perturbation Techniques," IEEE Trans. on Microwave Theory Tech., vol. MTT-29, no. 10, pp. 1041-1046, Oct. 1981.

[61] Lynch, A.C., "Precise Measurements on Dielectric and Magnetic Materials," IEEE Trans. on Instrum. Meas., vol. IM-23, no. 4, pp. 425-443, Dec. 1974.

[62] Bahl, I.J., and S.S.Stuchly, "Analysis of a Microstrip Covered with a Lossy Dielectric," IEEE Trans. on Microwave Theory Tech., vol. MTT-28, no. 21, pp. 104-109, Feb. 1980.

[63] Yanshend, X., "A Simple and Effective Method for Waveguides Loaded with Lossy Dielectrics or Magnetic Materials," Microwave and Optical Technology Letters, vol. 1, no. 3, pp. 93-95, May 1988.

[64] Sharpe, C.B., "Graphical Method for Measuring Dielectric Constants at Microwave Frequencies," IRE Transactions on Microwave Theory and Tech., vol.MTT-8, pp. 155-159, March 1960.

[65] Rzepecka, M.A., and M.A.K. Hamid, "Extension of Digital Automatic Method for Measuring the Permittivity of Thin Dielectric Films," IEEE Trans. on Microwave Theory and Tech., pp. 628-631, Sept. 1972.

[66] Roberts, S., and A. von Hippel, "A New Method for Measuring Dielectric Constant and Loss in the Range of Centimeter Waves," J. Appl. Phys., pp. 610-16, July, 1946.

[67] Dakin, T.W., and C.N.Works, "Microwave Dielectric Measurements," J. Appl. Phys., pp. 789-96, Sept. 1947.

[68] Bell, R.O., and G.Rupprecht "Measurement of Small Dielectric Losses in Material with a Large Dielectric Constant at Microwave Frequencies," IRE Trans. on Microwave Theory Tech., vol. MTT-9, pp. 239-242, May 1961.

[69] Arcone, S. A., and R.W. Larson, "Single-Horn Reflectometry In Situ Dielectric Measurements at Microwave Frequencies" IEEE Transactions on Geoscience and Remote Sensing, pp. 89-92, Jan. 1988.

[70] Azzeer, A.M., Leo M. Silber, Ian L. Spain, C. Patton and H.A. Goldberg, "Applicability of the Microwave Cavity Perturbation Method for Conductivity Measurements on Carbon Fibers," J. Appl. Phys., vol.57, no. 7, pp. 2529-2531, Apr. 1985.

[71] Itoh, T., "A New Method for Measuring Properties of Dielectric Materials Using a Microstrip Cavity," IEEE Trans. on Microwave Theory Tech., vol. MTT-22, pp. 572-576, May 1974.

[72] Nikolic, P.M., L.D.Zivanov and O.S.Aleksic, "Dielectric Properties of Strontium Hexaferrite in Microwave, Infrared and Far Infrared Ranges," Diel. Mat. Meas. and Appl., IEE: Conf. Publ. no. 289, pp. 332-35, June 1988.

[73] Krupka, J., "An Accurate Method for Permittivity and Loss Tangent Measurements of Low Dielectric Using TE-01 Dielectric Resonators," Diel. Mat. Meas. and Appl., IEE: Conf. Publ. no. 289, pp. 322-25, 27-30 June 1988.

[74] Sardos, R., J.-F. Escarment and E. Christorhe, "Anisotropic Measurement of Rubber Sheets with an X-Band Three-Wave Interferometer," IEEE Trans. on Microwave Theory Tech., vol. MTT-38, no. 3, pp. 330-33, March 1990.

[75] Gardiol, F.E., "Nomograms Save Time in Determining Permittivity," Microwaves, pp. 68-70, Nov. 1973.

[76] Musal, H.M., and D.C. Smith, "Universal Design Chart for Specular Absorbers," IEEE Trans. on Magnetics, vol. MAG-26, no. 5,pp.1462-1464, Sept. 1990.

[76] Rose, G.C., R.J. Churchill and K.R. Cook, "Determination of Complex Dielectric Constant of High-Loss Materials," IEEE Trans. on Instrum. Meas., vol. IM-21, pp. 286-287, Aug. 1972.

[77] Weir, W.B., "Automatic Measurement of Complex Dielectric Constant and Permeability at Microwave Frequencies," Proc. IEEE, vol. 62, no. 1, pp. 33-36, Jan. 1974.

[78] Hashimoto, O., and Y. Shimizu, "Reflecting Characteristics of Anisotropic Rubber Sheets and Measurement of Complex Permittivity Tensor," IEEE Trans. on Microwave Theory Tech., vol. MTT-34, no. 11, pp. 1202-1207, Nov. 1986.

[79] Chan, and B. Chambers, "Open Resonator Permittivity Measurement of Curved Dielectric Samples," Diel. Mat. Meas. and Appl., pp. 336-339, June 1988.

[80] Itoh, T., "A New Method for Measuring of Dielectric Materials Using a Microstrip Cavity," IEEE Trans. on Microwave Theory Tech., vol. MTT-22, pp. 572-576, May 1974.

[81] Ghodgaonkar, D.K., V.V.Varadan and V.K.Varadan, "A Free-Space Method for Measurement of Dielectric Constants and Loss Tangents at Microwave Frequencies," IEEE Trans. on Instrum. Meas., vol. IM-37, no. 3, pp. 789-793, June 1989.

[82] Rueggeberg, W., "Determination of Complex Permittivity of Arbitrarily Dimensioned Dielectric Modules at Microwave Frequencies," IEEE Trans. on Microwave Theory Tech., vol. MTT-19, no. 6, pp. 517-521, June 1971.

[83] Campbell, C.K., "Rapid Measurement of Dielectric Substrate Permittivity at X-band," IEEE Trans. on Instr. Meas., vol. IM-24, pp. 82-83, March 1975.

[84] Bussey, H.E., "Measurement of RF Properties of Materials a Survey," Proc. IEEE, vol-55, no. 6, pp. 1046-1053, June 1967.

[85] Nelson, S. O., LaVerne Stetson and C.W. Schlaphoff, "A General Computer Program for Precise Calculation of Dielectric Properties from Short-Circuited-Waveguide Measurements," IEEE Trans. on Instr. Meas., vol. IM-23, no. 4, pp. 455-460, Dec. 1974.

[86] Afsar, M.N., and G.W.Chantry, "Precise Dielectric Measurements of Low-Loss Materials at Millimeter and Submillimeter Wavelengths," IEEE Trans. on Microwave Theory Tech., vol. MTT-25, no. 6, pp. 509-511, June 1977.

[87] Rzepecka, M.A., and M.A.K. Hamid, "Modified Perturbation Method for Permittivity Measurements at Microwave Frequencies," J. of Microwave Power, vol. 9, no. 4, pp. 317-328, 1974.

[88] Rzepecka, M., "Permittivity Measurement," J. of Microwave Power, vol. 8, no. 1, pp. 3-11, 1973.

[89] Watkins, J., and D. Brown, "Calculation of the Complex Permittivity of Lossy Dielectric Materials Using the Roberts - von Hippel Standing-Wave Method," Elect. Let., vol. 5, no. 11, pp. 243-244, 1969.

[90] Naishadham, K., and P. Kadaba, "Measurement of the Microwave Conductivity of Polymeric Material with Potential Applications in Absorbers and Shielding," IEEE Trans. on Microwave Theory Tech., vol. 39, no. 7, pp. 1158-1164, July 1991.

[91] Hipp, J.E., "Soil Electromagnetic Parameters as Functions of Frequency, Soil Density, and Soil Moisture," Proc. IEEE, vol. 62, no. 1, pp. 98-103, Jan. 1974.

[92] Lynch, A.C., and S. Ayeres, "Measurement of Small Dielectric Loss at Microwave frequencies," Proc. IEE, vol. 119, no. 6, pp. 767-770, June 1972.

[93] Birchak, J., C. Gardner, J. Hipp and J. Victor, "High Dielectric Constant Microwave Probes for Sensing Soil Moisture," Proc. IEEE, vol. 62, no. 1, pp. 93-98, Jan. 1974.

[94] Khan, S., S. Yong, N. Maode, W. Zihua and X. De-Ming, "Dielectric Constant Measurement of High Loss Materials by Using Automatic Six-Port Reflectometer at W-band," Proc. of 3rd Int. Symp. Recent Advances in Microwave Technology (ISRAMT '91), pp. 149-152, Reno, Nevada, Aug. 18-21, 1991.

[95] Kent, G., "Nondestructive Measurements of Substrate Permittivity," Proc. of 3rd Int. Symp. Recent Advances in Microwave Technology (ISRAMT '91), pp. 153-156, Reno, Nevada, Aug. 18-21, 1991.

[96] Pournaropoulos, C., and D. Misra, "An Integral Equation Procedure for Electrical Characterization of Materials Using a Coaxial Microwave Sensor," Proc. of 3rd Int. Symp. Recent Advances in Microwave Technology (ISRAMT '91), pp. 157-, Reno, Nevada, Aug. 18-21, 1991.

[97] Kent, G., "A Dielectrometer for Measurement of Substrate Permittivity," Microwave Jour., pp. 72-82, Dec. 1991.

[98] Sequeira, H.B., "Extracting ε and μ of Materials from Vector Reflection Measurements," Microwave Jour., pp. 73-84, March 1991.

[99] Maze, G., J. Bonnefoy and M. Kamarey, "Microwave Measurement of the Dielectric Constant Using Sliding Short-Circuited Waveguide Method," Microwave Jour., pp. 77-88, Oct. 1990.

[100] Yansheng, X., "A Simple and Effective Method for Waveguides Loaded with Lossy Dielectrics of Magnetic Materials," Microwave and Optical Technology Letters, vol. 1, no. 3, pp. 93-95, May 1988.

[101] Riedel, C. H., M.B. Steer, M.R. Kay, J.S. Kasten, M.S. Basel and R. Pomerleau, "Dielectric Characterization of Printed Circuit Board Substrates," IEEE Trans. on Inst. Meas., vol. 39, pp. 437-440, Apr. 1990.

[102] Mattar, K., and M. Brodwin, "A Variable Frequency Method for Wide-Band Microwave Material Characterization," IEEE Trans. on Inst. Meas., vol. 39, pp. 609-614, Aug. 1990.

[103] Fidanboylu, K., S. Riad and A. Elshabini-Riad, "A New Time-Domain Approach for Determining the Complex Permittivity Using Stripline Geometry," IEEE Trans. on Inst. Meas., vol. 39, pp. 940-944, Dec 1990.

[104] Boifot, A.M., "Dielectric Measurements by Utilizing the Curvature of Pulses," IEEE Trans. on Inst. Meas., vol. 40, pp. 611-617, June 1991.

[105] Buckmaster, H.A., C.H. Hansen and T.H. van Kalleveen, "Design Optimization of a High Precision Microwave Complex Permittivity Instrumentation System for Use with High Loss Liquids," IEEE Trans. on Inst. Meas., vol. 39, pp. 964-968, Dec. 1990.

[106] Voss, W.A., and W.R. Tinga, "Materials Evaluation and Measurement Techniques," Chapter 5.1.19 in Microwave Power Engineering, (Okress, ed.), Academic Press.

[107] Nelson, S., A. Kraszewski and T. You, "Solid and Particulate Material Permittivity Relationships," J. Microwave Power and Electromagnetic Energy, vol. 26, no. 1, pp. 45-51, 1991.

[108] Risman, P., "Terminology and Notation of Microwave Power and Electromagnetic Energy," J. Microwave Power and Electromagnetic Energy, vol. 26, no. 4, pp. 243-250, 1991.

[109] Campbell, C.K., "Free-Space Permittivity Measurements on Dielectric Materials at Millimeter Wavelengths," IEEE Trans. on Inst. Meas., vol. IM-27, pp. 54-58, March 1978.

[110] Nicolson, A.M., and G.F. Ross, "Measurement of the Intrinsic Properties of Materials by Time-Domain Techniques," IEEE Trans. on Inst. Meas., vol. IM-19, pp. 377-382, Nov 1970.

[111] Moore, R.L, A. MacDonald and H. Ross Moroz, "Permittivity of Fiber-Polymer Composites: A Study to Determine the Effects of the Environment," Microwave Jour., pp. 67-82, Feb. 1991.

[112] Risman, P.O., and T. Ohlsson, Brief Communication: "Dielectric Constants for High Loss Materials, a Comment of Earlier Measurements," J. Microwave Power, vol. 8, no. 2, pp. 185-188, 1973.

[113] Li, S., C. Akyel, and R. Bosisio, "Precise Calculations and Measurements on the Complex Dielectric Constant of Lossy Materials Using TM_{010} Cavity Perturbation Techniques," IEEE Trans. on Microwave Theory Tech., vol. MTT-29, no. 10, pp. 1041-1048, Oct. 1981.

[114] Afsar, M.N., J.B. Birch, R.N. Clarke and G.W. Chantry, "The Measurements of the Properties of the Materials," Proc. IEEE, vol. 74, no. 1, pp. 183-199, Jan.1986.

[115] Afsar, M.N., et al., "A Comparison of Dielectric Measurement Methods for Liquids in the Frequency Range 1 GHz to 4 GHz," IEEE Trans. on Inst. Meas., vol. IM-29, pp. 283-288, Dec. 1980.

[116] Ayers, S., D. Marr and A.E. Parker, "Measurement of Dielectric Loss and Wall Loss in a Dielectric Filled Waveguides," IEEE Trans. on Inst. Meas., vol. IM-23, pp. 431-434, Dec. 1974.

[117] Ghodgaonkar, D. K., V.V.Varadan and V.K.Varadan, "Free-Space Measurement of Complex Permittivity and Complex Permeability at Microwave Frequencies," IEEE Trans. on Inst. Meas., vol. 39, no. 2, pp. 387-394, Apr. 1990.

[118] Varadan, V.V., R.D. Hollinger, D. K. Ghodgaonkar and V.K.Varadan, "Free-Space, Broadband Measurements of High-Temperature, Complex Dielectric Properties at Microwave Frequencies," IEEE Trans. on Inst. Meas., vol. 40, no. 5, pp. 842-846, Oct. 1991.

[119] Collet, E., "Digital Spectrometry Measurement of Dielectric Constants at Millimeter Frequencies," Microwave Jour., pp. 307-312, May 1986.

[120] Sun, J.-S., and C.-C. Wei, "Iterative Method Provides Accurate Resonator Analysis," Microwaves & RF, Dec. 1991.

[121] Paris, D.T., "An Extension of the TE_{01n} Resonator Method of Making Measurements on Solid Dielectrics," IEEE Trans. on Microwave Theory Tech., vol. MTT-12, no. 3, pp. 251-252, March 1964.

[122] Curtis, W.L., and R.J. Coe, "A Microwave Technique for the Measurement of the Dielectric Properties of Soils," IEEE Trans. on Microwave Theory Tech., vol. MTT-11, no. 5, pp. 211-212, May 1963.

[123] Nozaki, R., and T.K. Bose, "Broadband Complex Permittivity Measurements by Time-Domain Spectroscopy," IEEE Trans. on Inst. Meas., vol. 39, no. 6, pp. 945-951, Dec. 1990.

[124] Gelinas, S., V.N. Tran and R. Vaillantcourt, "Global Iterative Solution of Dielectric Spectroscopy Equations," IEEE Trans. on Inst. Meas., vol. 39, no. 4, pp. 615-620, Aug. 1990.

[125] Sequeira, H.B., "Extracting μ_r and ε_r of Solids from One-Port Phasor Network Analyzer Measurements," IEEE Trans. on Inst. Meas., vol. 39, no. 4, pp. 621-627, Aug. 1990.

[126] Magid, M., "Precision Determination of the Dielectric Properties of Nonmagnetic High-Loss Microwave Materials," IEEE Trans. on Inst. Meas., vol. IM-17, no. 4, pp. 291-298, Dec. 1968.

[127] Chudobiak, W., B.A. Syrett and H.M. Hafez, "Recent Advances in Broad-Band VHF and UHF Transmission Line Methods for Moisture Content and Dielectric Constant Measurement," IEEE Trans. on Inst. Meas., vol. IM-28, no. 4, pp. 284-289, Dec. 1979.

[128] Chudobiak, W., M.R. Beshir and J.S. Wight, "An Open Transmission Line UHF CW Phase Technique for Thickness/Dielectric Constant Measurement," IEEE Trans. on Inst. Meas., vol. IM-28, no. 1, pp. 18-25, March 1979.

[129] Scott, W.R., "A New Technique for Measuring the Constitutive Parameters of Planar Materials," IEEE Trans. on Inst. Meas., vol. 41, no. 5, pp. 639-645, Oct. 1992.

[130] Baker-Jarvis, J., R.G. Geyer and P.D. Domich, "A Nonlinear Least-Squares Solution with Causality Constraints Applied to Transmission Line Permittivity and Permeability Determination," IEEE Trans. on Inst. Meas., vol. 41, no. 5, pp. 646-652, Oct. 1992.

[131] Dudeck, K.E., and L.J. Buckley, "Dielectric Material Measurement of Thin Samples at Millimeter Wavelengths," IEEE Trans. on Inst. Meas., vol. 41, no. 5, pp. 723-725, Oct. 1992.

[132] Terselius, B., and B. Randby, "Cavity Perturbation Measurements of the Dielectric Properties of Vulcanizing Rubber and Polyethylene Compounds," J. Microwave Power, vol. 13, pp. 327-335, 1978.

[133] Schwarz, H.F., R.G. Bosisio, M.R. Wertheimer, and D. Couderc, "Microwave Curing of Synthetic Rubbers," J. Microwave Power, vol. 8, pp. 303-322, 1973.

[134] Jow, J., M.C. Hawley, M. Finzel, J. Asmussen, H.-H. Lin, and B. Manring, "Microwave Processing and Diagnosis of Chemically Reacting Materials in a Single-Mode Cavity Applicator," IEEE Trans. on Microwave Theory Tech., vol. MTT-35, no. 12, pp. 1435-1443, Dec. 1987.

[135] Martinelli, M., P.A. Rolla and E. Tombari, "A Method for Dynamic Dielectric Measurements at Microwave Frequencies: Application to Polarization Process Studies," IEEE Trans. on Inst. Meas., vol. IM-34, no. 3, pp. 723-725, Oct. 1992.

[136] Altschuler, H.M., "Dielectric Constant," ch. 9 in Handbook of Microwave Measurements, vol. II. (M. Sucher and J. Fox, eds.), Brookline, N.Y.: Polytechnic Press, 1963.

[137] Chao, S.H., "An Uncertainty Analysis for the Measurements of Microwave Conductivity and Dielectric Constant by the Short-Circuited Line Method," IEEE Trans. on Inst. Meas., vol. IM-35, no. 1, pp. 36-41, March 1986.

[138] Gao, J., "Effects of the Cavity Walls on Perturbation Measurements," IEEE Trans. on Inst. Meas., vol. 40, no. 3, pp. 618-622, June 1991.

[139] Berman,. M., and P.I. Somlo, "Efficient Procedures for Fitting Circles and Ellipses with Application to Sliding Termination Measurements," IEEE Trans. on Inst. Meas., vol. IM-35, no. 1, pp. 31-35, March 1986.

[140] Mathew, K.T., and U. Raveendranat, "Waveguide Cavity Perturbation Method for Measuring Complex Permittivity of Water," Microwave and Optical Technology Letters, vol. 6, pp. 104-106, Feb. 1993.

[141] Akyel, C., and R. Bosisio, "New Developments on Automated-Active Circuits for Permittivity Measurements at Microwave Frequencies," IEEE Trans. on Inst. Meas., vol. IM-38, no. 2, pp. 496-504, Apr 1989.

[142] Margineda, J., M. Rojo, J. Munoz and A. Hernandez, "Eliminating the Ambiguity of in Nonperturbation Microwave Measurenets of Permittivity," IEEE Trans. on Inst. Meas., vol. IM-38, no. 5, pp. 1010-1012, Oct. 1989.

[143] Weil, C.M., and W.A. Kissik, "The Electromagnetic Properties of Matrials Program at NIST," IEEE Instrumentation and Measurement Technology Conference, pp. 626-630, Atlanta, GA. May. 14-16, 1991.

[144] Janezic, M.D., and J.H. Grosvenor, "Improved Technique for Measuring Permittivity of Thin Dielectrics with a Cylindrical Resonant Cavity," IEEE Instrumentation and Measurement Technology Conference, pp. 580-584, Atlanta, GA. May. 14-16, 1991.

[145] Villamezet, J.F., M. Chatard-Moulin, P. Guilon and H. Jallageas, "Non Destructive Complex Permittivity Measurements of Absorbing Materials," IEEE Instrumentation and Measurement Technology Conference, pp. 232-235, Atlanta, GA. May. 14-16, 1991.

[146] Sugino, T., Y. Ito and M. Umeno, "Method of Measuring Microwave Relative Complex Permittivities of Film, Sheet and Plate Dielectric Materials," Electrical Engineering in Japan, vol. 109, pp. 28-37, no.3, May-June 1989.

[147] Ghannouchi, F.M., R. Guay and R.G. Bosisio, "Non-Destructive Automated Microwave Permittivity Measurements Using a Six-Port Reflectometer," 1988 Conference on Precision Electromagnetic Measurements (CPEM' 88) Digest, pp. 143-144, Tsukuba, Japan.

[148] Nishikawa, T., K. Wakino, H. Tanaka and Y. Ishikawa, "Precise Measurement Method for Complex Permittivity of Microwave Dielectric Substrates," 1988 Conference on Precision Electromagnetic Measurements (CPEM' 88) Digest, pp. 155-156, Tsukuba, Japan.

[149] Vanzura, E., and W. Kissick, "Advances in NIST Dielectric Measurement Capability Using a Mode-Filtered Cylindrical Cavity," 1989 IEEE MTT-S Digest, vol. III, pp. 901-904.

[150] Nelson, S.O., and T.-S. You, "Relationships Between Microwave Permittivities of Solid and Pulverized Plastics," Jouranl of Physics D: Applied Physics, vol. 23, no. 3, pp. 346-353, March 1990.

[151] Akyel, C., R.C. Labelle, A.J. Berteaud and R.G. Bosisio, "Computer-Aided Permittivity measurements of Moistened and Pyrolyzed Materials in Strong RF Fields (Part I)," IEEE Trans. on Inst. Meas., vol. IM-34, no. 1, pp. 25-31, March 1985.

[152] Arenata, J.C., M.E. Brodwin and G.A. Kriegsmann," High-Temperature Microwave Characterization of Dielectric Rods," IEEE Trans. on Microwave Theory Tech., vol. MTT-32, no. 10, pp. 1328-1335, Oct. 1984.

[153] Chan, W.P.F., and B. Chambers, "Measurement of Nonplanar Dielectric Samples Using and Open Resonator," IEEE Trans. on Microwave Theory Tech., vol. MTT-35, no. 12, pp. 1429-1434, Dec. 1987.

[154] Ganchev, S., J. Bhattacharyya, S. Bakhtiari, N. Qaddoumi, D. Brandenburgh and R. Zoughi, "Microwave Diagnosis of Rubber Compounds," IEEE Trans. on Microwave Theory and Tech., vol. MTT-42, no. 1, pp. 18-24, Jan. 1994.

[155] Gray, S., S. Ganchev, N. Qaddoumi, G. Beauregard, D. Radford and R. Zoughi, "Porosity Level Estimation in Polymer Composites Using Microwaves," To appear in Materials Evaluation, 1995.

[156] Zoughi, R., S. Gray and P. Nowak, "Microwave Nondestructive Estimation of Cement Paste Compressive Strength," To appear in the ACI Materials Journal, 1995.

[157] Tsankov, M.A., "Comments on Dielectric Measurements of Sheet Materials," IEEE Trans. on Inst. and Meas., vol. IM-23, pp. 248-249, 1974.

[158] Ganchev, S., S. Bakhtiari and R. Zoughi, "A Novel Numerical Technique for Dielectric Measurement of Lossy Dielectrics," IEEE Trans. on Inst. and Meas., vol. IM-41, pp. 361-365, 1992.

[159] Ganchev, S., S. Bakhtiari and R. Zoughi, "Open-Ended Rectangular Waveguide for Nondestructive Thickness Measurement and Variation Detection of Lossy Dielectric Slabs Backed by a Conducting Plate," IEEE Trans. on Inst. and Meas., vol. IM-42, Feb. 1993.

[160] Tsankov, M.A., "Measurable Values of Permittivity and Loss Tangent of Dielectrics and Ferrites for Waveguide Microwave Methods," Bulg. J. Phys., vol. 8, no. 4, pp. 403-414, 1981.

[161] Malhorta, V.M., and N.J. Carino, Editors, "Handbook on Nondestructive Tetsing of Concrete," CRC Press, p. 343, 1991.

[162] Zoughi, R., G.L. Cone and P.S. Nowak, "Microwave Nondestructive Detection of Rebars in Concrete Slabs," Materials Evaluation, vol. 49, no. 11, pp. 1385-1388, 1991.

[163] Zoughi, R., T. Nast and P.S. Nowak, "Preliminary Results of Microwave Reflectometry as a Nondestructive Tool for Studying Concrete Properties," Proceedings of the Conference on Nondestructive Evaluation of Civil Structures and Materials, Boulder, CO, May 10-13, 1992.

[164] Rzepecka, M.A., and M.A.K. Hamid, "Monitoring of Concrete Curing Process by Microwave Terminal Measurements," IEEE Trans. on Indus. Elec. and Control Inst., vol. IECI-19, no. 4, Nov. 1972.

[165] ACI Standard, "Recommended Practice for Selecting Properties for Normal and Heavy Weight Concrete," ACI 211.1-77, American Concrete Institute, Detroit, MI, 1997.

[166] Abrams, D.A., "Design of Concrete Mixtures," Structural Materials, Research Laboratory, Lewis Institute, Bulletin 1, Chicago, IL, 1918.

[167] Mindess, S., and J.F. Young, "Concrete," p. 671, Prentice Hall, New York, 1981.

CHAPTER 3

THICKNESS MEASUREMENT AND DISBOND EVALUATION IN MULTI LAYERED DIELECTRIC COMPOSITES

Microwave nondestructive techniques have shown tremendous potential for accurate thickness measurement of dielectric sheets as well as detecting minute thickness variations in dielectric slabs. The application of microwave NDE methods to a general multi layered dielectric composite may include:

- thickness measurement and thickness variation monitoring of a single sheet of material such as rubber, plastic, paper, etc.
- thickness measurement of a single dielectric coating on top of a metal backing such as paint and other dielectric laminates
- thickness measurement of a dielectric layer within several layers of a stratified composite
- since a disbond can be, in most cases, modelled as a thin layer of air (or vacuum), then disbond detection and evaluation are possible
- a pancake shaped void can similarly be detected and its thickness evaluated
- in all of the above cases detection of minute variation in the thickness of the desired layer is possible
- detection and evaluation of a disbond under a layer with varying thickness
- all of the above measurements may be conducted in contact or non contact basis requiring a standoff distance which may be carefully chosen to render increased measurement sensitivity

Inspection of a layered dielectric composite for the purpose of thickness measurement and variation detection can be conducted using either a far-field or near-field approach. In the far-field approach the medium under test is placed in the far-field of a microwave transducer, usually an antenna. Clearly, this is a non contact approach. In the far-field of an antenna plane waves are assumed to exist (similar to radar approach). In this case the theoretical analysis of the interaction between the electromagnetic waves and the material under test is relatively simple and straightforward. However, the measurement sensitivity of this approach is somewhat limited compared to the near-field approach. In

the near-field approach the material under examination is placed in close vicinity of a microwave transducer which is usually an open end of a well understood transmission line such as a rectangular or circular waveguide, a coaxial transmission line or a microstrip structure. Unlike the far-field approach, the theoretical description of the interaction between electromagnetic fields and material media in the near-field of a transducer is relatively complicated. In most cases no analytical solution may be found for this interaction and only through some simplifying assumptions and the utilization of numerical techniques it is possible to model the interaction of these fields with material media. However, much better measurement sensitivities (resolutions) are possible in the near-field approach as opposed to the far-field approach. One of the most important aspects of using microwaves for inspecting stratified dielectric composites is the utilization of optimization techniques for both the far- and near-field approaches. This means that once the interaction of microwaves with a given layered structure is modelled, the model can be used as a test bed to examine and find those parameters that render higher measurement sensitivities. These parameter include the operating frequency, the standoff distance (lift off) and the type of the sensor used. As will be seen later, such optimization techniques have resulted in coating thickness variation detection of less than a micron at around 10 GHz (wavelength of 3 cm!). Using such optimization techniques it is also possible to choose standoff distances, for a given application, in such a way that slight variations in this parameter does not cause a significant degradation in the measurement sensitivity. This is a very important practical issue since in many industrial applications the effect of vibrations (causing a variation in the standoff distance) is significantly minimized.

Microwave systems built for the purpose of thickness measurement, thickness variation detection, disbond detection and evaluation can be handheld, battery operated, relatively inexpensive, simple to operate by non-skilled operators and require minimal post signal processing, yet they can yield very fine thickness resolutions. Finally, these measurements are commonly conducted in a reflection mode which means that the transmitter and the receiver (usually one transducer is used to perform both tasks) is placed on the same side of the material under examination. Thus, access to both sides of the medium is unnecessary (i.e. the transmission through mode).

In this chapter the theoretical and experimental foundations of the above applications will be demonstrated along with some theoretical and experimental results.

FAR-FIELD OR PLANE WAVE APPROACH

As mentioned earlier this approach utilizes the properties of plane electromagnetic waves which are those fields present at some considerable distance from an antenna (transducer or sensor). A simple rule of thumb gives the far-field distance to be equal to $(2D^2/\lambda)$ away from an antenna, where D is the largest dimension of the antenna and λ is the operating wavelength [1] At this distance the maximum phase variation over an equal to the antenna aperture dimension is 22.5^o which is considered to be a reasonable assumption that a spherical wave front resembles a planar wave front (a planar wave front is an equi-phase wave front). For a given antenna higher frequencies result in longer far-field distances. Likewise, at a given frequency larger antennas result in longer far-field distances.

Commonly, an antenna is used as the transducer to launch electromagnetic waves. The antenna couples the waves into the free-space much more efficiently than an open-ended transmission line (to which the antenna is connected). Also, the use of an antenna results in increased signal gain in the desired incident direction, thus the fields can reach a material under test in the far-field, and adequate signal level can be picked up by such a directive antenna. One of the drawbacks of the plane wave approach is the fact that the footprint of the electromagnetic wave is usually relatively large in the far-field. Thus, fine spatial or lateral resolution is generally not attainable. This also limits the application to samples of relatively large extent. To reduce the far-field distance one may reduce the antenna size (for a given operating wavelength). However, this results in a wider antenna beamwidth and hence a larger footprint on the medium under test [1]. Sometimes (in the case of a horn antenna) a collimating lens may be used in conjunction with the antenna to reduce the footprint [1,2]. Therefore, one may conclude that the plane wave or the far-field approach is best to use when dealing with large structures (laterally) and when relatively small spatial or lateral resolutions are not required. When antennas are used in an array fashion or they are synthetically made to be very large (synthetic aperture imaging) the above limitations can be overcome at the expense of more complicated hardware and sophisticated signal processing [3].

Additionally, the plane wave approach does not provide as good of thickness and thickness variation resolutions as do the near-field approaches. Therefore, instead of the detailed theoretical and experimental description of the far-field approach, the reader is referred to several comprehensive references. They discuss different experimental aspects of this approach along with two theoretical

approaches used for modelling (transmission line and field coefficient approaches) [4-13].

NEAR-FIELD APPROACH

Much work has been done on rigorous theoretical analysis of near-field microwave probes/sensors/transducers, in particular, a rectangular waveguide radiating into a layered media. The applications at which these works have been aimed are just as diverse. Most of the earlier literature have addressed the problem of plasma covered aperture antennas [14-17]. More recent rigorous analysis have been presented predominantly in application to measurement of dielectric properties of materials and field interactions with biological tissues [18-22]. Considering typical measurement resolutions and accuracies in near-field examination of generally lossy composite media, most rigorous numerical results offer little practical advantage when taking into account the necessary computation time and difficulties involved in replicating the results by means of well-controlled experimental setups.

The approach adopted by Bakhtiari et al., [23] to model a general multi layered composite structure backed or unbacked by a conducting sheet was originally applied by Compton [16] in application to radiation from plasma covered aperture antennas. It is assumed that the aperture field distribution is that of the waveguide dominant mode. This approach was first implemented and tested for the practical case of thickness measurement and thickness variation detection of lossy dielectric slabs backed by a conducting plate [24]. Subsequently, the solution was expanded to include general N-layer stratified dielectric media which may be terminated by a conducting sheet or an infinite half-space. This is accomplished using a Fourier transform boundary matching technique to construct the field solutions in the layered medium outside the waveguide. A variational expression for the terminating aperture admittance in an infinite ground plane is used to construct the desired solution. Furthermore, the numerical results have been compared with several experimental measurements using a precise mechanical device built specifically for this purpose. Some important observations regarding both the numerical and experimental results have been acknowledged.

THEORETICAL FORMULATION

The detailed theoretical formulation of an open-ended rectangular waveguide radiating into a multi layered dielectric composite is given in [23]. Thus, only a brief explanation of this formulation is reported here. Variational expression for the terminating admittance of the open-

ended rectangular waveguide, depicted in Figs. 1a -1b, can be written as [16]

$$Y = G + jB = \frac{\iint_{aperture}\left[\overline{E}(x,y,0)\times\overline{W}(x,y)\right].\hat{a}_z\,dx\,dy}{\left[\iint_{aperture}\overline{E}(x,y,0)\cdot\overline{e}_0(x,y)dx\,dy\right]^2} \qquad (1)$$

where,

$$\overline{W}(x,y) = \overline{H}(x,y,0) + \sum_{i=1}^{\infty} Y_i\overline{h}_i(x,y)$$
$$x \iint_{aperture}\overline{E}(\eta,\xi,0).\overline{e}_i(\eta,\xi)d\eta\,d\xi \qquad (2)$$

and $\overline{E}(x,y,0)$ and $\overline{H}(x,y,0)$ represent the aperture field distributions. G and B are the aperture conductance and susceptance, respectively.

This admittance expression is constructed using transverse vector mode functions and their orthogonal properties [25]. $\overline{e}_i$ and $\overline{h}_i$ are the i^{th} vector mode functions and Y_i is the characteristic admittance of the the i^{th} waveguide mode. It has been shown that Equation (1) is stationary with respect to variations of the aperture E-field about its exact value [16,26,27]. Thus, a reasonable approximation for the electric field results in a good estimate of the aperture admittance. It must be noted that as standard practice, a square flange with sides greater than $1\lambda_0$ is a good approximation to the theoretical assumption of an infinite flange for near-field measurements [28].

With the TE_{10} mode incident on the aperture, a normalized symmetrical aperture electric field distribution can be written as

$$E_y(x,y,0) = \overline{e}_0(x,y) = \begin{cases}\sqrt{\dfrac{2}{ab}}\cos\left(\dfrac{\pi x}{a}\right) & \text{Over Aperture}\\ 0 & \text{Elsewhere}\end{cases} \qquad (3)$$

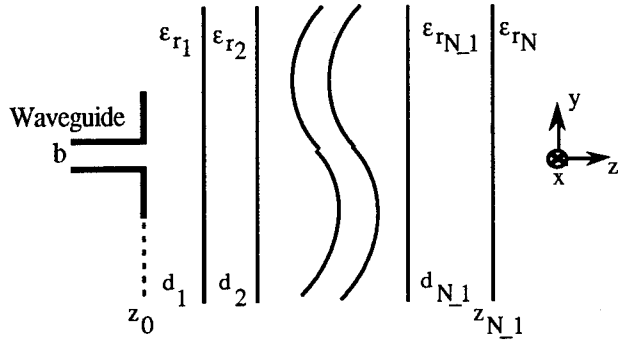

Fig. 1a: Cross-section of an N-layer stratified medium terminated by an infinite half-space, [23].

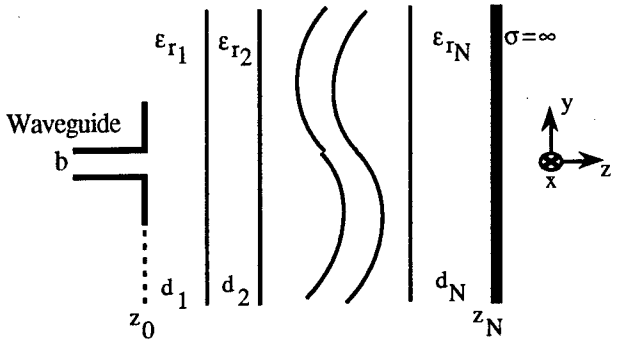

Fig. 1b: Cross-section of an N-layer stratified medium terminated by a conducting plate, [23].

where a and b are the large and small dimensions of the waveguide cross section respectively. A Fourier transform boundary matching technique is used to construct the field solutions in an N-layer stratified generally lossy dielectric medium. The transverse field components are expanded in each layer in terms of Fourier integrals. Subsequently, appropriate boundary conditions across each interface is enforced to solve for the unknown field coefficients in each medium. As shown in Figs. 1a-b the waveguide is radiating into a layered medium which may be terminated into an infinite half-space or a perfect conducting sheet respectively. Each layer is assumed to be homogeneous and nonmagnetic with relative complex dielectric constant ε_{rn}.

The fields outside the waveguide may be constructed using a single vector potential with two components [23]. In each layer, denoted by layer number n, fields must satisfy the source-free wave equation. These field components may be written as

$$\overline{E}^n(x,y,z) = -\nabla \times \overline{\Pi}^n \qquad (4a)$$

$$\overline{H}^n(x,y,z) = \frac{1}{j\omega\mu_o}\left[k_n^2 \overline{\Pi}^n + \nabla\nabla \cdot \overline{\Pi}^n\right] \qquad (4b)$$

where, $\overline{\Pi}^n = \Phi_n \hat{a}_x + \Psi_n \hat{a}_y$.

General solutions of Equations (4a) and (4b) may be expressed in terms of integrations over the entire mode space. Following the treatment given in the Appendix of reference [23], the admittance expression once normalized with respect to guide admittance can be expressed by Equation (7) in [23]. This expression has also shown to be fast converging and its numerical calculation can be performed on a PC which is an important practical advantage [23,24].

COATING THICKNESS MEASUREMENT

Using the derivation mentioned in the previous section, the potential of accurate measurement of coating thicknesses over conducting plates, as shown in Fig. 2, was investigated [24]. The measurements were conducted using an open-ended slotted waveguide [29].

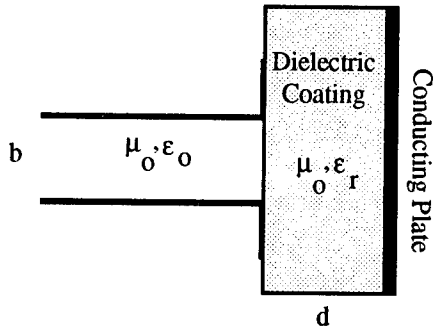

Fig. 2: An open-ended rectangular waveguide radiating into a dielectric coating on a conducting plate.

Tables I and II show the results of these measurements and their comparison with the theoretical results for two different dielectric coating (similar to carbon loaded rubber) at 10 GHz [24]. The first column shows the physically measured values of the coating using a micrometer. The second column shows the results of calculations via measuring the admittance of the waveguide aperture and recalculating the coating thickness. For both samples the calculated thickness values are within 3% of their actually measured values.

Table I: Coating thickness measurement results at 10 GHz for ε'_r = 7.25 and $tan\delta$ = 0.103, [24].

Measured d (mm)	Calculated d (mm)	% Error
3.91 ± 0.04	3.9 ± 0.05	0.26
5.92 ± 0.04	5.83± 0.05	1.52
7.77± 0.05	7.8± 0.1	0.40
11.56± 0.05	11.38± 0.19	1.56

Table I: Coating thickness measurement results at 10 GHz for ε'_r = 12.6 and $tan\delta$ = 0.19, [24].

Measured d (mm)	Calculated d (mm)	% Error
3.63 ± 0.07	3.59 ± 0.02	0.2
3.76 ± 0.05	3.76± 0.02	0.1
7.43± 0.06	7.45± 0.05	0.3
8.20± 0.05	12.20± 0.10	1.2
13.0± 0.05	12.64± 0.06	2.8

This measurement procedure may also be optimized to give maximum thickness measurement sensitivity. Since Fig. 2 shows a contact type measurement (no standoff distant between the waveguide aperture and the dielectric coating) then only the operating frequency can be used as an optimizing parameter. This means finding the most optimum operating frequency which results in the highest thickness measurement resolution. This optimization approach has been described in detail elsewhere [30]. Since this optimization procedure requires a swept frequency measurement technique a calibrated microwave bridge, as shown in Fig. 3, was used to conduct the measurements.

Fig. 3 depicts the measurement apparatus which is a dual-arm microwave reflectometer (bridge) [3]. The sweep oscillator generates the swept frequency signal which is then fed into a waveguide Tee. The Tee splits the input signal into two equal (phase and magnitude) signals each entering one of the reflectometer arms. In the upper arm the signal is fed into an open-ended waveguide which is in contact with the conductor backed dielectric slab. The reflected signal subsequently is coupled into the attached directional coupler and finally into the test port of a microwave network analyzer. The other half of the input signal enters the lower arm and is reflected off of a sliding short circuit.

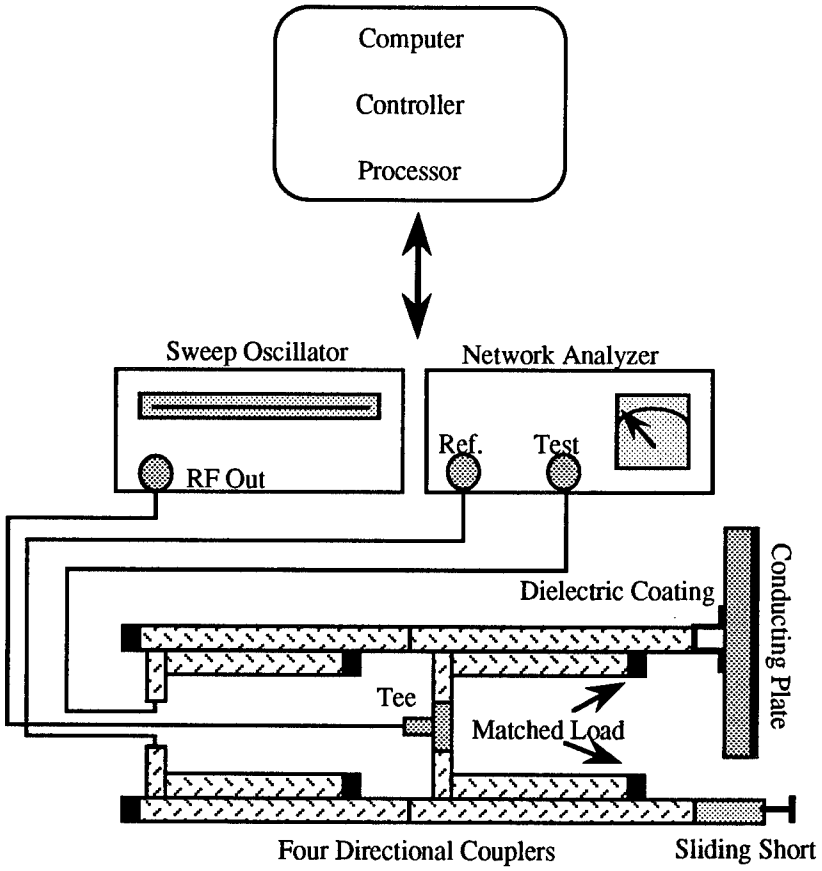

Fig. 3: X-band microwave bridge, [30].

The reflected signal in this arm is then fed into the reference port of the network analyzer for comparison (phase and magnitude) with the test signal. The sliding short in the reference arm allows compensation for the extra length of the waveguide in the test arm over the entire range of frequency sweep. Once the device is calibrated with respect to a short circuit at the test port, any detected change in the measurement parameters would be as a result of changes in the dielectric-conductor medium. The use of a computer controller via an A/D board allows real time processing and display of the measurement results over the swept bandwidth.

To better understand the measurement resolution and sensitivity due to small variations in the dielectric material thickness an experiment was conducted on a 2 mm coating of a material commonly used as thermal barrier coating (TBC) in extremely high temperature environments [3]. This coating on top of a conducting plate may be considered in the category of low-loss, high permittivity ceramics. The relative dielectric

constant of this coating was measured to be ε_r = 20 - j0.02 at 9 GHz. Typically the accuracies by which the permittivity and loss factor are measured are around 5% and 10%, respectively. The thick solid line (not smooth) in Fig. 4 represents the measured results from 8 to 9.5 GHz of the thermal barrier coating sample. The thin solid line is the theoretical predication. Clearly the two results are in fairly good agreement. The deviation of these two lines from each other is attributed to the factors stated earlier. Subsequently, the theoretical results for a 50 micrometer change (2.5% variation) in the thickness of this coating were obtained and are shown as the dashed lines in Fig. 4.

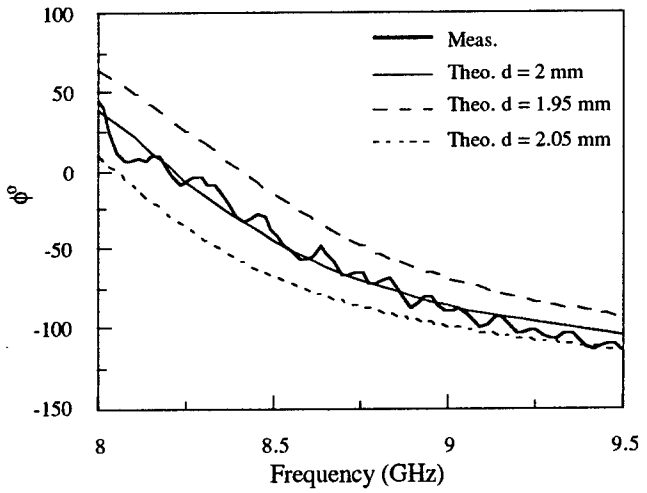

Fig. 4 : Comparison between experimental and theoretical results for a low-loss dielectric sample (TBC) of thickness ε_r = 20 - j 0.02 and thicknesses of d = 2.0 mm, d = 1.95 mm and d = 2.05 mm, [30].

The results indicate that at frequencies higher than 9.5 GHz the resolution is relatively poor. However, in the range of 8 - 8.5, a 50 micrometer thickness change causes about 25^o of phase change. This translates to a resolution of about 2 *microns* per degree. It is important to note that ϕ can be measured accurately within one degree. Clearly, the choice of operating frequency strongly affects the measurement resolution. From Fig. 4 it is also evident that lower than 8 GHz may render higher measurement sensitivity (the measurement apparatus here was limited to X-band region). The most important conclusion that may be drawn from this analysis is that resolutions in the few micron range can be achieved even at relatively low microwave frequencies.

Normally this type of resolutions are associated with operating frequencies in the millimeter wave range.

Fig. 5 shows the theoretical and experimental results for two samples of lossy dielectric material of (synthetic rubber) ε_r = 12.4 - j2.4 with thicknesses of 2.08 mm and 2.18 mm respectively on top of a conducting sheet [30]. Once again the theory was used to deduce information about the appropriate range of frequency in the X-band region which would result in maximum measurement sensitivity. The results show significant difference between the two phases, both theoretical and experimental, due to 0.1 mm change in the material thickness. Calculation of the phase difference between the two samples at around 10.3 GHz (about 150°) shows variations of less than 1 *micron* per degree.

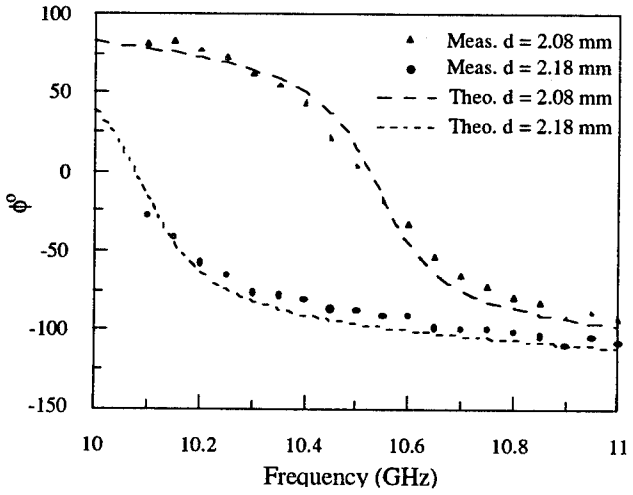

Fig. 5: Comparison between theoretical and experimental results for two lossy dielectric samples of ε_r = 12.4 - j 2.4 and thickness d_1 = 2.08 mm, and d_2 = 2.18 mm, [30].

To further analyze the resolution and sensitivity theoretically, the thicknesses of the two samples were varied by 10 microns and their respective phase differences (w.r.t. the actual thickness of each sample) were studied [30]. Fig. 6 shows both the theoretical and experimental phase differences of samples in Fig. 5 along with two theoretical simulation results displaying the variations of phase difference due to 10 microns of change in the thickness of each sample. There is a difference of about 30° for both samples due to 10 microns of thickness variation.

This difference roughly translates to a change of less than 1 micron per three degrees. Keeping in mind that phase can be measured with about 1^{o} accuracy in the laboratory, this results indicates better than *one micron* measurement resolution. There is a nonlinear dependence between the phase difference and thickness change, as expected. Taking into account that these measurements are performed at X-band, one can see the tremendous potential of such swept microwave nondestructive method for accurate measurements of minute changes in material thickness.

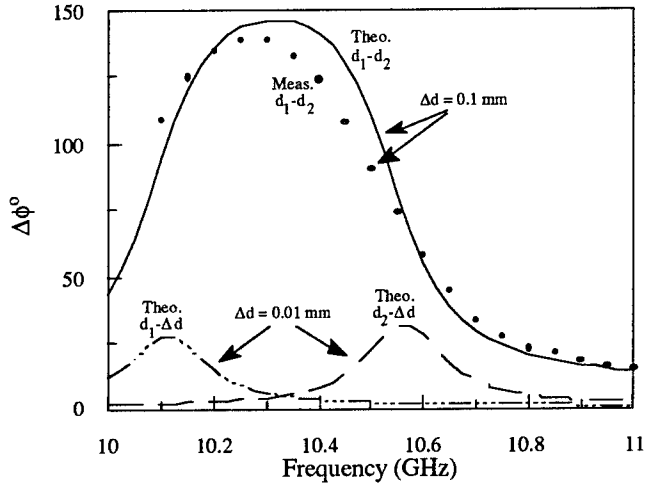

Fig. 6: Comparison between theoretical and experimental results of phase difference for two lossy dielectric samples of ε_r = 12.4 - j 2.4 and thickness d_1 = 2.08 mm, and d_2 = 2.18 mm, along with theoretical results due to 0.01 mm variation of thickness of each sample, [30].

THICKNESS MEASUREMENT OF DIELECTRIC SLABS AND DISBONDS IN MULTI LAYERED COMPOSITES

The complex reflection coefficient, R is related to normalized complex admittance, y_s, by $\Gamma = (1-y_s)/(1+y_s)$, [23]. The magnitude and phase of Γ can be measured directly from *VSWR (SWR)* and shift in the location of the standing wave null compared to a short circuited waveguide [31]. The apparatus utilized to conduct experimental measurements incorporated a slotted line and a mechanical setup with two sliding sample holders which allowed accurate adjustment of the sample positions, via two micrometers, in front of the waveguide aperture. Figs. 7a-b depict the two basic geometries realized by this apparatus.

The measurements presented here were performed at a frequency of 10 GHz using dielectric sheets with mean permittivity and loss tangent of $\varepsilon'_r = 8.4$ and $tan\delta = 0.107$ (synthetic rubber sheets), respectively. The experimental results presented here are the average value of several independent measurements.

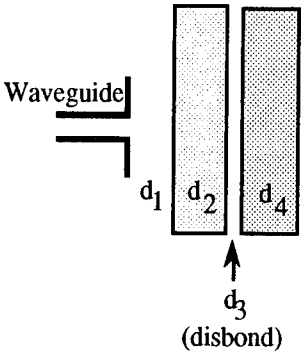

Fig. 7a: Cross sectional geometry termination into free-space, [23].

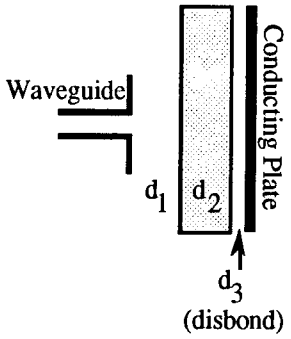

Fig. 7b: Cross sectional geometry termination into a conducting sheet, [23].

TERMINATION OF LAYERED MEDIA INTO AN INFINITE HALF-SPACE

To examine the validity and limitations of the numerical results, initially variations of *VSWR* and phase were monitored as a function of distance between the aperture and the sample (air gap) using a single slab terminated into free-space. The geometry configuration of the measurement is derived from Fig. 1a with a dielectric sample thickness of $d_2 = 7.55$ mm, and with d_3 and d_4 equal to zero. The measured slab thickness, using a micrometer thickness gauge, is the mean value over the aperture area. The results of the theoretical and measured *VSWR* and

phase for a range of air gap values are shown in Fig. 8. There is a good agreement between the measurement and numerical results. As expected, the air gap size (i.e. standoff distance or liftoff) dictates the degree of the field coupling into the dielectric slab and can be manipulated for measurement purposes.

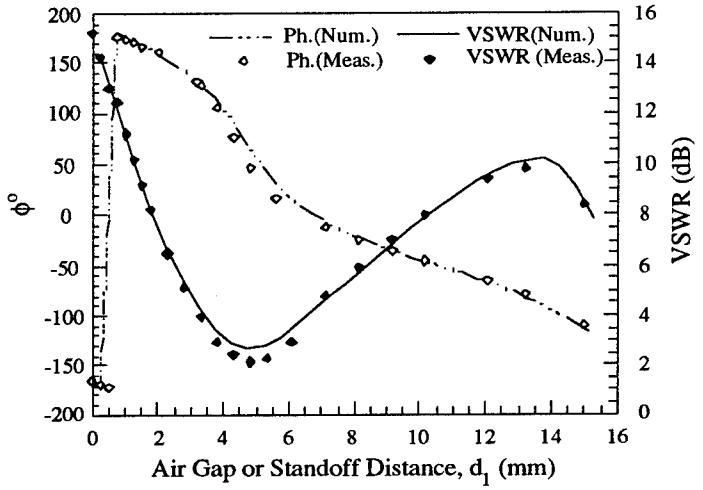

Fig. 8: Comparison of numerical and experimental results for *VSWR* and phase as a function of air gap d_1 for a two layer media terminated into free-space, [23].

Next, variations of VSWR and phase were investigated as a function of the slab thickness for a fixed arbitrary air gap distance d_1. Once again Fig. 7a illustrates the geometry for this case with d_3 and d_4 equal to zero. Figs. 9 and 10 show the numerical results at 24 GHz along with both the numerical and experimental results at 10 GHz for different slab thicknesses. Figs. 9a-b show variations of *VSWR* and phase respectively for an air gap of d_1 = 2 mm. The numerical results of phase variation at 24 GHz shows a change of around 120 degrees over the first 4.5 mm range of slab thickness. With a measurement resolution of about one degree, this indicates that for this case thickness variations as small as 0.04 mm may be detected. Figs. 10a-b display the results for an air gap of d_1 = 5 mm. The measured phase at 10 GHz shows significant variation over this thickness range which is also predicted by the theory. Due to greater signal attenuation at larger air gaps and increase in electrical length of the lossy sample at higher frequencies, variations of *VSWR* and phase are expected to degrade as shown for the 24 GHz results in Fig. 10. Such observations are made to indicate that the measurement resolution (accuracy) may be

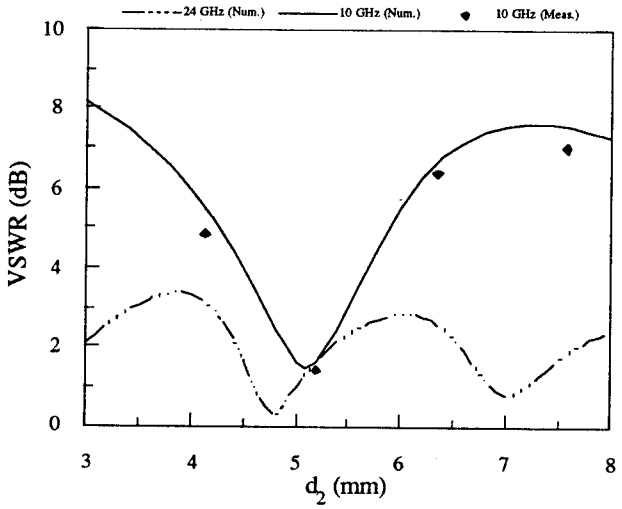

Fig. 9a: Comparison of numerical results at 10 and 24 GHz along with experimental results at 10 GHz for *VSWR* as a function of slab thickness for an arbitrary air gap of $d_1 = 2$ mm, [23].

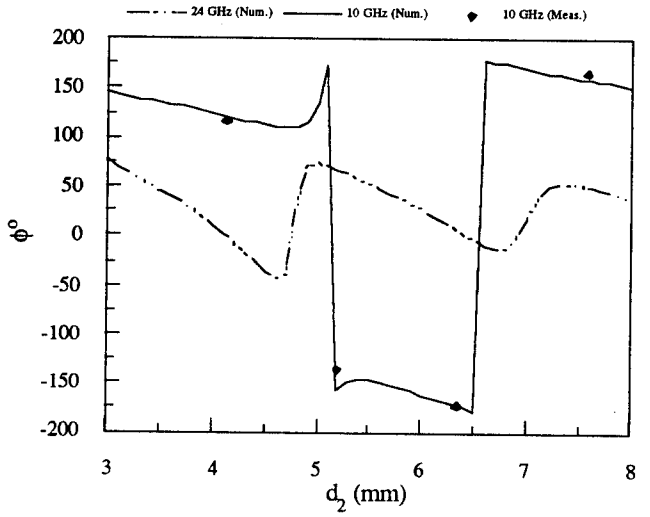

Fig. 9b: Comparison of numerical results at 10 and 24 GHz along with experimental results at 10 GHz for phase as a function of slab thickness for an arbitrary air gap of $d_1 = 2$ mm, [23].

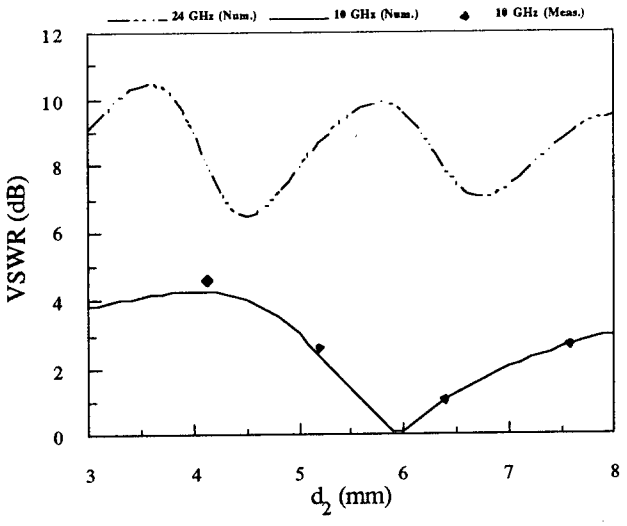

Fig. 10a: Comparison of numerical results at 10 and 24 GHz along with experimental results at 10 GHz for *VSWR* as a function of slab thickness d_2 for an arbitrary air gap of d_1 = 5 mm, [23].

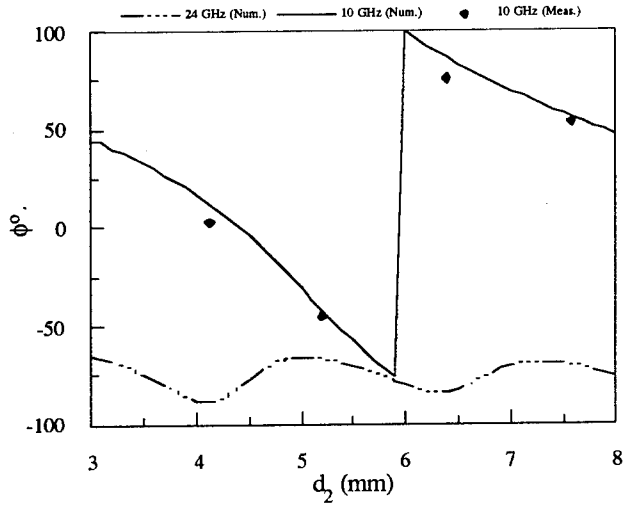

Fig. 10b: Comparison of numerical results at 10 and 24 GHz along with experimental results at 10 GHz for phase as a function of slab thickness d_2 for an arbitrary air gap of d_1 = 5 mm, [23].

maximized by using the theory to optimize the air gap distance and the operating frequency based on the sample thickness and its dielectric properties. Moreover, having such resolutions at X-band suggests that one may not need to go to much higher frequencies to achieve high resolutions for examination of the type of dielectric samples used here, although higher frequencies may eventually render better accuracies for thin and low-loss materials.

To examine the effect of disbond in a stratified composite medium an experiment was conducted in which the separation (disbond) between two slabs of the same dielectric material was varied for a fixed air gap. Once again, Fig. 7a depicts the geometry of this case for $d_2 = 5.15$ mm, $d_4 = 7.55$ mm, and with both slabs having the same dielectric constant as before. Layers 1, 3, and the infinite half-space in the back have free-space permittivity. Fig. 11 shows the numerical and experimental results for $d_1 = 5$ mm as d_3 varies. The measurement outcomes, which are in good agreement with the theory, clearly indicate that for this specific case, the phase of the reflection coefficient shows much more sensitivity to the disbond dimension than *VSWR*. The phase drops around 15 degrees over the first 0.5 mm variation of disbond in the layered medium.

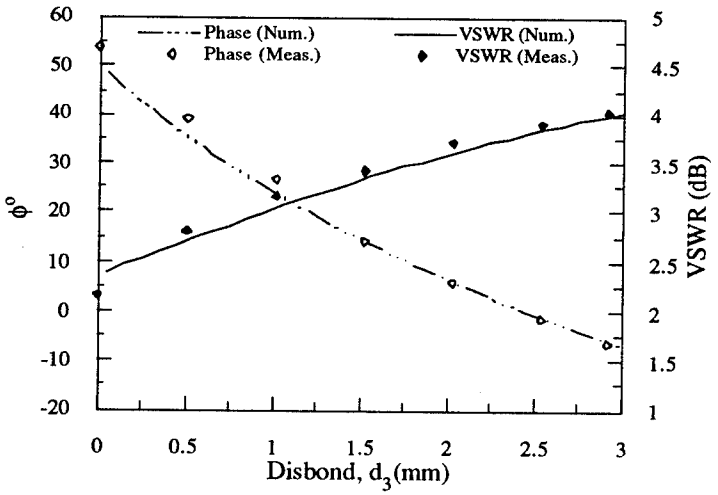

Fig. 11: Comparison of numerical and experimental results for *VSWR* and phase as a function of disbond d_3, $d_1 = 5$ mm, $d_2 = 5.15$ mm, $d_4 = 7.55$ mm, [23].

TERMINATION OF LAYERED MEDIA INTO A CONDUCTING SHEET

Similar measurements were performed for the case where the medium is backed by a conducting plate. Referring to Fig. 7b, a slab with thickness of $d_2 = 7.55$ mm was first placed flush against a metal plate ($d_3 = 0$), and d_1 varied. The numerical and experimental results for VSWR and phase are shown in Fig. 12. Comparing *VSWR* in Fig. 12 with its counterpart in Fig. 8 where the conductor in not present one can clearly observe the effect of strong reflection from the surface of the metal plate causing slower damping of the *VSWR* variation in Fig. 12. Similarly comparison between the phase of these two cases shows the strong influence of the conductor backing both in terms of a shift in position and change of slope in the phase variation.

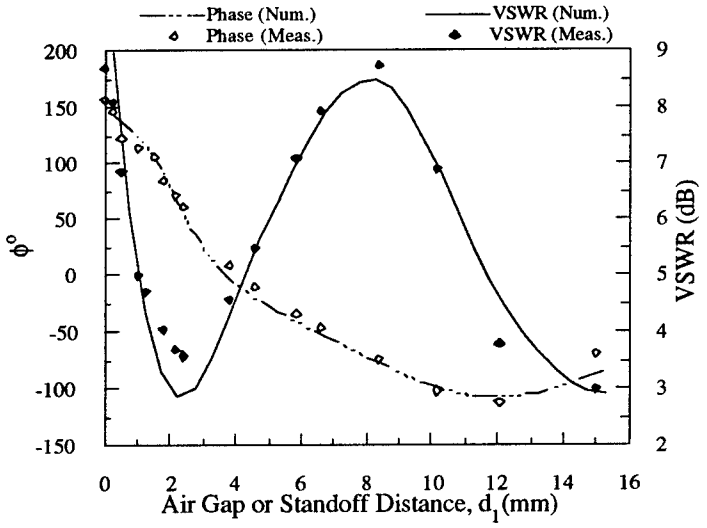

Fig. 12: Comparison of numerical and experimental results for *VSWR* and phase as a function of d_1, $d_2 = 7.55$ mm, $d_3 = 0$, [23].

Fig. 13 displays variations of *VSWR* and phase as a function of disbond thickness variation, d_3, between the dielectric sheet and the metal plate for an air gap of $d_1 = 5$ mm. Both *VSWR* and phase values, which are in close agreement with the theory. Comparing the phase variation for the initial 1 mm change of disbond d_3 in Fig. 13 with that of Fig. 11 indicates a much greater change due to variation of disbond. These results clearly illustrate the utility of this approach for detecting a disbond at its early stages of development.

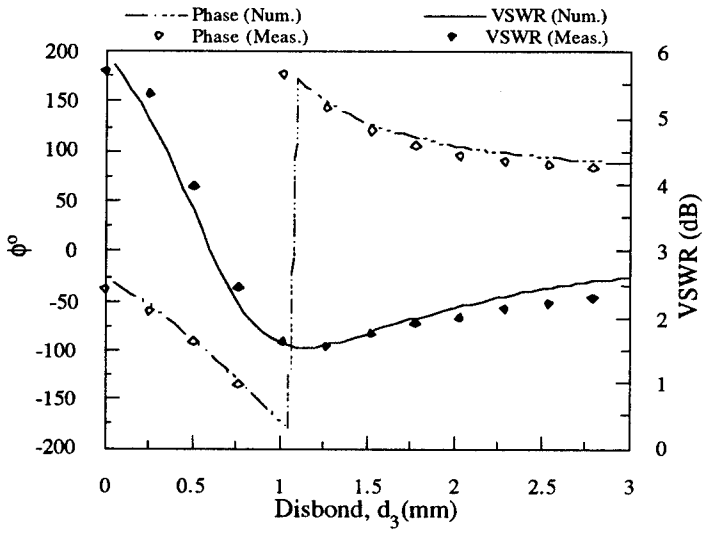

Fig. 13: Comparison of numerical and experimental results for *VSWR* and phase as a function of d_3., d_1 = 5 mm, d_2 = 7.55 mm, [23].

Depending on the measurement requirements (in many industrial applications), the disbond detection and its thickness estimation may need to be conducted independent of small variations in the prescribed thickness d_2 of the coating (geometry shown in Fig. 7b) [32]. This may be achieved by optimizing the operating frequency. Thus, the influence of varying the coating thickness d_2 on $\Delta\phi^o$ was investigated at 10 GHz. Fig. 14 shows the calculated phase difference between several disbond thicknesses and the zero disbond case versus the thickness of the coating at a fixed standoff distance of d_1 = 5.05 mm. At this frequency and standoff distance, there is maximum sensitivity to disbond presence in the thickness interval of 7 - 8 mm and to a lesser extent in the range of 12 - 13 mm. It must be noted that for these intervals, despite the attractive sensitivity, a small change in the coating thickness (d_2) will not result in an accurate estimation of the disbond thickness. Conversely, in the thickness intervals of 5-6 mm and 9-11 mm, the disbond detection and its thickness estimation is nearly independent of changes in the coating thickness. For these areas the disbond detection sensitivity is less; however, it may be adequate for most practical applications (as will be seen later). To experimentally verify these results several measurements with different coating thicknesses (d_2 = 5.2, 6.33, 8.8, and 10.1 mm) were performed at 10 GHz (Fig. 15). This figure may be obtained from Fig. 14 for fixed values of d_2, while changing the disbond thickness, d_3. There is good

agreement between the measured (discrete points) and the theoretical (lines) results. If these lines are approximated to be straight (not true for all cases), their slope will be the measure of sensitivity to disbond detection. For example for d_2 = 6.33 mm a sensitivity of 2.8°/50 μm is calculated (for the considered range of disbond thicknesses). Such sensitivity is sufficient in many production environments. Usually higher sensitivity requirements are accompanied with production of dielectric coatings with tight thickness tolerances, and in those cases the thicknesses around maximum detection sensitivity intervals (Fig. 14) may be used.

For the geometry depicted in Fig. 7a (layered dielectrics terminated by infinite half-space), calculated and measured $\Delta\phi^o$ for a standoff distance of d_1 = 2.5 mm, dielectric thicknesses of d_2 = 5.2 mm and d_4 = 6.33 mm, and a varying disbond thickness at 9.5 GHz is presented in Fig. 16 [32]. In this case the sensitivity to disbond thickness (calculated from the slope) is 1.3°/0.1 mm. Generally, better disbond detection sensitivity is achieved for the conductor backed case. The theoretical curve for 8.2 GHz demonstrates that the sensitivity is frequency dependent.

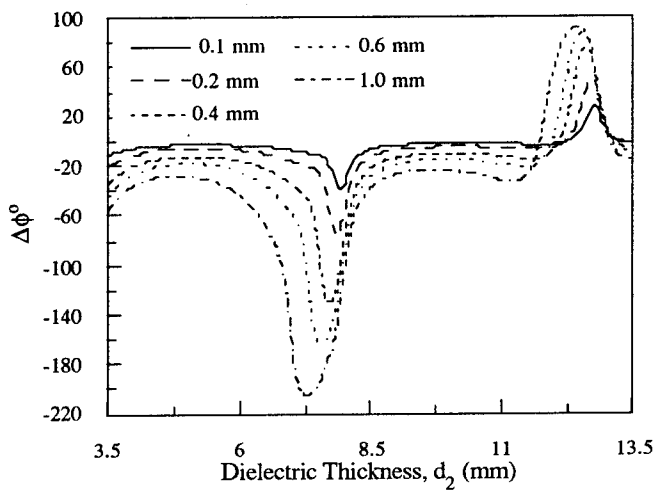

Fig. 14: Phase difference versus dielectric layer thickness d_2 for several fixed disbonds at 10 GHz, [32].

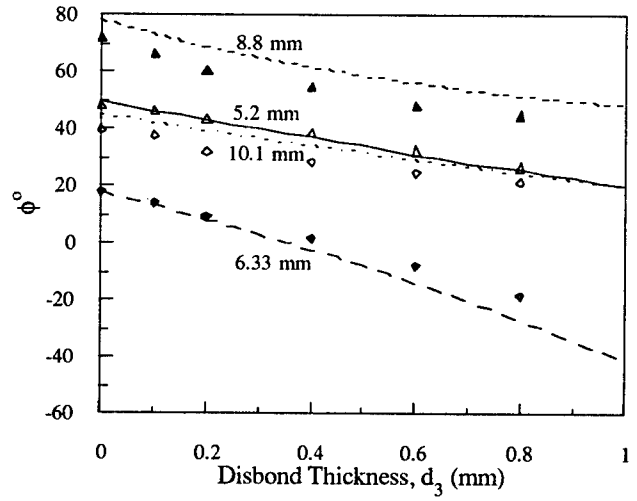

Fig. 15: Phase versus disbond thickness d_3 for several thicknesses of the dielectric (d_2 = 5.2, 6.33, 8.8, and 10.1 mm), [32].

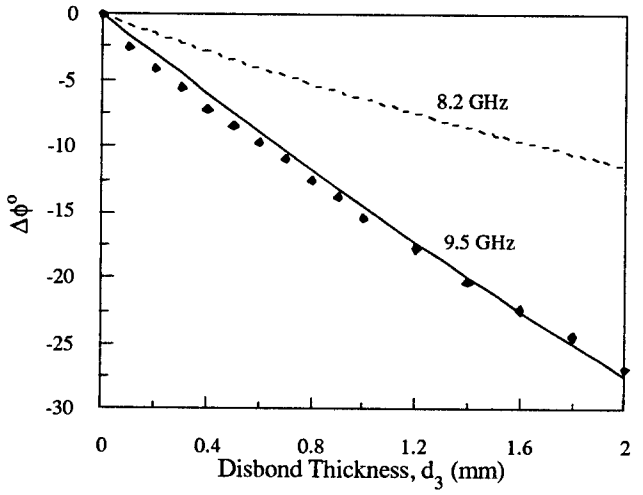

Fig. 16: Phase difference versus disbond thickness d_3 for 9.5 GHz (together with the measurement points) and 8.2 GHz (theory). The geometry used is that of Fig. 7a where d_1 = 5.05 mm, d_2 = 5.2 mm and d_4 = 6.33 mm, [32].

SUMMARY

Microwave NDE approaches are very attractive for dielectric slab, dielectric coating and disbond thickness measurement and thickness variation evaluation. These approaches utilize far-field or near-field techniques. The advantages and drawbacks of of the far-field measurements were discussed in detail. Ample references were provided that describe the theoretical and the experimental foundation of the far-field approach.

A theoretical model along with experimental results were presented in application to microwave *in situ* NDE of layered dielectric media terminating into either free-space or a conducting sheet. The theoretical analysis is based on a Fourier transform boundary matching technique to construct the field components in a layered media outside an open-ended rectangular waveguide coupled with the variational form of the terminating admittance of the flange-mounted aperture. The integrity of the numerical results have been examined by conducting several measurements using a precise mechanical device built specifically to duplicate the geometry of the theoretical model. The measurements presented here were performed at 10 GHz using generally lossy slab-like samples. Variation of *VSWR* and phase of the reflection coefficient as a function of parameters such as the air gap between the sample and the waveguide, and sample thickness were investigated. Furthermore, numerical and experimental results were presented demonstrating the possibility for detection of small disbond thicknesses in a layered media. The experimental results showed good agreement with the numerical outcomes. These results clearly indicate that high resolutions may be achieved in examination of generally lossy dielectric samples without the need to operate at very high frequencies. Furthermore, they demonstrate the sensitivity of such versatile NDE technique as it applies to the interrogation of layered composite media, and the importance of a fast and reliable numerical model as a tool to gain real time a priori knowledge of the underlying process. It is concluded that the theoretical model can render important information for optimization of such measurement parameters as position of the sensor and operating frequency leading to better resolutions.

For dielectric coating thickness measurements, the same technique was used which yielded a measurement error less than 3% for lossy dielectrics. To obtain maximum measurement accuracy or resolution, the choice of the operating frequency depends on the dielectric properties of the slab and its thickness in a manner that is difficult to simply guess for. The results of the thickness measurement using the approach outlined here showed that at some frequencies measurement accuracies of better than one micron are possible. Whereas, at a slightly

different frequency in the same microwave band the measurement accuracy is degraded drastically. The results of this study also indicated that detection of thickness variations in the order of a few microns is quite possible. This is important since these measurements were conducted in the 8.2 - 12.4 GHz region, and not in the millimeter wave region.

The optimization of air disbond detection using an open-ended rectangular waveguide sensor, was also presented for layered dielectric materials terminated by conductor or infinite-half space. The sensitivity of the disbond detection is dependent on the frequency of operation and the geometry of the layered dielectric composite. Depending on the measurement requirements, the disbond detection and the estimation of its thickness may be independent of the changes in the dielectric coating thickness. Conversely, the measurement system may be adjusted to achieve maximum sensitivity to disbond presence at certain depths from the surface. An array of sensors may be tuned each to be sensitive to disbonds between different layers of a multi layered composite.

REFERENCES

[1] Balanis, C.A., "Antenna Theory, Analysis and Design," Chapter 2, Harper and Row, New York, NY, 1982.

[2] Gopalsami, N., S. Bakhtiari, S.L. Dieckman, A.C. Raptis and M.J. Lepper, "Millimeter-Wave Imaging for Nondestructive Evaluation of Materials," Materials Evaluation, vol. 52, no.3, pp. 412-415, March 1994.

[3] Ulaby. F.T., R.K. Moore and A.K. Fung, "Microwave Remote Sensing, Active and Passive," vol. II, Chapter 9, Artech House, Dedham, MA, 1982.

[4] Ulaby. F.T., R.K. Moore and A.K. Fung, "Microwave Remote Sensing, Active and Passive," vol. I, pp. 233-244, Artech House, Dedham, MA, 1981.

[5] Lavelle, T.M., "Microwave Nondestructive Testing," Materials Evaluation, vol. 25, pp. 254-258, Nov. 1967.

[6] Bahr, A., "Microwave Nondestructive Methods," Gordon and Breach Science Publishers, New York, NY, 1982.

[7] Zoughi, R., and M. Lujan, "Nondestructive Microwave Thickness Measurement of Dielectric Slabs," Materials Evaluation, vol. 48, pp. 1100-1105, Sept. 1990.

[8] Botsco, R.J., "Nondestructive Testing of Plastics with Microwaves," Materials Evaluation, vol. 27, pp. 25A-32A, June 1969.

[9] Zoughi, R., and S. Bakhtiari, "Microwave Nondestructive Detection and Evaluation of Disbonding and Delamination in Layered-Dielectric-Slabs," IEEE Trans. on Inst.and Meas., vol. IM-19, no. 6, pp. 1059-1063, Dec. 1990.

[10] Zoughi, R., and S. Bakhtiari, "Microwave Nondestructive Detection and Evaluation of Void in Layered Dielectric Slabs," Research in Nondestructive Eval., vol. 2, no. 4, pp. 195-205, 1990.

[11] Bakhtiari, S., and R. Zoughi, "Microwave Thickness Measurement of Lossy Layered Dielectric Slabs Using Incoherent Reflectivity," Research in Nondestructive Eval., vol. 2, no. 3, pp. 157-168, 1990.

[12] Zoughi, R., J. Edwards and S. Bakhtiari, "Swept Microwave Frequency Nondestructive Detection and Evaluation of Delamination in Stratified Dielectric Media," J. of Wave-Material Interaction, vol. 7, no. 1, pp. 427-438, Jan. 1992.

[13] Edwards, J., and R. Zoughi, "Microwave Sensitivity Maximization of Disbond Characterization in Conductor Backed Dielectric Composites," J. of Nondestructive Evaluation, vol. 12, no. 3, pp. 193-198, Sept. 1993.

[14] Galejs, J., "Admittance of a Waveguide Radiating into Stratified Plasma," IEEE Trans. Antennas Propagation, vol. AP-13, no. 1, pp. 64-70, Jan. 1965.

[15] Villeneuve, A. T., "Admittance of Waveguide Radiating into Plasma Environment," IEEE Trans. Antennas Propagation, vol. AP-13, no. 1, pp. 115-121, Jan. 1965.

[16] Compton, R. T., "The Admittance of Aperture Antennas Radiating into Lossy Media," Ph.D. dissertation, Ohio State University, 1964.

[17] Croswell, W. F., W. C. Taylor, C. T. Swift and A. R. Cockrell, "The Input Admittance of Rectangular Waveguide-Fed Aperture Under an Inhomogeneous Plasma: Theory and Experiment," IEEE Trans. Antennas and Propagation, vol. AP-16, pp.475-487, July 1968.

[18] Teodoridis, V., T. Sphicopoulos and F. E. Gardiol, "The Reflection From an Open Ended Rectangular Waveguide Terminated by Layered Dielectric Medium," IEEE Trans. Microwave Theory Tech., vol. MTT-33, no. 5, May 1985.

[19] Jamieson, A.R., and T. E. Rozzi, "Rigorous Analysis of Cross Polarization in Flangemounted Waveguide Radiators," Electron. Lett., vol. 13, pp. 742-744, Nov. 24, 1977.

[20] Decreton, M. C., and F. E. Gardiol, "Simple Non-Destructive Method for Measurement of Complex Permittivity," IEEE Trans. Inst. Meas., vol. IM-23, pp. 434-438, Dec. 1974.

[21] MacPhie, R. H., and A. I. Zaghloul, "Radiation From a Rectangular Waveguide With Infinite Flange - Exact Solution by the correlation Matrix Method," IEEE Trans. Antennas Propagation, vol. AP-28, no. 4, pp. 497-503, July 1980.

[22] Nikita, K. S., and N. K. Uzunoglu, "Analysis of The Power Coupling From a Waveguide Hyperthermia Applicator Into a Three-Layered Tissue Model," IEEE Trans.Microwave Theory Tech., vol. MTT-37, no. 11, pp.1794-1801, Nov. 1989.

[23] Bakhtiari, S., N. Qaddoumi, S. Ganchev and R. Zoughi, "Microwave Noncontact Examination of Disbond and Thickness Variation in Stratified Composite Media," IEEE Trans. on Microwave Theory and Tech., vol. 42, no.3 , pp. 389-395, March 1994.

[24] Bakhtiari, S., S. Ganchev and R. Zoughi, "Open-Ended Rectangular Waveguide for Nondestructive Thickness Measurement and Variation Detection of Lossy Dielectric Slabs Backed by a Conducting Plate," IEEE Trans. Inst. Meas., vol. 42, no.1, pp. 19-24, Feb. 1993.

[25] Harrington, R.F, "Time Harmonic Electromagnetic Fields," McGraw-Hill, New York, p. 381, 1961.

[26] Collin, R. E., "Field Theory of Guided Waves," McGraw-Hill, New York, 1960.

[27] Galejs, J., "Antennas in Inhomogeneous Media," Pergamon Press, 1969.

[28] Croswell, W. F., R.G. Rudduck and D. M. Hatcher," Admittance of a Rectangular Waveguide Radiating into a Dielectric Slab," IEEE Trans. Antennas Propagation, vol. AP-15, no. 5, pp.627-633, Sept. 1967.

[29] Altschuler, H.M., "Dielectric Constant," In Handbook of Microwave Measurements, vol. II, Chapter IX, pp. 495-546, Polytechnic Press, Brooklyn, NY, 1963.

[30] Bakhtiari, S., S. Ganchev and R. Zoughi, "Microwave Swept-Frequency Optimization fro Accurate Thickness or Dielectric Property Monitoring of Conductor-Backed Composites," Materials Evaluation, vol. 51, no. 6, pp. 740-743, June 1993.

[31] Ganchev, S., S. Bakhtiari and R. Zoughi, "A Novel Numerical Technique for Dielectric Measurement of Lossy Dielectrics," IEEE Trans. Inst. Meas., vol. IM-41, no. 3, pp. 361-365, June 1992.

[32] Ganchev, S., N. Qaddoumi, E. Ranu and R. Zoughi, "Detection Optimization of Disbond in Layered Dielectric Composites with Varying Thicknesses Using an Open-Ended Rectangular Waveguide," To appear in the IEEE Trans. on Inst. and Meas., 1995.

CHAPTER 4

MICROWAVE TECHNIQUES FOR SURFACE CRACK DETECTION AND SIZING IN METALS

Microwaves do not penetrate inside conductors (metals). However, they are very sensitive to conductor surface perturbation such as surface roughness and surface cracks. There are certain advantages in using microwave metal surface crack detections (particularly when using open-ended waveguide probes) such as:

- novelty of the approach. Fresh look at fatigue crack detection and sizing. Yet to be tapped capabilities
- the method is fast, reliable and relatively inexpensive
- the sensor may or may not be in contact with the surface under examination
- cracks may be filled or covered with dielectric materials such as paint, dirt, rust, etc.
- the same probe which detects and characterizes the properties of a crack under coating, may also (without any alteration to its design) measure the thickness of the coating and its material characteristics
- cracks may be on non-ferromagnetic as well as ferromagnetic metals or alloys
- cracks on the surface of graphite composites may also be detected and characterized.
- microwave techniques work with coarse-grained materials (metals)
- the surface under examination may be in a high temperature environment
- the detected signal is only due to surface defects and not to interior flaws
- the technique may be applied to curved and other complicated surfaces
- dimensions of a crack can be estimated
- crack orientation, edge and tip locations can be detected
- no special operator skills, in the fields of microwaves or signal interpretation are needed
- very little surface preparation is required
- the technique is environmentally compliant, operator friendly and safe

- the required microwave power is in low milliwatt range
- such a system may be battery operated and portable and handheld
- the results are obtained in real-time
- the technique is not a source EMI pollution and insensitive to EMI. These allow testing during normal operating conditions, thus reducing repair related down time
- capability of inspecting large areas in a relatively short time (e.g. use of sensor arrays)
- defects in laminates and thick composites (disbond, void, inhomogeneity, impact damage, under cure, fiber bundle orientation and breakage, etc.) covering a metal specimen may also be detected and evaluated
- adaptable to automatic (no operator involvement) detection routines

The following is a review of the previous works on metal surface crack detection using microwave techniques [1,2]. Generally speaking, these techniques can be divided into two categories, i.e. far-field and near-field measurement techniques. Far-field techniques use antennas as transmitters and receivers. The near-field techniques usually use open-ended sensors such as waveguides and coaxial lines. Three different types of probes are commonly used: waveguide probes, planar transmission line probes, and ferromagnetic resonance probes.

WAVEGUIDE PROBES

The first reported work on microwave crack detection was conducted by Feinstein et al., [3,4]. One of their earliest methods is based on rotating the polarization of the incident wave and associating a particular polarization component in the scattered signal with the crack signature. The crack is considered to be a polarization filter which scatters maximally when the incident electric field is perpendicular to its long dimension, in other words, the crack converts part of the incident wave (a mode) to an orthogonally polarized wave (an independent mode). Hence, this method can be considered as a mode conversion (by the crack) technique. The rotation of the incident polarization at first was achieved by a mechanically rotated waveguide joint and later by an electrically modulated Faraday rotator. A bridge was used to null out the background signal under the condition that the distance between the probe and the specimen remains constant. The disadvantages of this method are the additional signal loss due to the bridge and the poor reliability and the low modulation frequency of the mechanically rotated waveguide joint. This system was used to detect the growth of fatigue cracks and was reported to be capable of detecting a crack with a depth of less than 0.001 in.

Another type of mode conversion was also introduced by Hruby and Feinstein [5]. A rectangular dominant mode (TE_{10}) was converted to higher order cylindrical TM_{01} or TE_{01} mode through a mode converter. These modes are non-polarized so that crack orientation is not important. However, they are not stable and will be converted to cylindrical dominant mode TE_{11} and then to rectangular dominant mode in the slot. The reflected wave from the slot will be converted back to cylindrical TE_{11} mode in the circular waveguide and thus separated from other modes through a tapered filter. A Faraday rotator was used to further reduce the background signal and then the signal was amplified by a VSWR amplifier. The signal source operated at 30.5 GHz with a power level of 100 mW. This method was claimed to be capable of measuring very deep cracks (up to 50 mm).

Bahr [6] also used mode conversion for crack detection, but at 100 GHz. A linearly polarized incident wave is partially converted to an orthogonally polarized wave when the incident polarization is at an angle to the slot that is between 0 and 90 degrees. This crack signal was separated from the co-polarized background signal through an orthomode coupler. The antenna used was a lens-focused horn with a beamwidth of about 3.5 mm at the focal point. The measurements were performed on aluminum plates with slots which were 0.25 mm wide and with different depths and lengths. The plate was perpendicularly aligned to the microwave propagation direction and the long dimension of slots was at an angle of about 60^{o} to the electric polarization vector of the incident wave to ensure part of the incident energy would be coupled into the orthogonally polarized mode by slots. The experiments showed that it was also possible to determine the depth of cracks. This may be due to the fact that the test frequency was higher than the resonance frequency of the slot and thus allowed the wave to propagate into the slot. In other words, if the test frequency is below the resonance frequency of the slot, slot depth will not produce a detectable phase change for different slot depths in a polar display, similar to that for eddy current testing. The sensitivity of the system depends on the degree to which the transmitting and the receiving portions of the system can be isolated in the absence of a crack by the decoupler. This is critically dependent upon the flatness of the plate and its alignment with respect to the probe. This dependence is considered a major disadvantage of this approach. In [7], Bahr has also used a 6-dB directional coupler and a circular polarizer to replace the orthomode coupler to excite the probe for fatigue crack detection. The circular polarizer combined with a rectangular waveguide behaves like an orthomode coupler and provides a 10 dB rejection of the unwanted background signal. Using a circularly polarized wave makes the detection independent of crack orientation, however, this causes a 3 dB loss in signal power when compared to that produced by an optimally

aligned, linearly polarized incident wave. Instead of the far-field lens probe, a near-field, 1.1 mm (O.D.), dielectric waveguide probe was used. The latter should provide higher sensitivities because not only does it confine the incident fields to the vicinity of the crack, but it also receives stronger signal scattered by a crack. A good match was provided between the air-filled circular waveguide and the dielectric waveguide by tapering one end of the dielectric guide. This method can not detect crack with a width of less than one micron. However, detection was possible if cracks are a few microns wide. The depths of cracks can also be measured according to the phase angles of the signals displayed in a way similar to that for eddy current testing if cracks are sufficiently open, have high quality factor (as a resonator) and if crack lengths are larger than one half wavelength.

PLANAR TRANSMISSION LINE PROBES

Microstrip lines (or planar transmission lines) may also be built as microwave eddy-current probes for crack detection [8,9]. This type of a probe uses the near-field, since they must be brought close to the metal surface to be inspected in order to sense the crack. Compared to waveguide type probes, higher sensitivity is the major advantage of this type of probes because near field interaction is used and also because impedance-matching network can be readily incorporated into the probe structure.

Robinson and Gysel developed a coupled-stripline probe for surface crack detection. Two adjacent strip lines are coupled together to support two orthogonal TEM modes, the even mode and the odd mode. For the even mode, the two strip lines are at the same potential with respect to the ground, while, for the odd mode, their potentials are of the same magnitude but different polarities. For crack detection, the metal surface under test is used as one of the two ground plates. If the pair of strips are symmetrical and excited in the even mode, there will be no conversion to the odd mode. However, if there is a surface crack in the ground plate which perturbs the current flow under one strip but not the other, part of the exciting power will be converted into the odd mode. Thus, such a set-up can be used for crack detection and mode conversion is also used to reject unwanted background signal so that higher sensitivities can be achieved. The test frequency of this system was around 10 GHz. The exciting signal was pulse-modulated at 1 KHz. An in-phase power divider was used to excite the even mode and the odd mode was picked up by a rat-race hybrid. Quadrature detection and subsequent squaring and adding produced a phase-sensitive output. However, it is not easy to isolate the LO signal from the modulated signal and an isolator with more than 40 dB of isolation was required. It was found possible to achieve 50-75 dB of dynamic range if the

variable attenuator and the phase shifter connected to the output of the probe were properly adjusted. The advantages of this method are that: a) the strip lines can be as long as desired and b) by using a flexible dielectric substrate, the probe can follow the curved surface to achieve constant coupling. EDM notches 0.001" long, 0.0015" wide and 0.005" deep were successfully detected by this method. However , it was not easy to keep good isolation between the even and odd modes during the scan and this is a major disadvantage of this technique.

Husain and Ash [10] used a planar transmission line to design a "microwave scanning microscope." It consisted of a two-port resonator having a small aperture in the ground plane. When the probe was very close to the metal surface the lateral spatial resolution was in the order of the aperture diameter, which was much smaller than a wavelength. A microwave bridge and a mixer were used to null out the unwanted background signal and to improve the sensitivity. This system was able to detect fatigue cracks with a width of less than 2 microns at 10 GHz. The signal strength could also be related to slot depth.

Bahr and Watjen [11] designed a different transmission line probe. Quarter-wave long microstrip resonators are short-circuited to the ground at one end and capacitively coupled to a 50 Ω microstrip line at the other end. Using Duroid 5880 for the substrate material, an unloaded Q in excess of 300 was obtained. The purpose of the resonator is to match the low impedance to the 50 Ω source impedance and thereby maximize the sensitivity of the probe. 1 GHz was used to have a reasonable size for the probe. Using two of these kind of resonators back to back and surrounded by a metal shield a differential probe was formed with the tip unshielded to interact with the metal surface under test. The 1 GHz signal was down-converted to 100 kHz for display in a form similar to that for eddy current testing. The sensitivity of this system to open slots was found to be higher than that of a commercial 100 KHz eddy current system, however, its sensitivity to closed cracks was close to that of commercial probes. One of the problems with this system was the isolation characteristics of the bridge.

FERROMAGNETIC RESONANCE PROBE

The ferromagnetic resonance (FMR) probes may be considered as high frequency eddy current probes [12-20]. The extension of conventional eddy current probes to higher operating frequencies is hampered by the difficulty of fabricating the very small search coils required and by the frequency limitations imposed by the type of ferrite core materials used [16]. An alternative approach to high frequency eddy current testing involves the use of electron spin precession resonances in ferromagnetic

crystals such as Yttrium Iron Garnet (YIG). The availability of such materials and technique makes it possible to built very compact eddy current probes operating at frequencies in the range from 0.5 GHz to 4 GHz. In addition to their small size, these probes have an advantage of being resonant devices, thereby increasing their detection sensitivity. A small sphere (with a diameter less than one millimeter) of YIG was prepared by optically polishing and was placed in a DC magnetic bias field and excited with a single coupling loop containing the DC magnetic bias in its plane. A single turn loop, fed by a coaxial cable, is sufficient to provide good coupling to the resonator. This is due to the fact that ferromagnetic crystals exhibit very high magnetic permeabilities and quality factors. DC magnetic field of 200 to 800 Oe necessary to provide resonance frequency of about 0.5 to 2 GHz may easily be created with small-sized samarium-cobalt permanent magnets. Resonance of the YIG sphere takes the form of a uniform precession of the magnetization about the applied DC magnetic field. The DC magnetization of the sphere aligns along this direction, but application of an RF magnetic field h_{RF} by means of a small excitation coil causes a time varying deviation of the magnetization m_{RF}. Since the magnetization has a spin angular momentum associated with it, m_{RF} does not follow h_{RF} directly but precesses about the direction of the applied DC magnetic bias. One significant difference between FMR and conventional eddy current probes lies in the spatial distribution of eddy currents induced in the metal surface under examination. This is due to the fact that the magnetic field of an FMR probe rotates once every cycle about the DC magnetic field, whereas the field of a conventional single coil probe remains stationary. In order to satisfy the boundary conditions there is an infinite number of magnetostatic resonant modes existing in the sphere and each has its own characteristic distribution of magnetization within the sphere and a characteristic frequency that depends on H_{DC}. A conducting material (the specimen) placed near the FMR probe introduces losses and couples the modes to each other, causing changes in both the amplitude and frequency of the modes. Time-varying magnetic fields created outside the sphere by the rotating magnetic dipole moment interact with a flaw and produce a perturbed signal in a way similar to that of conventional eddy current testing. Experiments have shown that FMR probes were 40 times more sensitive than a 100 KHz conventional eddy current probe.

There have also been some other investigations in this area besides the ones mentioned above [20-30].

In recent years, Yeh et al., have used open-ended waveguides for surface crack detection in metals [31-34]. Their investigations have shown the potential of using a dominant mode technique for long and finite lengthed cracks detection in addition to detecting fatigue cracks

using a higher order mode technique. They also formulated two different approaches to sizing the width, depth and the length of a crack. A brief explanation of their approaches are given here.

LONG SURFACE CRACK DETECTION USING AN OPEN-ENDED RECTANGULAR WAVEGUIDE

In mid-1992 several experiments, using an open-ended waveguide, were conducted to investigate the feasibility of using this probe to detect long surface cracks in metals [31]. In this context, long refers to a crack whose length is greater than or equal to the broad dimension of a waveguide. Various long cracks of different widths and depths were milled on top of flat metal sheets. Preliminary experiments were conducted by moving (using a computer-controlled stepping motor) the cracked metal surface over the aperture of the open-ended waveguide while monitoring the standing-wave characteristics inside the waveguide. Subsequently, it was observed that when the crack axis (length) is parallel to the broad dimension of the waveguide (orthogonal to the electric field of the dominant TE_{10} mode) the standing wave experiences a pronounced shift in location when the crack is exposed to the aperture of the waveguide compared to when the crack is outside the aperture (a short-circuit condition). This shift indicates changes in the reflection coefficient properties of the metal surface perturbed by the crack. It was also observed that this shift is highly dependent on the relative location of the crack within the waveguide aperture (i.e. whether the crack is at the edge or at the center of the aperture). Figs. 1a-1b show the geometry of a crack with width W, depth d and length L and a waveguide aperture with dimensions a and b ,when the crack length is parallel to the broad dimension of the waveguide, and δ is a dimension indicating the location of the crack relative to an arbitrary location on the small dimension of the waveguide aperture, b. It was also observed that when the crack was not parallel to the broad dimension of the waveguide, the level of change in the standing wave decreased, and when the crack became parallel to the smaller dimension of the waveguide (parallel to the dominant TE_{10} mode electric field) there was no measurable perturbation in the characteristics of the standing wave. This is due to the fact that in this case the surface currents on the metal surface are parallel to the crack length which does not disturb the surface currents. It must be noted here that most fatigue and stress cracks in real life are not straight. However, they can usually be considered fairly straight along their lengths.

Fig. 2 shows a simple measurement apparatus that was used for these experiments. An oscillator feeds a (slotted) waveguide terminated by a metal plate in which there is a crack.

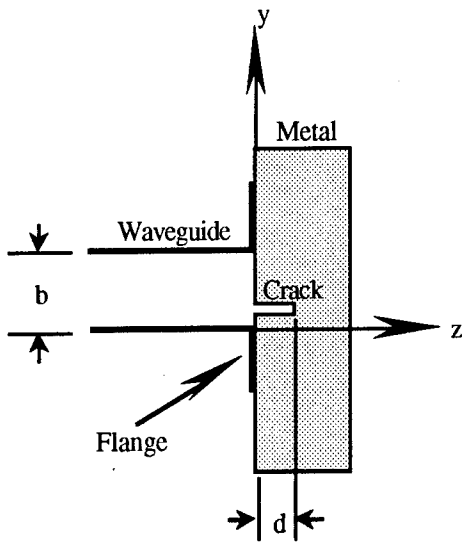

Fig. 1a: Side view of the relative geometry of a surface crack and a waveguide aperture, [31].

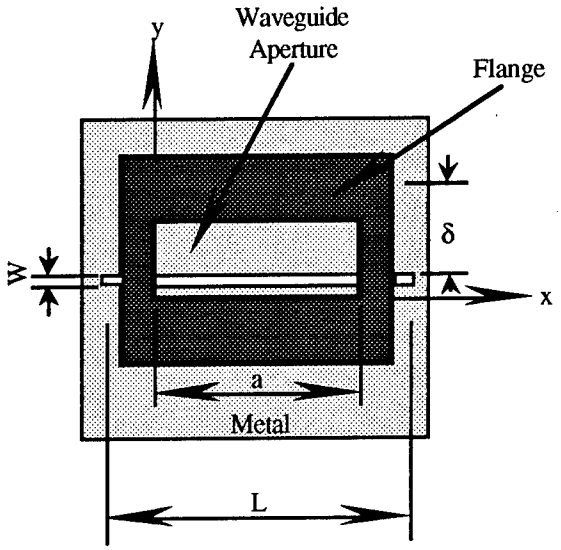

Fig. 1b: Plan view of the relative geometry of a surface crack and a waveguide aperture, [31].

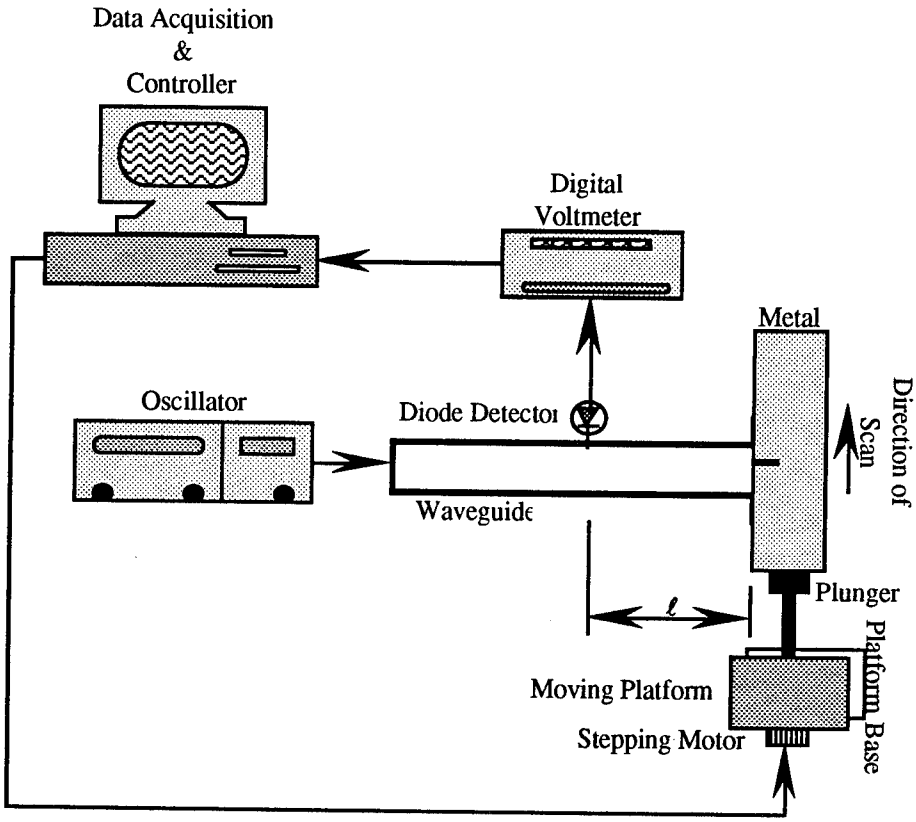

Fig. 2: Measurement apparatus, [31].

Placing the diode detector a distance ℓ away from the waveguide aperture, the metal plate can be scanned by the waveguide aperture and the standing voltage recorded. As will be seen later, different detector locations, ℓ, will change the difference between the measured signals for the short-circuit case and when the crack is in the middle of the aperture. If ℓ is chosen such that the detector is located between a maximum and a minimum on the standing-wave pattern, this difference is maximized.

At 24 GHz, a long crack with $L > 10.7$ mm, $W = 0.84$ mm and $d = 1.03$ mm was scanned over the aperture of a K-band waveguide ($a = 10.67$ mm and $b = 4.32$ mm). The diode output voltage measured at $\ell = 9.45$ cm is shown in Fig. 3 (the solid line). The results indicate that while the crack is outside the waveguide aperture the diode registers very little voltage variation due to the fact that the waveguide is terminated by a short circuit. The noise-like feature associated with the signal is due to the quantization resolution of the A/D converter and the internal noise of the voltmeter. As the crack begins to appear within the

waveguide aperture the voltage experiences a rapid magnitude change which is an indication of rapid phase change in the reflection coefficient at the aperture. The same phenomenon occurs when the crack leaves the waveguide aperture. The voltage value does not change very much while the crack is inside the aperture; however, its value is still different than that of a short-circuit case. The diode output voltage as a function of δ (hereon referred to as the *crack characteristic signal*) is clearly an indication of the presence of a crack (*detection*), since the absence of the crack results in a fairly constant voltage.

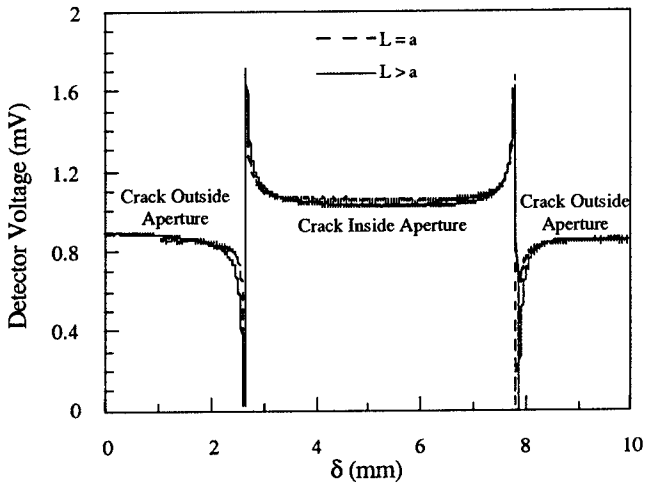

Fig. 3: Experimental characteristic signal at 24 GHz for a crack with W = 0.84 mm, d = 1.03 mm: (_____) L > 10.7 mm, (------) L = 10.7 mm, [31].

THEORETICAL FOUNDATION

To theoretically model this phenomenon an effort was made to simplify the geometry of the crack with respect to the waveguide. It was decided to investigate the effect of crack length on the characteristic signals. The idea was that if the length of the crack is approximated to be equal to the broad dimension of the waveguide aperture, a, then the problem could be modeled as a large waveguide feeding a much narrower short-circuited waveguide with the same broad dimension. Subsequently, an experiment was conducted in which a crack with the same width and depth as those used for the solid line in Fig. 3 but with L = 10.7 mm (equal to the broad dimension of the waveguide) was used to determine its characteristic signal at 24 GHz. The dashed line in Fig. 3 shows the results of this experiment. Comparing the solid and the dashed line

clearly indicates that, for thin cracks (small W), once the length extends beyond the waveguide aperture there will not be any considerable perturbation in the standing-wave pattern. Thus, in the subsequent theoretical derivations we can assume that the length of a crack is equal to the broad dimension of the waveguide, a. The slight widening of the characteristic signal at around $\delta = 2.5$ mm for the long crack (solid line) is attributed to a small amount of radiation through the long crack. This problem becomes much less important as the width of a crack becomes small which is the case for many fatigue cracks.

The crack dimension is Wxdxa. The dominant mode propagating in the $+z$ direction is incident upon the waveguide aperture. The reflected wave propagates in the $-z$ direction, and a standing wave is formed inside the waveguide. The properties of the standing wave are influenced by the crack size and its location within the waveguide aperture. The reflected wave arises as a direct consequence of forcing the boundary conditions inside and outside the crack at all times. For brevity the detailed formulation of the theoretical modelling will not be given here and the reader is referred to reference [31] for the detailed formulation.

COMPARISON OF THE THEORETICAL AND EXPERIMENTAL RESULTS

To compare the results of the theoretical derivations with experimental results, $|E_y|^2$ for a crack with W = 0.84 mm and d = 1.53 mm was calculated at ℓ = 9.45 cm away from the aperture (between a standing-wave null and maximum) at 24 GHz. Fig. 4 shows the normalized (with respect to the maximum value of each signal) results of the diode output voltage for the experimental case and $|E_y|^2$ for the theoretical case. The agreement between the two results is very good. The slight difference between the normalized signal levels is attributed primarily to the crack geometry not having 90° corners as assumed by the theory, and a small airgap present between the metal surface and the waveguide aperture during the measurements. The diode detector may not always operate in the square-law region (particularly for high input signal values) which may also attribute to this difference. The distance between the arrows marked 1 is equal to the width of the crack plus the small dimension of the waveguide ($W + b$). However, due to the causes mentioned above, experimentally the distance between the arrows marked 2 is approximated by ($W + b$). Our experiments have shown that the error associated with measuring a thin crack width in this manner is less than 10% if the airgap is kept to a minimum. Therefore, the characteristic signal can be used to estimate crack width reasonably accurately.

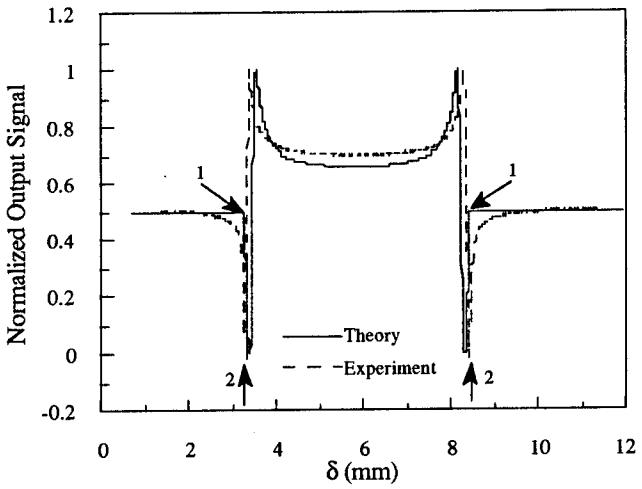

Fig. 4: Theoretical (_____) and experimental (-------) characteristic signals for a crack with $W = 0.84$ mm, $d = 1.53$ and $L = 10.7$ mm at 24 GHz, [31].

Fig. 5 shows the calculated standing-wave pattern inside the waveguide, as a function of ℓ, for a short circuit and when the above crack is at the center of the aperture ($y = b/2$). The shift in the standing-wave pattern that was mentioned earlier is apparent. It is also evident that if the diode detector were at locations 1 and 3 there would be a minimal amount of signal (voltage) difference between the short-circuit and the crack-terminated cases. However, when the diode detector probes the standing wave at location 2 there will be a maximum signal (voltage) difference between the two cases.

Fig. 6 shows the characteristic signals for a long crack with $W = 0.277$ mm and two depths of 0.96 mm and 1.488 mm at 24 GHz. The results of these experiments indicate that the distance between the voltage reversals remains unchanged since this distance is primarily a function of the crack widths. However, the signal magnitudes in the middle of the aperture are different and once calibrated may serve as an estimator of crack depth (as will be seen later, [34]).

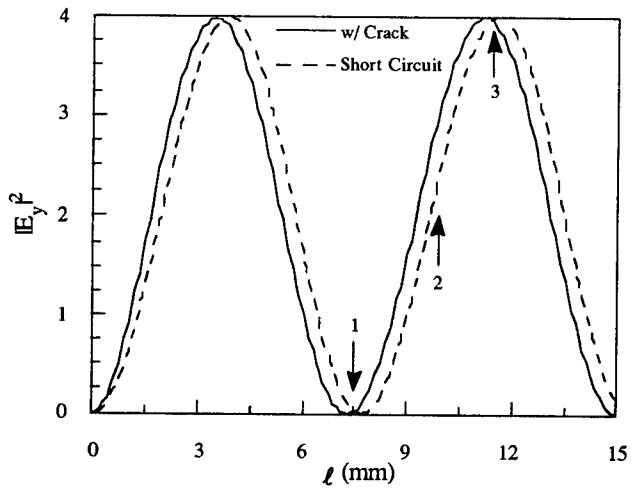

Fig. 5: Calculated standing-wave pattern inside the waveguide at 24 GHz: (_____) short circuit, (-------) crack with W = 0.84 mm and d = 1.53 mm at the center of the aperture, [31].

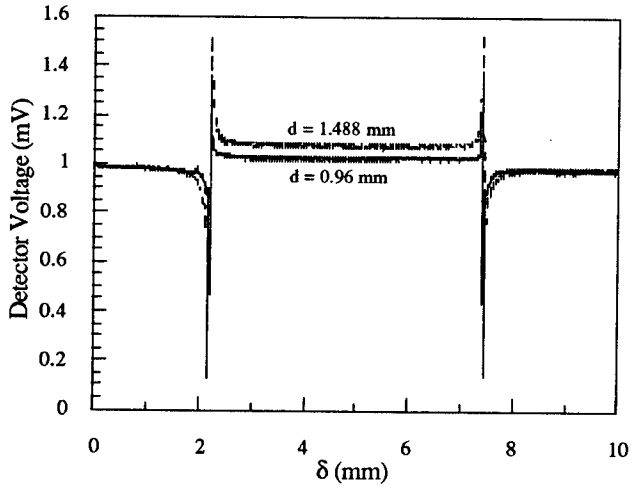

Fig. 6: Experimental characteristic signal for two cracks with W = 0.277 mm and different depths at 24 GHz, [31].

FINITE LENGTHED SURFACE CRACK DETECTION

A similar approach may be used to detect cracks whose lengths are smaller than the broad dimension of a waveguide, [31]. The theoretical derivation for this case is much more involved than for the long crack case. The reader is referred to reference [32] for the detailed derivation for this case. Fig. 7 shows the crack geometry with respect to the waveguide aperture for this case.

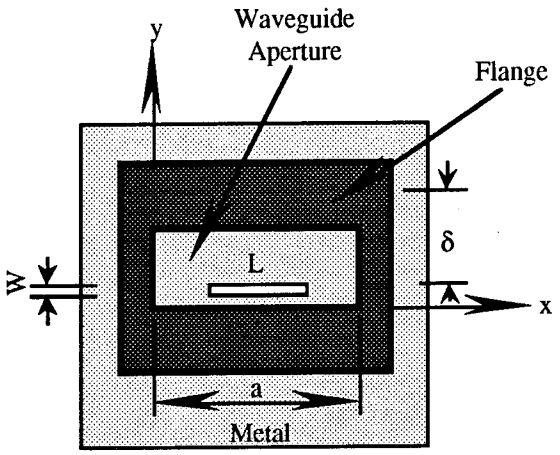

Fig. 7: Relative geometry of a finite crack and a waveguide aperture, [34].

A surface crack (slot) of 2 mm wide, 2 mm deep and 3.5 mm long was milled on an aluminum plate [32]. The two ends of this crack were cylindrical in shape due to the milling process. To reduce the computational complexity for comparing the theoretical and the experimental results, we used such a wide crack. A comparison of the theoretical and experimental results of this crack was conducted, at 38 GHz, to verify the integrity of the theoretical model for finite surface crack detection. The normalized (with respect to their respective short circuit values) theoretical and experimental crack characteristics signals for this crack are shown in Fig. 8. There is good agreement between the two results. The experimental crack characteristic signal is slightly wider than the theoretical one partly due to the presence of a slight airgap between the waveguide aperture and the sample (this effect is more apparent on the right hand side due to the uneven alignment between the sensor and the test surface). The difference in the middle part of these two characteristics signals is mainly due to the nonlinear properties of the diode detector, and partly due to the presence of the airgap.

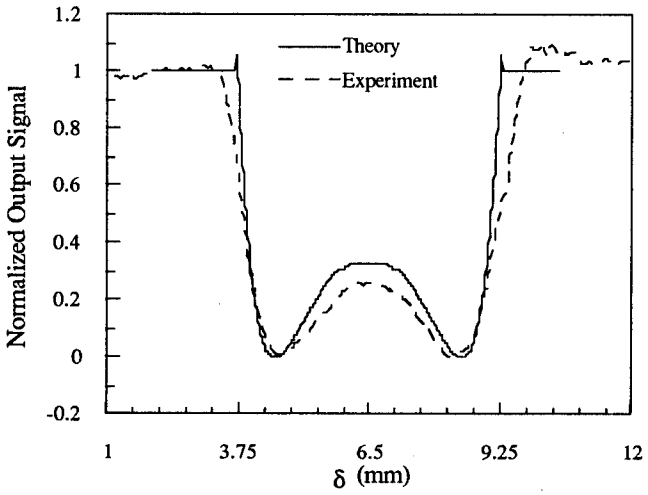

Fig. 8: Theoretical and experimental characteristic signals for a 2 mm wide, 2 mm deep, and 3.5 mm long crack at 38 GHz, [32].

When a crack is located closer to the center of the waveguide aperture in the x-direction, the magnitude of the incident electric field on the crack aperture is maximum. However, the change in the phase of the associated reflection coefficient is not so significant. This is because the reflection coefficient is determined by the over-all boundary conditions on the waveguide aperture (metal surface and the crack aperture). Since for finite cracks the crack length is smaller than the broad dimension of the waveguide (a), the effect of the perturbation due to the crack is less than when the crack length is equal to a. Hence, for a finite crack at different locations in the x-direction, there is not much difference in the corresponding characteristic signals. Fig. 9 shows the crack characteristic signals for a crack of 2 mm wide, 2 mm deep and 3.5 mm long at three different locations in the x-direction when the waveguide aperture scans the crack in the y-direction. The solid line illustrates the results for when one end of the crack is in contact with one of the small walls of the waveguide; the dotted line is for when the crack is at the center of the waveguide aperture; and the dashed line is for when the crack is located somewhere between the former two locations. Comparing these three characteristic signals, two observations can be made. The first observation is that the upper part of the solid line is wider than that of the other two. This is because in this case the perturbation due to the *finite* crack is less so that the airgap effect is more significant (i.e. radiation through the airgap widens the characteristic signal).

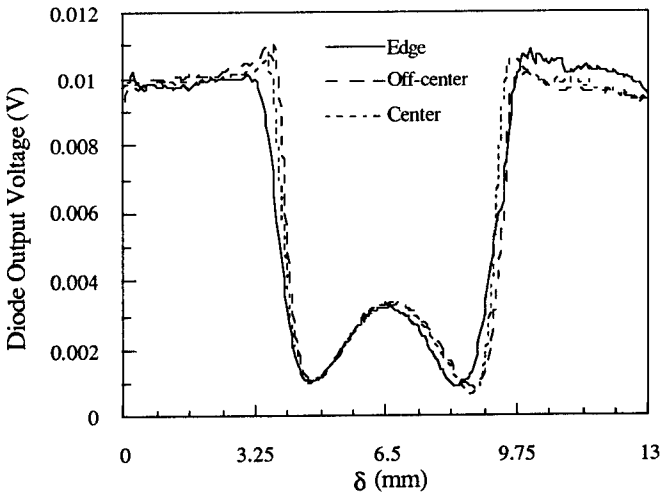

Fig. 9: Characteristic signals at 38 GHz for a 2 mm wide, 2 mm deep, and 3.5 mm long crack located in the x-direction at: a) center, b) edge, c) off-center within the waveguide aperture, [32].

The second observation is that the distance between the two outermost dips for the solid line is shorter than those of the other two characteristic signals. This feature may be used for crack location identification.

Fatigue cracks are the most difficult cracks to be detected nondestructively because they are very tight in nature. Hence, detecting fatigue cracks is the best way to test the capability of a technique. Pre-notched aluminum specimens were subjected to cycling load to produce fatigue cracks on them. A sketch of the specimen with a fatigue crack (with a width ranging between 2 to 5 microns, a length of 5.5 mm and an unknown depth) is given in Fig. 10. This crack was scanned with an open-ended waveguide sensor operating at 38 GHz [32]. The crack characteristic signal is shown in Fig. 11. During the test, only part of the crack length (about 4.5 mm) was within the waveguide aperture to simulate a finite crack. The test was conducted many times, and the results showed to be very repeatable. The distance between the two dips is about 4 mm which is slightly wider than the small dimension of the waveguide, 3.56 mm. This may be due to the small airgap between the specimen surface and the waveguide aperture. The general shape of the curve is similar to that shown in Fig. 8.

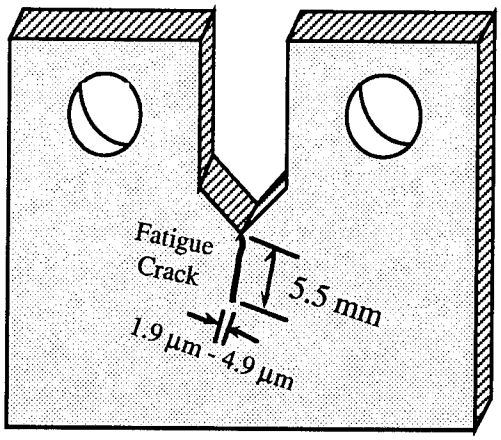

Fig. 10: Fatigue crack specimen used to obtain the characteristic signal shown in Fig. 11, [32].

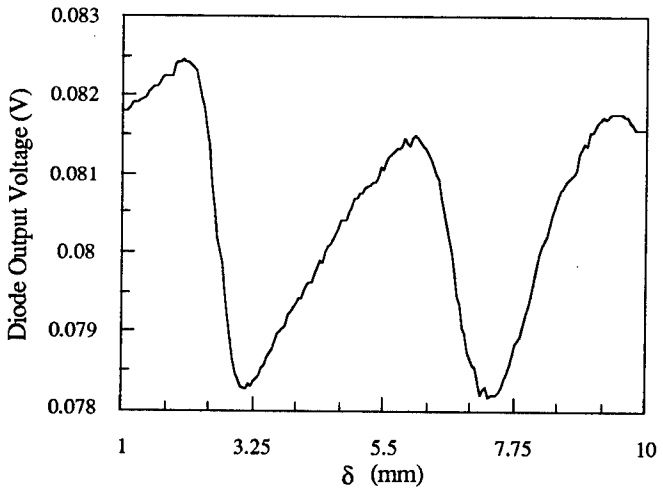

Fig. 11: Experimental characteristic signal at 38 GHz for a fatigue crack with W = 2 to 5 microns, L = 5.5 mm, and an unknown depth, [32].

CRACK DETECTION USING HIGHER ORDER WAVEGUIDE MODES

As mentioned earlier, in the absence of the crack only the dominant (incident and reflected) electric fields exist, namely $E_y(z)$. However, the presence of the crack generates an infinite number of reflected higher order TM (Transverse Magnetic) modes (for long cracks) in addition to the dominant mode. Assuming a dominant TE_{10} (Transverse Electric)

mode incident on the metal surface, the reflected TE_{10} and the higher order TM modes can be determined by forcing the boundary conditions at the metal surface and the boundaries inside the crack as the waveguide aperture scans over it [31].

In his case the x directed electric field component of the higher order modes can be measured for detecting a crack by appropriately placing a probe in the waveguide [33]. The reason for exploring the characteristics of these higher order TM modes for fatigue/surface crack detection is that in the absence of a crack there are no higher order modes present, hence theoretically the magnitude of the measured signal associated with higher order modes is zero. However, the presence of a crack generates higher order modes, and subsequently a finite amount of signal is measured. Hence, theoretically a signal-to-noise ratio (SNR) of equal to infinite is achieved which results in very sensitive (to the presence of a crack) measurements. In practice, however, the noise characteristics of the measurement system dictates the noise level. This high measurement sensitivity renders small fatigue/surface cracks (i.e. at their early stages of development) easily detectable. Moreover, it implies that for a given range of crack widths lower microwave frequencies can be used with relatively high detection sensitivity [33].

Fig. 12 shows the apparatus used for measuring the x-component of the overall electric field of the reflected higher order TM modes, $E_x(z)$. $E_x(z)$ is measured (via a crystal detector) by a small probe located at a distance ℓ near the waveguide aperture. The measured voltage, which is proportional to the power associated with the higher order modes (i.e. crystal detector operating in its square law region), is then recorded as a function of the scanning distance, δ. $\mathcal{T}$ is the distance between the probe and the waveguide wall, and as will be seen later the proper choice of this value can substantially increase the crack detection capability of this technique. Fig. 13 shows a close-up geometry of the relative location of the probe and the waveguide aperture.

Higher order TM modes are evanescent, i.e. their magnitudes decay exponentially with the distance from the waveguide aperture, ℓ [35]. However, close to the aperture their presence can be detected by sensing and measuring $E_x(z)$. Fig. 14 shows $|E_x(z)|^2$ as a function of ℓ for a crack with W = 0.5 mm, d = 0.5 mm and L = 10.67 mm at 24 GHz when the crack is at the edge of the waveguide. $|E_x(z)|^2$ represents the square law property of the crystal diode detector which is used in the actual measurements. The exponential decay of $|E_x(z)|^2$ as a function of ℓ is evident, and as ℓ increases beyond 1 mm the signal level substantially decreases.

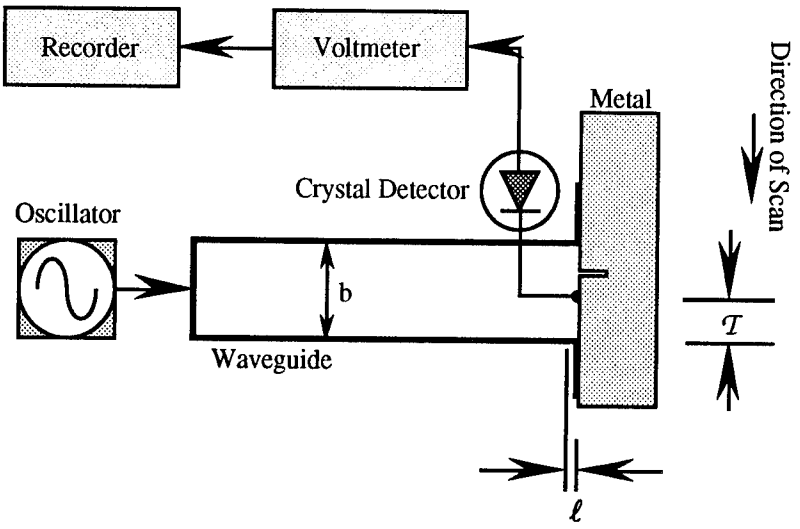

Fig. 12: Measurement apparatus, [33].

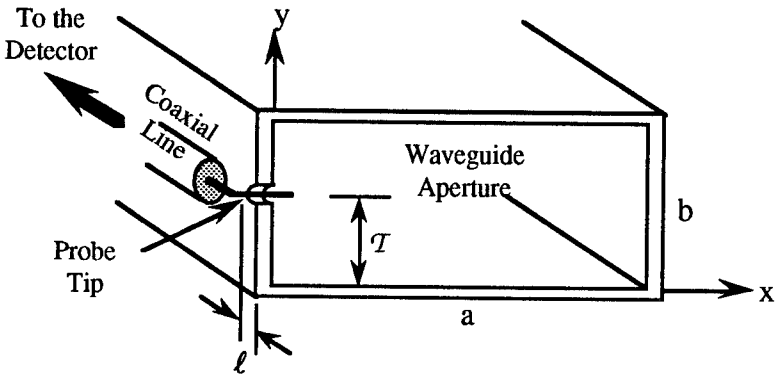

Fig. 13: A close-up geometry of the relative location of the probe and the waveguide aperture, [33].

To examine the optimal probe location for detecting the maximum magnitude of $E_x(z)$, two cracks with equal widths of 0.5 mm, equal lengths of 10.67 mm and respective depths of 1 mm and 1.5 mm were theoretically scanned. Fig.15 shows $|E_x(z)|^2$ as a function of $\kappa = (\mathcal{T}/b)$ at 24 GHz. The results show that maximum signal level occurs at $\kappa \approx 0.17$. The optimal probe location for any given crack size turns out to be a function of the waveguide dimension, b, and the operating frequency and is approximately in the range of $0.11 \leq \kappa \leq 0.20$ for the frequency range of 12.4 - 40 GHz.

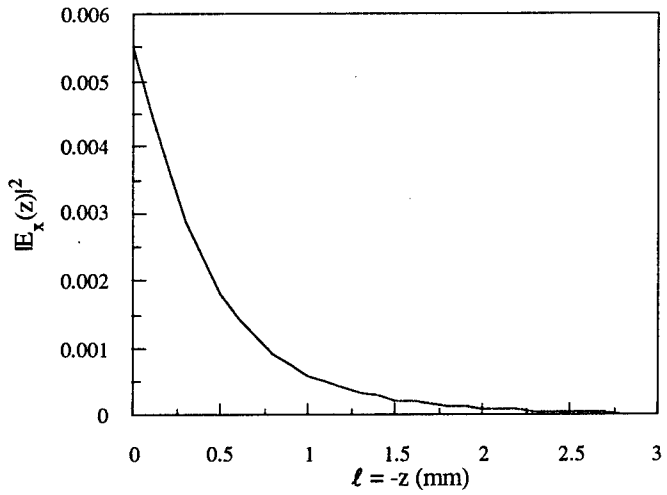

Fig. 14: $|E_X(\ell)|^2$ as a function of ℓ for a crack with W = 0.5 mm, d = 0.5 mm and L > 10.67 mm at 24 GHz, [33].

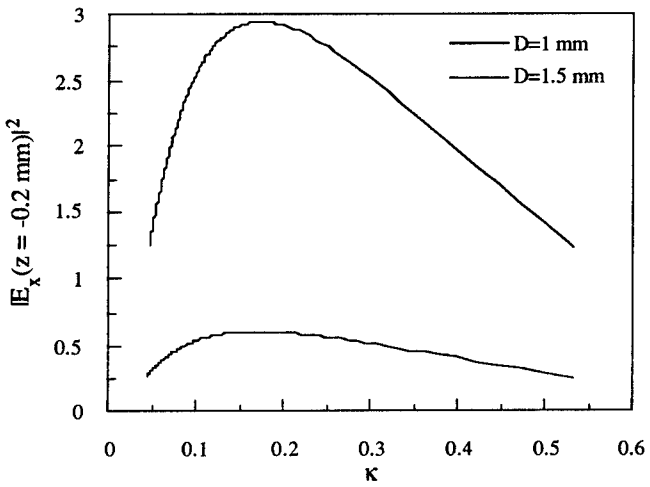

Fig. 15: Theoretical optimum probing location, $\kappa = T/b$, at 24 GHz for two cracks with equal widths of W = 0.5 mm, equal lengths of L = 10.67 mm and two different depths, [33].

Fig. 16 shows the theoretical variation of $|E_x(z)|^2$ as a function of the scanning distance δ for three different values of κ for a crack with W = 0.144 mm, d = 1.2 mm and L = 22.86 mm at 12.4 GHz. When the probe is in the middle of the waveguide (dashed line) two equal peak signal amplitudes are seen as the crack enters and exits the waveguide. When the probe location is at a distance $b/3$ from the broad wall of the waveguide (thick solid line) two unequal peak signal amplitudes are produced. The unequal peak signal amplitudes are due to the fact that when the crack enters the waveguide aperture it is closer to the probe than when it exits the waveguide aperture. Hence, the probe is influenced differently by the generated higher order TM modes. Finally, at the optimal probe location (thin solid line) the same phenomenon, as in the previous case, occurs. However, this time due to the optimal choice of the probe location, the higher of the two unequal peak signal amplitudes is at a higher level than its counterpart in the previous case. Clearly, the correct choice of probe location increases the crack detection capability.

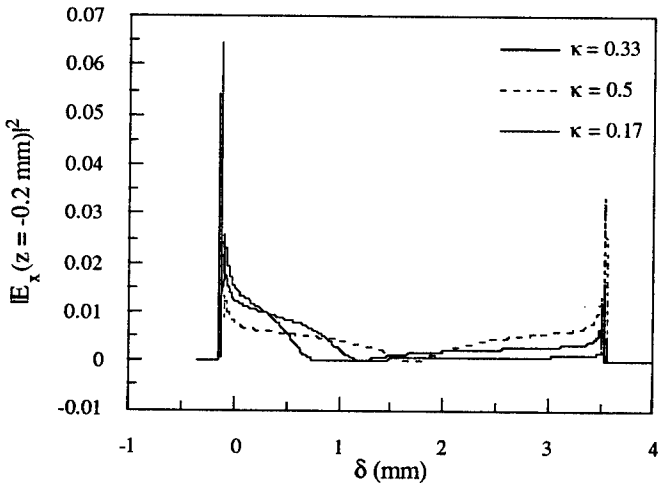

Fig. 16: $|E_x(z)|^2$ at z = -0.2 mm as a function of three different probe locations for a crack with W = 0.144 mm, d = 1.2 mm, and L = 22.86 mm at 12.4 GHz, [33].

Figs. 17 and 18 show the experimental results for the crack mentioned in Fig. 16 for two probe locations of κ = 0.5 and κ = 0.17, respectively. These results closely match, both in shape and relative magnitude, with the theoretical findings shown in Fig. 16. The results shown in Figs. 16-18 were calculated and measured at ℓ = 0.2 mm.

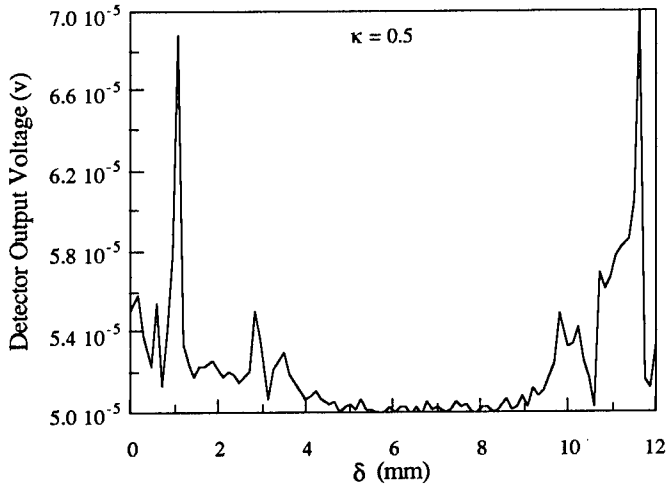

Fig. 17: Experimental result for a crack with $W = 0.144$ mm, $d = 1.2$ mm, and $L = 22.86$ mm at 12.4 GHz for $\kappa = 0.5$, [33].

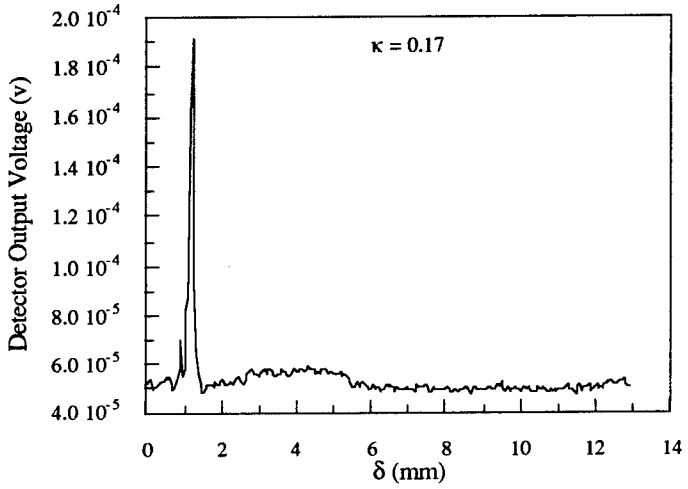

Fig. 18: Experimental result for a crack with $W = 0.144$ mm, $d = 1.2$ mm, and $L = 22.86$ mm at 12.4 GHz for $\kappa = 0.17$, [33].

To demonstrate the capability of this technique to detect very small cracks, a standard fatigue specimen was subjected to cyclical loading until a fatigue crack was generated as shown in Fig. 10. This crack was scanned by an open-ended waveguide operating at 38 GHz. Fig.19 shows the results of this experiment. The results show the capability of this technique to detect this fatigue crack (this experiment was repeated many times and each time the same results were obtained). The experiment was conducted in such a way as to ensure that the notch associated with the fatigue specimen was not exposed to the waveguide aperture during the scanning. From Fig. 19 a SNR $\cong$ 3 dB is evident which is quite adequate for detection. However, it must be mentioned that the voltmeter used in this experiment suffered from internal noise problem ($\approx$ 65 microvolts), but this was the only voltmeter in our laboratory compatible with the computer/recorder system. Not using a computer run recording system, we obtained data with a more sensitive voltmeter which had better, by an order of magnitude, noise characteristics (less than 6 microvolts). This translates to a SNR $\cong$ 13 dB. Another important measurement criterion is the resolution of the scanner which scans the waveguide over the metal surface (or vice versa).

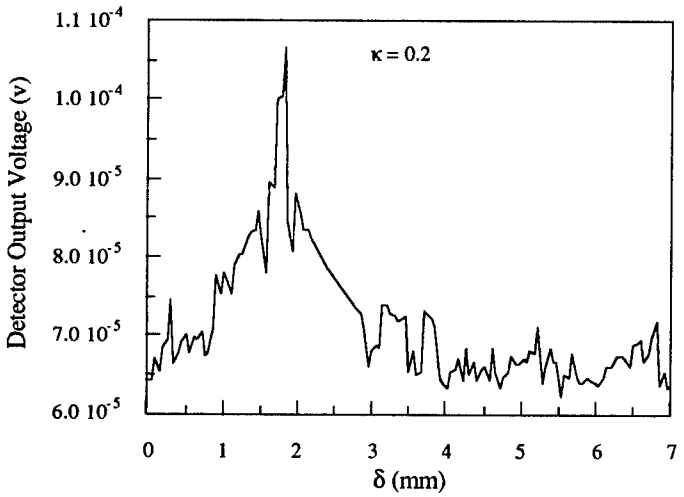

Fig. 19: Experimental result for the fatigue crack with shown in Fig. 10 at 38 GHz for κ = 0.20, [33].

COVERED CRACK DETECTION USING THE DOMINANT MODE APPROACH

The dominant and the higher order mode crack detection approaches which were discussed here have also been applied to covered cracks [36,37]. A covered cracks may be viewed from several different stand points, namely:

- a metal surface may be covered with a dielectric layer/coating such as paint
- the dielectric coating may be stratified such as paint, composites, etc.
- a non-coated or coated surface may be inspected by placing a layer of known dielectric material at the waveguide aperture to enhance crack detection sensitivity
- the presence of an airgap between the waveguide aperture and an exposed crack may be used as an optimization parameter
- the presence of an airgap provides for conducting noncontact measurements

Figs. 20a-20b show a covered crack with two different types of dielectric coatings [36]. These cracks may also be filled with the same dielectric or another material.

To demonstrate the potential and effectiveness of using an open-ended waveguide for covered crack detection several experiments were conducted. These experiments follow the dominant mode detection technique described earlier [31]. We used a metal specimen in which a long crack (slot) with a width of $W = 0.84$ mm and a depth of $d = 1.032$ mm was machined. This crack was scanned once without any dielectric coating on it (flush) at 24 GHz. Subsequently, the crack was scanned three times and each time an additional layers of a 0.1 mm-thick dielectric sheet (similar in properties to conventional paint) was used to cover the crack. The characteristic signals for these four cases are shown in Fig. 21. The sharp peaks, characteristic to measuring the uncovered crack, consistently broadened when the crack was covered with additional layers of the dielectric. This effect is due to radiation within the dielectric material. This is to say that the edges of the crack are exposed to the radiation before the edge of the waveguide aperture and the crack edge are lined up. Hence, during the measurement it is unlikely that due to a coarse scan step size, the transition corners are jumped over and not detected. This is an important practical issue since a scanner does not need to have a fine spatial scanning resolution to detect covered cracks. Thus, one may conclude that this microwave technique detects a surface crack easier when the crack is covered than when it is exposed.

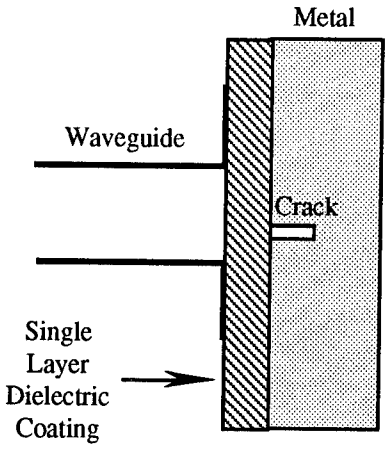

Fig. 20a: A crack covered with a single layer of a dielectric coating, [36].

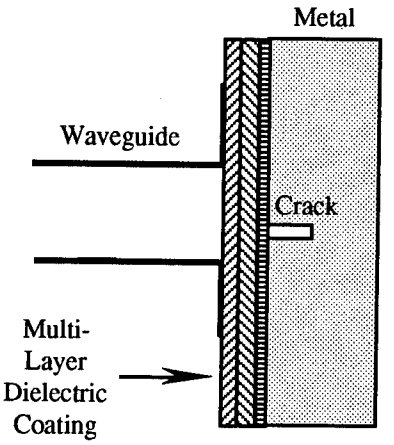

Fig. 20b: A crack covered with a stratified dielectric coating, [36].

COVERED CRACK DETECTION USING THE HIGHER ORDER WAVEGUIDE MODES

To demonstrate the potential and effectiveness of using higher order modes for covered crack detection several experiments were conducted. A metal specimen with a long crack with a width of $W = 0.277$ mm and a depth of $d = 2.475$ mm was used. This crack was scanned once without any dielectric coating on it (flush) at 12 GHz using the technique outlined earlier. Next, it was scanned two times and each time an additional layer of tissue paper was used to cover the crack. At 12 GHz tissue paper has the same dielectric properties as common paint, plastic, kevlar, synthetic rubber, etc.

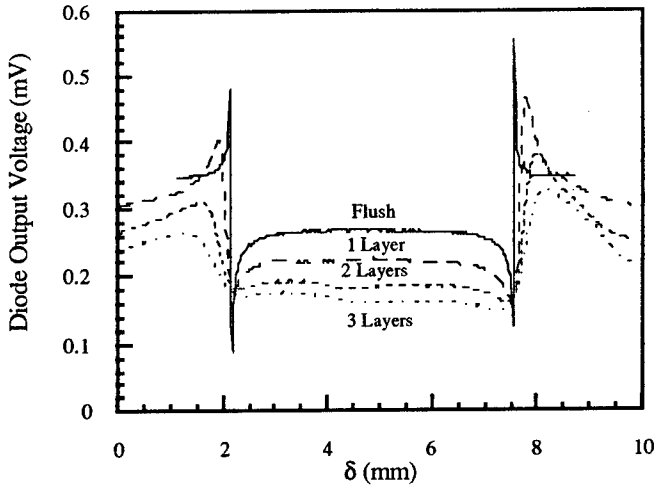

Fig. 21: Measured characteristic signals for a long crack with $W = 0.84$ mm and $d = 1.032$ mm at 24 GHz, exposed (flush) and covered.

Moreover, tissue paper has a relatively uniform thickness of about 0.1 mm. Fig. 22 shows the results of these measurements. The uncovered (flush) crack has a similar characteristics signal to those shown earlier. The sharp peak, characteristic to measuring the uncovered crack, consistently broadens when the crack is covered with additional layers of paper, and the signal amplitudes decay exponentially. This effect is due to radiation within the dielectric material (paper). Hence, during the measurement it is unlikely that due to a coarse scan step size, the transition corners are jumped over and not detected. This is an important practical issue, since a scanner does not need to have a high spatial scanning resolution.

Theoretically only one peak should show up when scanning the cracked surface. The difference seen in Fig. 22 is explained with an imperfect alignment between the waveguide and the metal surface under test. Nevertheless, even with a certain degree of misalignment, the crack was detected in all four cases. For a thicker and lossier dielectric coating the overall signal level will decrease.

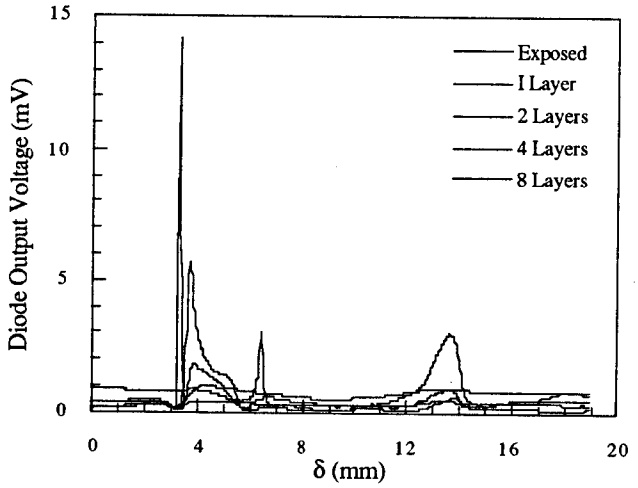

Fig. 22: Measured characteristics signals for a long crack with W = 0.277 mm and d = 2.475 mm at 12 GHz, uncovered (flush) and covered with paper.

CRACK SIZING

There are two basic approaches for determining the width and depth of a long crack using an open-ended waveguide probe [34]. Both of these approaches use the dominant mode detection scheme. In the first approach the characteristic signal of a crack is used to determine the width and the depth of a crack. This approach was mentioned briefly when discussing the dominant mode *crack characteristic signal.* Yeh and Zoughi have shown that using this method the width of a crack may be determined within ±20% and the depth within ±18% [34].

Since depth estimation is much more important in repair and fracture analysis, then accuracy of ±18% may not be sufficient for many applications. For this reason a swept frequency method was developed by which the depth of a crack may be estimated to within 1%, independent of how well the width may have been estimated [34].

Suppose the crack has a width equal to the small dimension of the waveguide aperture, b (unrealistic, but used here only for discussion purposes), the phase of the reflection coefficient (measured at the waveguide aperture) is then a linear function of the crack depth. In this case, when the crack depth is exactly equal to one quarter of the guide wavelength the phase of the reflection coefficient is 0^{o}. However, for

practical cases where the crack (slot) width is narrower than b, the change in the phase of the reflection coefficient becomes less abrupt as a function of crack depth. Since there is an induced current flowing along the crack surface, a mutual inductance exists between the two faces of the crack. The interaction between these currents causes a phase lag (maximum 90°) in addition to the phase lag which is a linear function of the crack depth $2d$. For narrower cracks this inductance is small until the crack depth reaches one quarter of the guide wavelength so that the currents on the two crack faces are in phase. In other words, for a narrow crack, when the crack depth reaches a certain value the phase of the reflection coefficient changes more abruptly than that for a wider crack, and this phase transition occurs at a larger depth. Fig. 23 shows three such transitions at 24 GHz for three cracks with widths of W = 20, 50 and 200 microns, respectively. It is evident that the transition is steeper for narrower cracks. Since the phase of the reflection coefficient for a narrower crack has a steeper transition characteristics and shifts to the right, it intersects with that for a wider crack at the lower part of the curve (e.g. around -115° in Fig. 23). From Fig. 23 one can see that the phase is not so sensitive to the variation of crack width. In other words, for a negative phase angle, the depth corresponding to a width of W =20 micron is not much different (in percentage) from that for a width of W = 50 microns or 200 microns. This is particularly true if the operating frequency is tuned such that a phase value of around -115° is detected.

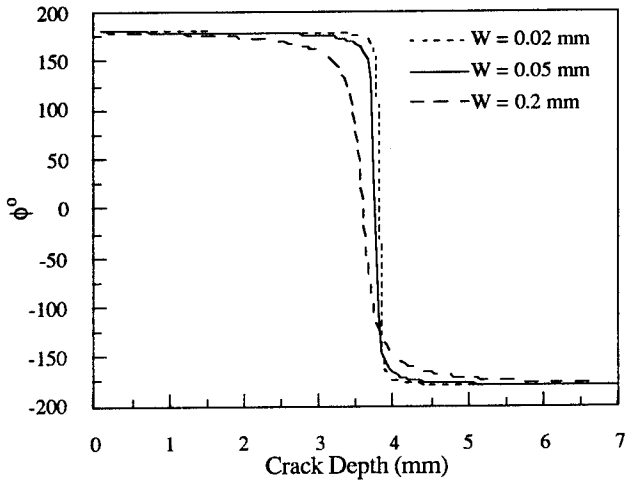

Fig. 23: Phase of the reflection coefficient vs. crack depth at 24 GHz for three crack widths of 20 microns, 50 microns and 200 microns, [34].

The reader is encouraged to consult with reference [34] since the topic of crack sizing deserves more detailed explanation that has been furnished here.

SUMMARY

In this chapter an attempt was made to familiarize the reader with different microwave methods for surface crack/slot detection and sizing. However, any extensive investigation in this area seemed to have halted by early 1980s. However, in the past four years there has been substantial activity in this area using open-ended rectangular waveguide methods. Thus, a detailed description of these recent activities was presented in this chapter.

A new, simple and sensitive method for detecting long straight surface cracks in metals using an open-ended rectangular waveguide was described. This method, established via numerous experimental investigations, was also modelled electromagnetically. The modelling approach relies on properly forcing boundary conditions at the waveguide aperture. The significant phase reversal, when the crack is at the waveguide edges, makes this technique a very sensitive one for crack detection. Thus, this method is capable of detecting very thin cracks (fatigue and stress) at relatively low microwave frequencies. As expected, higher frequencies can be used to detect cracks with widths as narrow as a few microns. This technique is also suitable for estimating the crack dimensions. The use of this approach for filled and covered cracks was also presented.

A novel microwave open-ended waveguide technique, using higher order modes, for detecting fatigue/surface cracks in metals was described. The theoretical foundation of this technique was also given. The results of several experiments were given to verify the theoretical findings and the capability of this technique for detecting very small fatigue/surface cracks. This technique offers several important advantages over the existing non-microwave and microwave techniques the least of which is the overall simplicity. It was shown that the design of the open-ended waveguide probe can be optimized for maximum detection capability. The inherent high SNR (theoretically SNR $\cong \infty$) associated with this technique makes it suitable for detecting very small cracks at relatively low microwave frequencies. The results showed that a fatigue crack whose width was less than 5 micrometer could be repeatedly detected at 38 GHz with consistently high SNR. It must be noted that the length of the probe inside the waveguide must be kept very short such that it does not interfere with the signal inside, and yet long enough to pick up the signal for detection. This usually means that, depending on the operating frequency, the length of the probe

should be a fraction of a millimeter. Although modifications to the open-ended waveguide will allow detection of cracks on curved surfaces, the present approach can still be applied to surfaces with large curvatures (aircraft wings) at frequencies lower than 38 GHz.

Successful covered crack detection was also demonstrated using two different approaches: the dominant mode and the higher order mode detection.

Two simple microwave techniques for crack sizing on metal surface were mentioned. It was briefly discussed that crack width and depth can be measured with an accuracy of about ±20% using crack *characteristics signals*, while using a swept frequency approach crack depth can be measured with an accuracy of better than 1% independent of how accurate the width is estimated.

REFERENCES

[1] Yeh, C.Y., "Detection and Sizing of Surface Cracks in Metals Using Open-Ended Rectangular Waveguides," Ph.D. Dissertation, Electrical Engineering Department, Colorado State University, May 1994.

[2] Bahr, A. J., "Microwave Nondestructive Testing Methods," Volume I, Gordon and Breach Science Publishers, 1982.

[3] Feinstein, L., and R.J. Hruby, "Surface Crack Detection by Microwave Methods," 6th Symp. on Nondestructive Evaluation of Aerospace and Weapons Systems Components and Materials, San Antonio, Texas, 1967.

[4] Feinstein, L., and R.J. Hruby, "AIAA Paper 68-321, AIAA/ASME 9th Structures, structural Dynamics, and Materials Conference," Apr. 1968.

[5] Hruby, R. J., and L. Feinstein, "A novel Nondestructive, Noncontacting Method for Measuring the Depth of Thin Slits and Cracks in Metals," Rev. of Sci. Inst., vol 41, no. 5, pp. 679-683, May 1970.

[6] Bahr, A.J., "Microwave Eddy-Current Techniques for Quantitative Nondestructive Evaluation," in Eddy-Current Characterization of Materials and Structures, ASTM STP 722, G. Birnbaum and G. Free eds., American Society for Testing and Materials, pp. 311-331, 1981.

[7] Bahr, A.J., "Microwave Eddy-Current Techniques for Quantitative Nondestructive Evaluation," Proceedings of DARPA/AF Review of Progress in Quantities NDE, La Jolla, California, July 1980.

[8] Gysel, U.H., and L. Feinstein, "Design and Fabrication of Stripline Microwave Surface-Crack Detector for Projectiles," Final Report, Contract DAAG46-73-C-0257, SRI Project 2821, Stanford Research Institute, Menlo Park, California, Aug. 1974.

[9] Robinson, L.A., and U.H. Gysel, "Microwave Coupled Stripline Surface Crack Detector," Final Report, Contract DAAG46-72-C-0019, SRI Project 1490, Stanford Research Institute, Menlo Park, California, Aug. 1972.

[10] Husain, A., and E. A. Ash, "Microwave Scanning Microscopy for Nondestructive Testing," Proc. of the 5th European Microwave Conf., Hamburg, Germany,pp 213-217, Microwave Exhibitions and Publishers Ltd., Kent, England, Sept. 1975.

[11] Bahr, A.J., and J.P. Watjen, "Novel Eddy-Current Probe Development," Semiannual Report, Contract F33615-80-C-5025, SRI Project 1908, SRI International, Menlo Park, California, Feb. 1981

[12] Auld, B.A., "Theory of Ferromagnetic Resonance Probes for Surface Cracks in Metals," G.L. Report 2839, E.L. Ginzton Laboratory, Stanford University, Stanford, CA, July 1978.

[13] Auld, B.A., A. Ezekial, D. Pettibone and D.K. Winslow, "Surface Flaw Detection with Ferromagnetic Resonance Probes," Proceedings of DARPA/AF Review of Progress in Quantitative NDE, La Jolla, California, July 1979.

[14] Auld, B. A., F. Muennemann and D.K. Winslow, "Surface Flaw Detection with Ferromagnetic Resonance Probes," Proceedings of DARPA/AF Review of Progress in Quantitative NDE, La Jolla, California, July 1980.

[15] Auld, B.A., "Theoretical Characterization and Comparison of Resonant-Probe Microwave Eddy-Current Testing with Conventional Low-Frequency Eddy-Current Methods," in Eddy-Current Characterization of Materials and Structures, ASTM STP 722, G. Birnbaum and G. Free eds., American Society for Testing and Materials, pp. 332-347, 1981.

[16] Auld, B. A., "Ferromagnetic Resonance Flaw Detection," Phys. Tech, Vol. 12, July 1981, pp.149-154.

[17] Auld, B. A., F. Muennemann and D.K. Winslow, "Eddy-Current Probe Response to Open and Closed Surface Flaws," J. Nondestr. Eval., vol. 2, March 1981, pp. 1-21.

[18] Auld, B. A., F. Muennemann and D.K. Winslow, "Observation of Fatigue-Crack Closure Effects with the Ferromagnetic Resonance Eddy-Current Probe," G. L. Report No. 3233, E. L. Ginzton Laboratory, Stanford University, Stanford, California, March 1981.

[19] Auld, B.A., and D.K. Winslow, "Microwave Eddy-Current Experiments with Ferromagnetic Resonance Probes," in Eddy-Current Characterization of Materials and Structures, ASTM STP 722, (G. Birnbaum and G. Free eds.), American Society for Testing and Materials, pp. 348-366, 1981.

[20] Prince, J.M., and B.A. Auld, "Development of Active Microwave Ferromagnetic resonance Eddy Current Probes and Associated Signal Processing Method," Review of Prioress in QNDE, vol.3, Proceedings of the Tenth Annual Review, Santa Cruz, CA, pp. 1369-1376, 7-12 Aug. 1983.

[21] Ash, E.A., and A. Husain,"Surface Examination Using a Superresolution Scanning Microwave Microscope," Proc. of the 3rd European Microwave Conf., pp c.15.2., 1973.

[22] Auld, B.A., "New Methods of Detection and Characterization of Surface Flaws," Proceedings of DARPA/AF Review of Progress in Quantitative NDE, Cornell University, New York, June 1977.

[23] Auld, B.A., G. Elston, D.K. Winslow and C.M. Fortunko, "Surface Flaw Detection with Ferromagnetic Resonance Probes," Proceedings of DARPA/AF Review of Progress in Quantitative NDE, La Jolla, California, July 1978.

[24] Bahr, A.J., "Using Electromagnetic Scattering to Estimate the Depth of a Rectangular Slot," IEEE Trans Antennas Propagation, vol. AP-27, pp. 739-746, Nov. 1979.

[25] Bahr, A.J., "Microwave Eddy-Current Techniques for Quantitative Nondestructive Evaluation," Proceedings of DARPA/AF Review of Progress in Quantities NDE, La Jolla, California, July 1980.

[26] Bahr, A.J., "System Analysis of Eddy-Current Measurements," Review of Progress in QNDE vol. I, Proc. of the Eight Air Force/Defence Advanced Research Projects Agency Symposium on QNDE, Boulder, Colorado, 2-7 Aug., 1981, pp. 375-386.

[27] Dalton, B. L., "Microwave Noncontact Measurement and Instrumentation in Steel Industry," Jour. of Mic. Power, vol. 8, no. 3, pp. 235-244, 1973.

[28] Ash, E.A., and A. Husain,"Surface Examination Using a Superresolution Scanning Microwave Microscope," Proc. of the 3rd European Microwave Conf., pp c.15.2., 1973.

[29] Ishii, T., "Microwave Sensing Technique of Surface Hair Line Cracks of Fast Moving Objects," J. of Microwave Power and EM Energy, vol. 23, no.3, pp. 176-182, 1988.

[30] Ostapenko, V.D. and N.P. Kalinin, "Microwave Eddy-Current Transducer for Monitoring Metals," Sov. J. Nondestr. Test., vol. 19, no 1, Jan. 1983, pp. 40-44.

[31] Yeh, C.Y., and R. Zoughi, "A Novel Microwave Method for Detection of Long Surface Cracks in Metals," IEEE Trans. on Inst. and Meas., vol. IM-43, no. 5, pp. 719-725, Oct. 1994.

[32] Yeh, C.Y., and R. Zoughi, "Microwave Detection of Finite Surface Cracks in Metals Using Rectangular Waveguide Sensors," To appear in the Research in Nondestructive Evaluation, 1995.

[33] Yeh, C.Y., E. Ranu and R. Zoughi, "A Novel Microwave Method for Surface Crack Detection Using Higher Order Waveguide Modes," Materials Evaluation, vol. 52, no. 6, pp. 676-781, June 1994.

[34] Yeh, C.Y., and R. Zoughi, "Sizing Techniques for Surface Cracks in Metals," To appear in the Materials Evaluation, 1995.

[35] Pozar, D.M., "Microwave Engineering", Addison Wesley, Chapter 4, New York, NY, 1990.

[36] Huber, C., and R. Zoughi, "Microwave/mm-Wave Detection of Surface cracks Under Stratified Dielectric Coatings Using an Open-Ended Rectangular Waveguide," ASNT Fall Conference'94, Atlanta, GA, Sept. 19-23, 1994.

[37] Huber, C., and R. Zoughi, "Higher Order Modes as Indicators of Surface Cracks Under Stratified Dielectric Coatings Using an Open-Ended Waveguide," To appear in the Review of Progress in Quantitative NDE, vol. 14, 1995.

CHAPTER 5

DEFECT DETECTION IN THICK COMPOSITES

The utility of microwave and millimeter wave inspection of dielectrics has been mentioned several times throughout this report. The application of microwave and millimeter wave NDE to thick dielectric composites will be discussed in this chapter along with the presentation of examples associated with some recent investigations in this area.

The increased use of thick composites both for industrial and military applications presents quite a challenge to nondestructive testing (NDT). Difficulties arise from the inherent anisotropy and physical property variations of these materials, as well as their relative high density causing excess absorption and scattering of signals used in several conventional NDE methods. The ability of microwaves to penetrate deeply inside dielectric materials makes microwave NDT&E techniques very attractive for interrogating such type of materials. The same applies to structures made of thick composites. Additionally, the sensitivity of microwaves to the presence of dissimilar layers in these materials allows for accurate thickness variation measurement in the range of a few micrometers at 10 GHz as discussed in Chapter 3.

Microwave NDT techniques, applied to thick composites are performed on a contact or non-contact basis. In addition, these measurements may be conducted from only one side of the sample (reflection techniques). When compared with ultrasonic techniques, microwave methods require no coupling material (e.g. oil or water), and do not suffer as much from high signal attenuation due to internal scattering. Microwave NDT techniques are also easily adaptable to on-line measurement environments which offer the possibility of in-process control during the manufacturing of thick composites. This feature produces results such that the final product may not need extensive post process inspection, and may only require occasional testing once under loading for detection of in-service created defects.

Microwave NDT techniques are also capable of material characteristic identification and classification as discussed in Chapter 2. It has also been shown that microwaves have the ability to detect voids, delaminations and porosity variations in a variety of dielectric materials. The same is particularly applicable to thick composite structures. The

polarizability of microwave signals enables the study of fiber bundle orientation or misalignment during manufacturing. This same feature may also provide information about cut or broken fiber bundles inside a thick composite member. The accurate sizing of flaws and defects should also be possible with microwave techniques. Furthermore, a modulated microwave technique may provide information about the depth of a defect.

As discussed in Chapter 3, there are two basic approaches for inspecting thick composites, namely the far-field and the near-field methods. The same advantages and disadvantages that were discussed in Chapter 3 apply here as well. Most if not all of the theoretical investigations in imaging embedded defects consider the far-field case since a plane wave approach renders significantly less complicated and rigorous theoretical derivations. Quite a few of these investigations have dealt with the issue of probing radars (references [170-194] of Chapter 1). There has also been some recent activities in the theoretical realm of microwave imaging [1,2]. Other investigators have incorporated dielectric lenses for obtaining a smaller footprint when imaging a composite structure [3-6].

Near-field microwave imaging has received considerable attention recently. These efforts have included looking into concrete structure, thick glass reinforced composites, thick sandwich composites and impact damage which is considered a surface defect [7-10]. The primary focus of this chapter will be on these recent activities.

NEAR-FIELD IMAGING OF THICK GLASS REINFORCED COMPOSITES

A set of experimental results obtained using a simple microwave technique to inspect thick composite structures with embedded defects is presented here [8]. Images of thick composite panels with known defects were created using a voltage signal related to the amplitude or phase of the reflection coefficient (or the reflected wave). The effect of standoff distance and frequency for image enhancement is also investigated.

The sample materials used in this study were fabricated from S-2 glass reinforced polyester composite. This suite of samples was developed by the Army Research Laboratory for a series of NDE tests; they were not specifically intended for microwave measurements. However, they do contain intentionally introduced flaws and defects and they have been tested and characterized using a variety of NDE techniques [11]. Some of the defects, such as inclusions, were embedded in during hand lay-up prior to cure. Others, such as flat bottom holes, were drilled into the

cured panel. The nominal sizes of the panels are 200 mm square by 38 mm thick and 190 mm square by 25 mm thick. The density of the panels is 1.7 g/cm^3.

The setup used to conduct the measurements described here is shown in Fig. 1 which depicts the side and plan views of an open-ended waveguide sensor scanning a thick composite panel with an embedded defect, [8]. As the open-ended rectangular waveguide transmits a microwave signal into the thick composite, the voltage related to the phase or magnitude of the reflection coefficient, detected in the same probe, is continuously recorded while the waveguide scans over the thick composite.

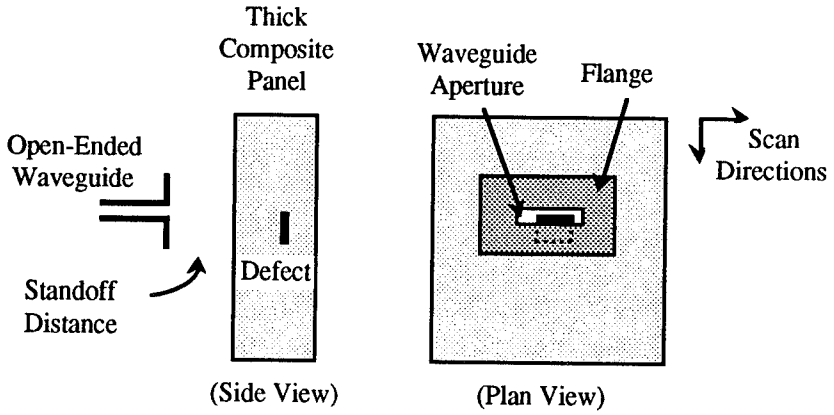

Fig. 1: Side and plan views of the relative geometry of an open-ended waveguide sensor and a thick composite panel with an embedded defect, [8].

To conduct this experimental study three thick composite panels from the suite of characterized standard materials were used. Fig. 2 shows a section of a 38 mm (1.5") thick glass reinforced polymer composite panel with three embedded aluminum inclusions of 25.4 mm x 25.4 mm, 12.7 mm x 12.7 mm and 6.35 mm x 6.35 mm, (all 0.8 mm thick) at a depth of 19 mm from the surface. This sample was scanned at a frequency of 10.5 GHz (wavelength of 28.6 mm in free-space), with the waveguide sensor in contact with the sample surface. Fig. 3 shows the plan view of an amplitude scan (i.e. the voltage measured is related to the amplitude of the reflection coefficient at the aperture of the waveguide) conducted in a contact fashion. The scanned area was 150 mm by 58 mm. The horizontal and the vertical scan steps were 0.5 mm and 2 mm, respectively, for this and all the subsequent scans of this study. Using these raw data without any signal/image processing

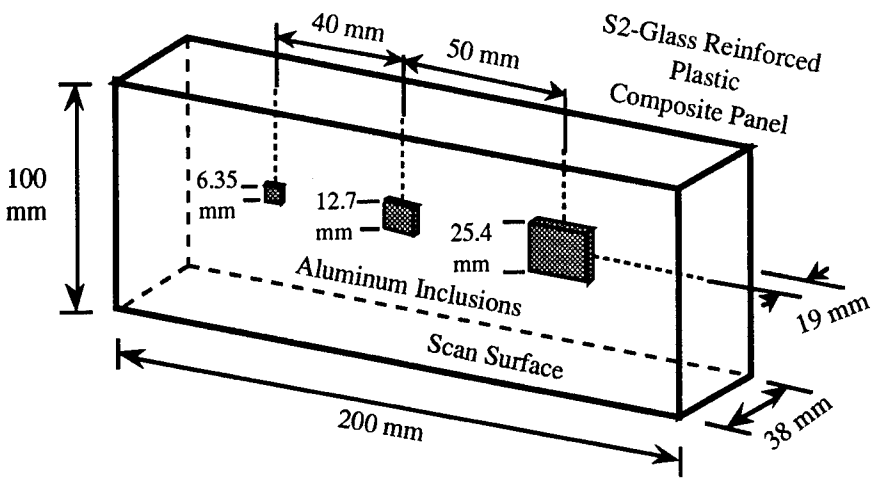

Fig. 2: Geometry of a thick composite panel with 3 aluminum defects of different sizes at the same depth, [8].

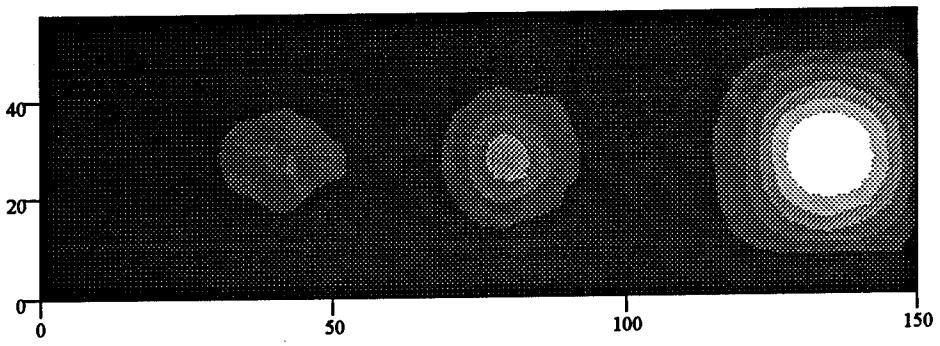

Fig. 3: A plan view amplitude scan of the composite shown in Fig. 2 at 10.5 GHz, the contour plot dimensions are in mm, [8].

enhancement, and without any optimization of the measurement parameters (frequency and standoff distance), all three defects are distinctly detected. A strong indication of the relative size of each defect is also evident. The measured distances between the centers of the defects obtained from the image correspond well with the actual distances.

The second panel which was also made of a 38 mm thick glass reinforced polymer composite is shown in Fig. 4, [8]. The area scanned from this sample had two flat bottom holes with diameters of 6.35 mm at 19 mm and 25.5 mm from the surface of the sample, respectively. The scanned area was 100 mm by 22 mm. A scan of this sample was conducted in a contact fashion at a frequency of 24 GHz (wavelength of 12.5 mm in free-space), since this frequency showed to be more sensitive to the presence of these holes (additionally at higher frequencies the waveguide aperture is smaller and hence the measurements are more sensitive, spatially, to the presence of objects). The raw data image shown in Fig. 5 shows a clear indication of both holes (voids) and the signal strength in each case is related to the depth of each hole. The darker spot is due to the deepest hole (the one with its bottom closer to the scan surface). The measured distance between the two hole centers on the image closely matches the actual distance between the centers on the panel. Two adjacent regions of relative high intensity are seen on each side of the holes. They are attributed to the hole walls, and the possible interference between the hole side walls. It is important to note that other NDE techniques that had been used to study this particular sample (ultrasonics and thermal imaging) did not detect these holes [11]. Difficulties with ultrasonics and thermal imaging was found to be a result of the interference caused by a very large area disbond in near surface laminates. This additional unintentional masking defect did not interfere with the microwave measurements because microwaves could penetrate through the disbond and interrogate the following layer. It is important to note that the detection of near surface disbonding and voids with microwaves could also be possible with some tuning of the measurement parameters in such a way that the measurement results would be sensitive to the presence of disbonded layers.

To improve the contrast (difference between the signal due to the defect and the background signal) in the image, other amplitude scans at several standoff distances were conducted, [8]. Fig. 6 shows an image of a non-contact scan at 24 GHz of the same panel at a standoff distance of 0.5 mm. The indications of the holes on this image are much stronger than those shown in Fig. 5 (i.e. higher contrast). This illustrates the importance of the choice of the standoff distance. This is an example of how a measurement may be optimized for contrast enhancement. It has been shown that the frequency of operation and the standoff distance may be tuned to increase measurement sensitivity including sensitivity to the presence of a defect.

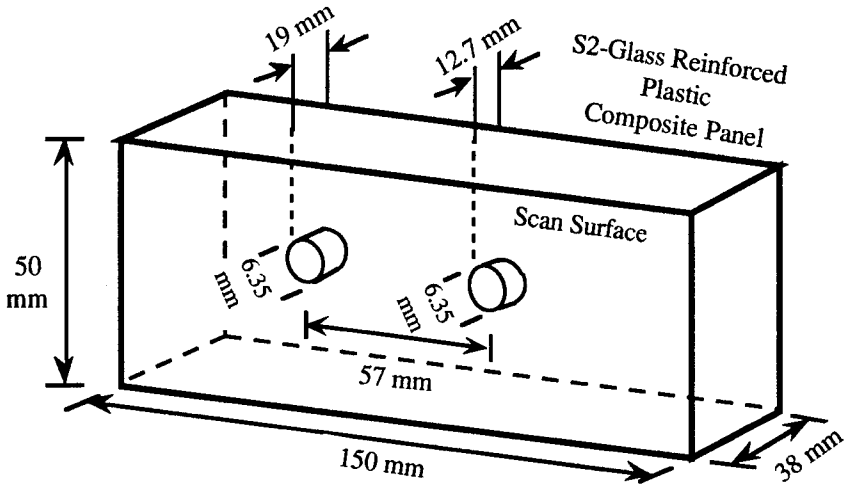

Fig. 4: Geometry of a thick composite panel with two flat bottom cylindrical holes cut out of the panel, [8].

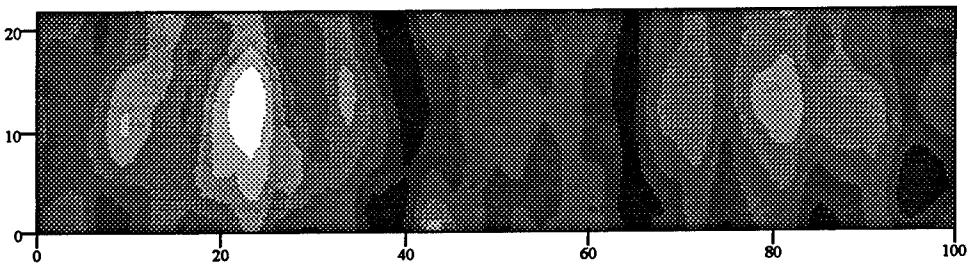

Fig. 5: A plan view of an amplitude scan of the composite shown in Fig. 4 at a frequency of 24 GHz, [8].

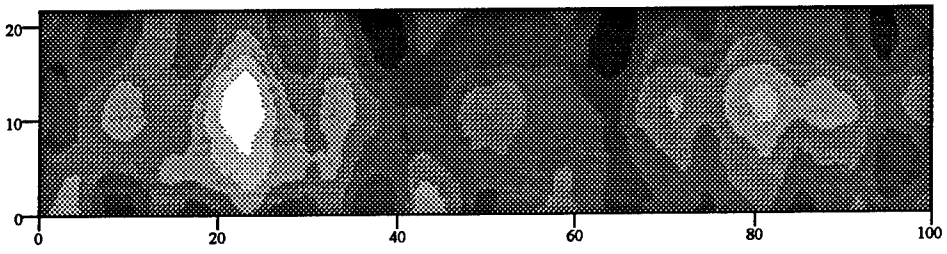

Fig. 6: A plan view of an amplitude scan of the composite shown in Fig. 4 at a frequency of 24 GHz and a standoff distance of 0.5 mm, [8].

The third panel, shown in Fig. 7, was made of a 25.4 mm (1") thick glass reinforced polymer composite, [8]. This sample had an aluminum inclusion of 6.35 mm x 6.35 mm x 0.8 mm located at a distance of 12.7 mm from the surface of the sample. A phase scan (i.e. the voltage used to generate the image is related to the phase of the reflection coefficient at the waveguide aperture) was performed at a frequency of 10.5 GHz in a contact fashion. The scan covered an area of 85 mm by 98 mm. Fig. 8 shows the plan view of this scan. The contrast is very high, and defect is clearly visible.

As was mentioned earlier, the measurement parameters (frequency of operation and standoff distance) may be varied to optimize for a given measurement. To demonstrate this, two measurements were performed in which the standoff distance between the sensor and the surface of the sample was changed. In the first measurement the sensor was pointing directly at the defect (maximum signal), and in the second one it was pointing at a non-defect area (background or minimum signal). Subsequently, the standoff distance was changed, and the voltage proportional to the phase of the effective reflection coefficient at the aperture of the waveguide was recorded (Fig. 9). The results show that operating at a standoff distance of 0 mm (in contact) and at this frequency (10.5 GHz) the difference between the signals due to defective and non defective areas is maximum. On the other hand, if a standoff distance of around 5 mm or 13 mm is used, there will be no distinction between these two areas of the panel. Another observation is that, operating at a standoff distance of between 5 mm to 13 mm the contrast in the image is reversed. Also, operating in the range where the phase variation as a function of the standoff distance is almost constant (7-10 mm) is important from a practical point of view since slight changes in the standoff distance do not influence the outcome significantly. To illustrate these observations, a phase scan of this sample at a standoff distance of 9 mm was produced. Fig. 10 shows that the contrast is reduced (i.e. the dynamic range is less) and reversed (compared to the results of Fig. 8). However, at this standoff distance, the fiber bundle orientation seems to be more visible than that of Fig. 8. This is another indication of the sensitivity of the standoff distance to different sample characteristics (e.g. small thickness variation).

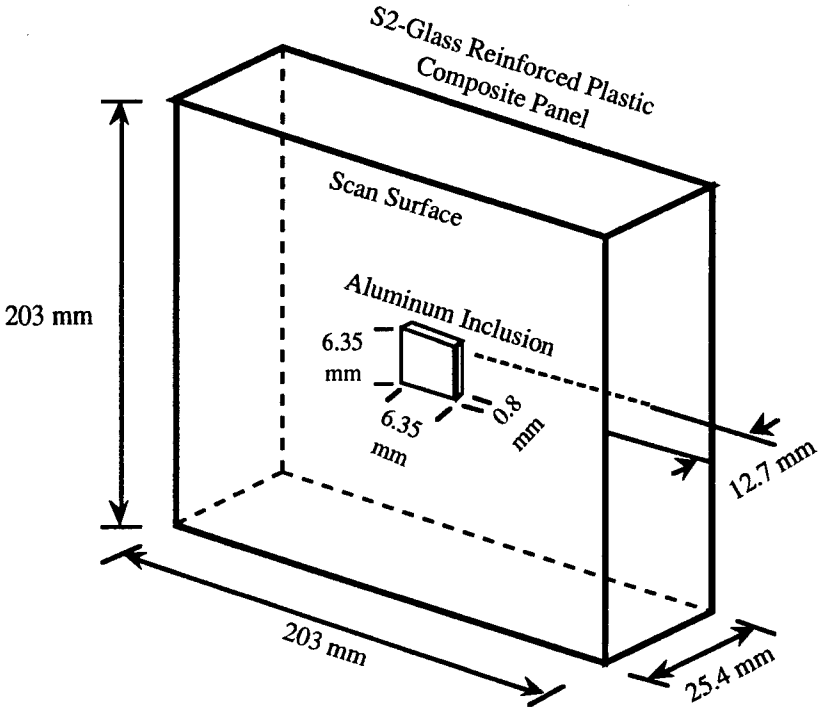

Fig. 7: Geometry of a thick composite panel with an aluminum inclusion embedded at the center of the panel, [8].

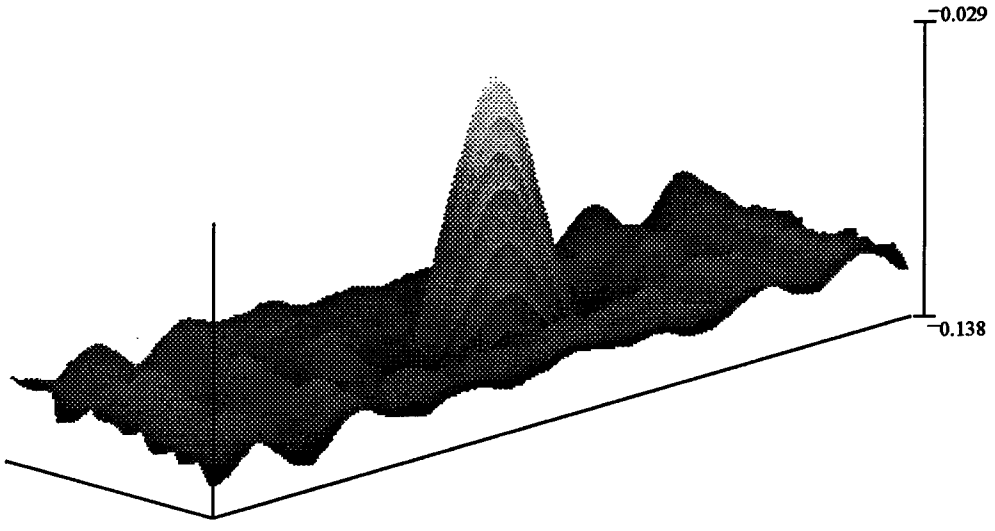

Fig. 8: An in-contact intensity level phase scan of the composite shown in Fig. 7 at a frequency of 10.5 GHz, [8].

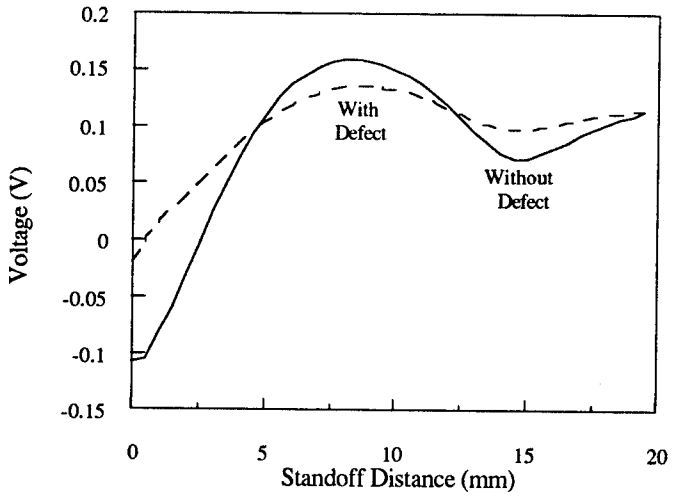

Fig. 9: The voltage (related to the phase) with and without a defect as a function of the standoff distance, [8].

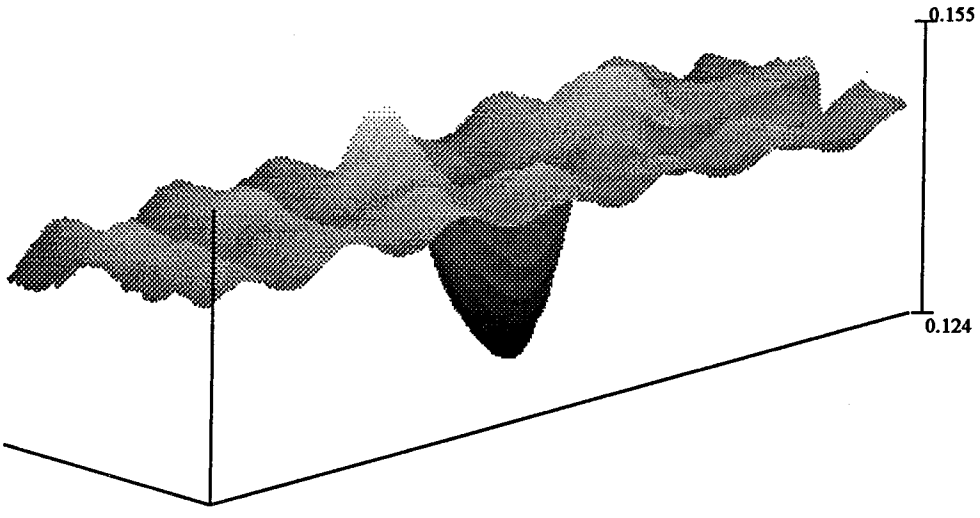

Fig. 10: A intensity level phase scan of the composite shown in Fig. 7 at a standoff distance of 9 mm and a frequency of 10.5 GHz, [8].

NEAR-FIELD IMAGING OF THICK SANDWICH COMPOSITES

Two thick sandwich composite samples (foam and honeycomb) were specially prepared for this study [9]. Each sample was made of fiberglass epoxy laminate skin and core material (foam or honeycomb), backed by a conducting sheet as shown in Fig. 11. Special defects including two delaminations between sample layers and an impact damage to the sample surface were created in the samples during the sample production. Two 76.2 mm (3") diameter pieces of 0.127 mm (5 mil)-thick mylar were used to simulate delaminations. The edges of the mylar circles were held together with a mylar tape (approximately 0.076 mm (3 mils) thick), so that the edges of the disbond are thicker. A skin delamination (defect 2) was produced as described and was placed between the skin and the core. Defect 3 was a disbond placed between the core and the conducting sheet. Defect 1 was a surface impact damage, created after cure, from a 5 kg (11 lb.) steel ball dropped on the sample with a 67.8 J (50 ft-lb.) energy.

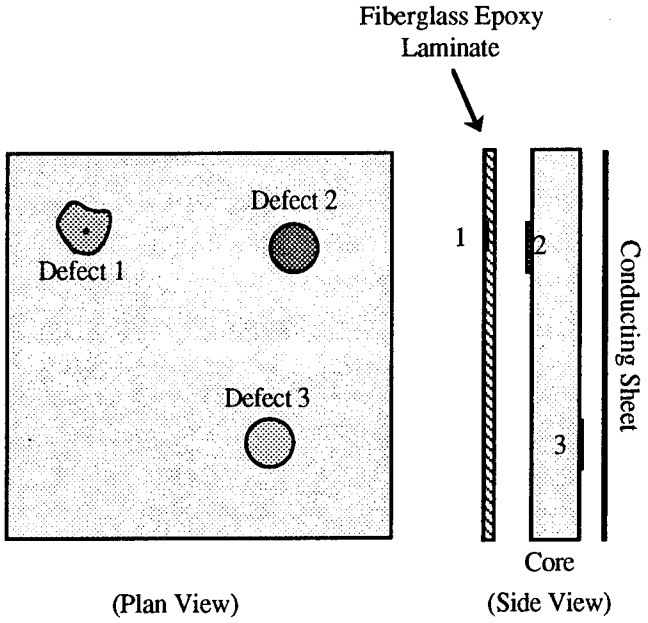

Fig. 11: Sketch of the sandwich composite sample showing its structural components as well as induced defect locations. (a) plan view; (b) side view. The thickness of the laminate skin is 2.54 mm (0.1") and the core thickness is 45 mm (1.77"); the area of the sample is 609.6 mm by 609.6 mm (24" by 24"), [9].

Upon optimization of the standoff distance and the operating frequency the following images were produced [9]. The image of the skin delamination in the foam composite is shown in Fig. 12 at a frequency of 12.0 GHz and at a standoff distance of 1.5 mm. The contour plot clearly shows the defect and the raised ridges. The raised areas are the spots near the left and right edges of the image. They are immediately followed by a spot caused by a depression in the surface. In the center of the image, a circular shape is readily apparent indicative of the circular nature of the delamination. This image may be understood taking into account the sample preparation procedure as described earlier. According to this procedure the edges of the mylar disks are thicker because of the tape used to hold them together. Fig. 13 shows the skin delamination for the foam sample for a frequency of 24 GHz using a 1 mm-thick plexiglass sheet to set the standoff distance. The scanning area in this case was 154 mm x 150 mm. Fig. 13 clearly shows that the area outside delamination is different, quite uniform and seems to indicate the skin fiber bundles and their orientation. The image possesses much better spatial resolution than the previous one (Fig. 12) which is due to the higher operating frequency (24 GHz compared to 12 GHz).

The results of a scan of defect 3 of the honeycomb sample at 9.1 GHz and at a 17 mm standoff distance shows a circular patch in the center of the scan (Fig. 14) approximately the size of the expected delamination, [9]. Although Fig. 14 presents a clear picture of the delamination, it also contains an unexplained anomaly. The spot located in the lower right corner of the image is curious. Upon sample examination, a surface feature that might produce this signal was not found. It is hypothesized that the adhesive used to hold the sample layers together may have dripped down into the honeycomb pockets of the core prior to cure and hardened there.

NEAR-FIELD INSPECTION OF IMPACT DAMAGE/FATIGUE

The useful life of a glass fiber/epoxy composite subjected to impact fatigue loading is an important issue in the future design of numerous industrial components. Lifetime predictions have been a problem particularly due to the difficulties encountered in monitoring damage accumulation in composites. It is hypothesized that there is a build up of micro damage, such as matrix micro-cracks and micro-delaminations, even though there is no apparent change in material compliance. A critical level is finally reached at which time the properties of the composite begin to fall and compliance change is evident, [10].

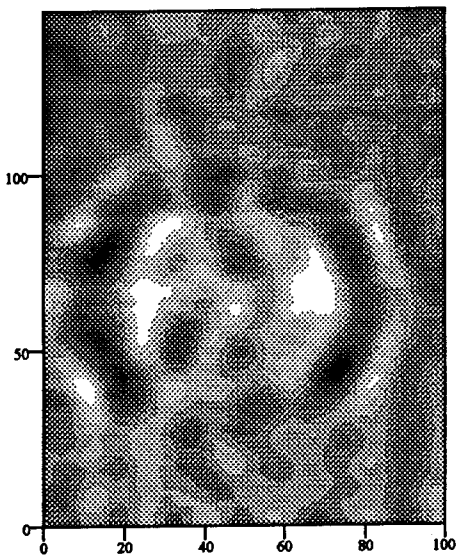

Fig. 12: The contour plot of the scan of the skin delamination (defect 2) for the foam sample at 12 GHz and 1.5 mm standoff distance. The contour plot dimensions are in mm, [9].

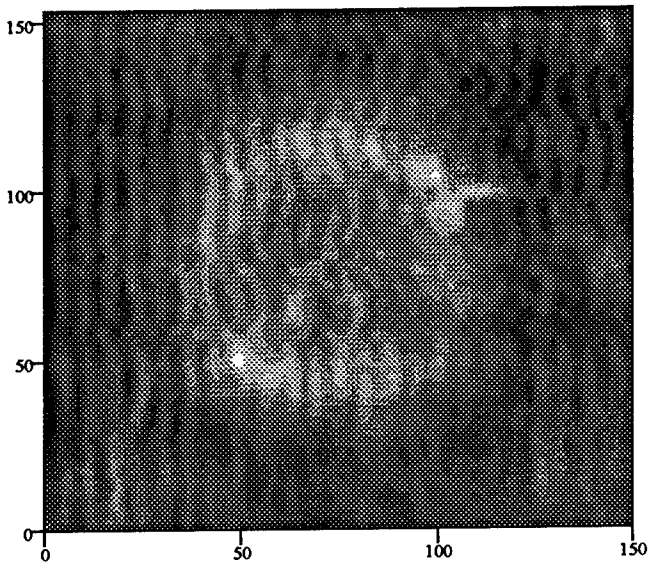

Fig. 13: The contour plot of the scan of the skin delamination (defect 2) for the foam sample at 24 GHz using a 1 mm-thick plexiglass sheet. The contour plot dimensions are in mm, [9].

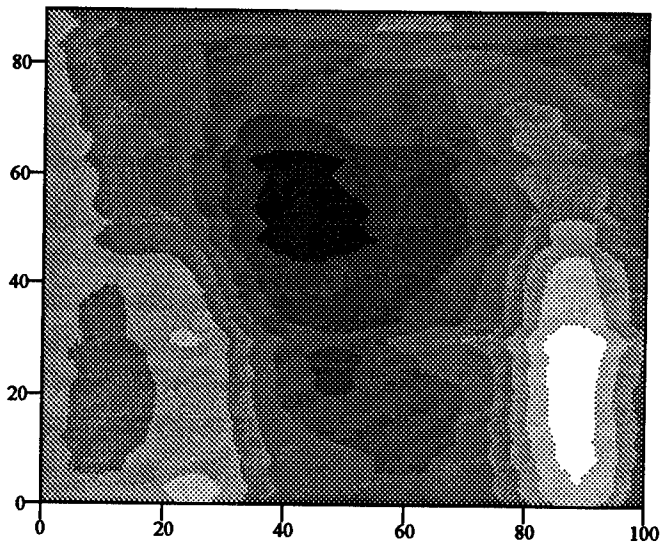

Fig. 14: The contour plot of the scan of the defect 3 for the honeycomb sample at 9.1 GHz and 17 mm standoff distance. The contour plot dimensions are in mm, [9].

As fiber reinforced composite materials mature as a technology and become more commonplace in our society they are being considered for an ever increasing number and variety of applications. The carefully monitored operating environments of the high technology industries which have constituted the bulk of the composite structural applications are becoming less common as composite materials technology moves into the arena of consumer products, automotive and industrial equipment. In many of these new applications extended lifetimes are expected under conditions of repetitive loading and repetitive impact. The damage which results can grow slowly, as do fatigue flaws, and ultimately cause catastrophic failure. Predictive capabilities do exist for common cyclic loading such as fatigue, as well as for the degradation of the material after sustaining a single impact; however, the mechanisms of repetitive high cycle impact damage are unknown. In addition to limited understanding of the mechanisms leading to damage initiation and propagation in composite materials, present techniques of early detection are few and are often cumbersome and difficult to apply in a service environment. Millimeter wave nondestructive investigation (NDI) techniques possess certain advantages over the other NDI approaches mentioned. In particular, millimeter wave NDI techniques are well suited for inspecting dielectric materials such as polymers, ceramics and composites. This is partially due to the fact that millimeter

waves easily penetrate dielectric materials and the reflected or transmitted signal can be related to the dielectric properties of the material. Subsequently physical and mechanical properties can be determined based upon these millimeter wave signals. It is this ability to yield information relating to the changing physical properties of materials that makes the application of millimeter wave NDI to damage detection in composites so interesting [10].

Thus, as part of the inspection of the sandwich composites, an image of the foam core sandwich impact damage (defect 1) at 24 GHz is presented in Fig. 15 [9]. A 3.2 mm-thick plexiglass sheet was inserted in between the sample and the waveguide. By keeping the waveguide in contact with the surface of the plexiglass, a constant standoff distance was maintained. The strongest signals (Fig. 15) occur along the warp/weave crossovers in the fiberglass epoxy laminate indicating damage at these locations. This may be a result of induced debond and/or porosity at these locations. When viewing the three dimensional surface (intensity) plot of the scan in Fig. 15b, a spherical indentation in the center can be plainly discerned. It is very likely that this shape is the result of the spherical ball used to create the impact.

To study the effect of cyclical impact on composite materials, specific polymer reinforced epoxy samples were subjected to cyclical impact fatigue [10]. The general experimental approach applied to this preliminary set of composite test specimens was to introduce cumulative damage by repetitive impact. At predetermined intervals the specimens were evaluated, visually and by millimeter wave scanning, for signs of damage. The results obtained by millimeter wave NDI were compared to the visual information as well as to the changes in mechanical performance recorded by the impact fatigue test apparatus [10].

Out-of-plane impact fatigue test specimens were molded in a disk geometry of 63.5 mm diameter and 3.2 mm thickness. These composite specimens were made up of either 4 or 8 layers of 10 oz satin weave fiberglass fabric in an Epon 813 epoxy resin matrix. The plies were stacked in a mid-plane symmetric, quasi-isotropic fashion with a fiber volume fraction of approximately 20% for the 4 ply and 40% for the 8 ply specimens. Cure was performed at room temperature and care was taken during mold filling to minimize the inclusion of air. Finally, specimens were carefully ground and polished to a thickness of approximately 2.5 mm to ensure flat and parallel surfaces for optimal millimeter wave NDI sensitivity, [10].

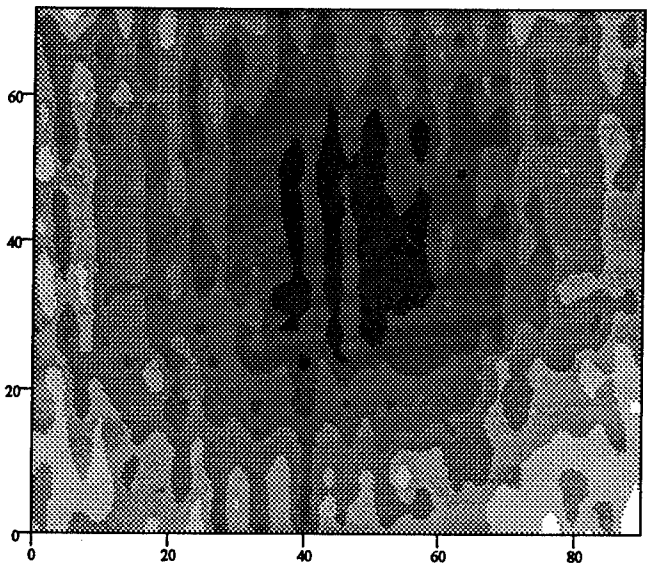

Fig. 15a: The contour plot of the scan of the impact damage (defect 1) for the foam sample at 24 GHz using a 3.2 mm-thick plexiglass sheet. The contour plot dimensions are in mm, [9].

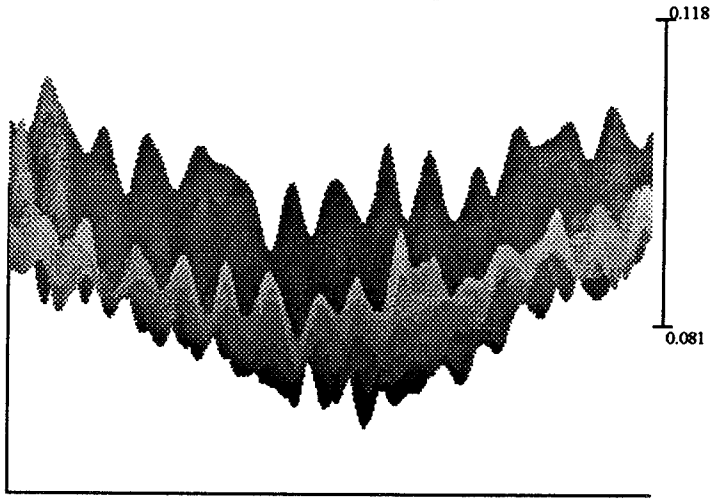

Fig. 15b: The surface plot of the scan of the impact damage (defect 1) for the foam sample at 24 GHz using a 3.2 mm-thick plexiglass sheet. The surface plot amplitude is in Volts, [9].

Impact fatigue testing involves impacting a single specimen a large number of times while measuring the resulting load degradation. The lack of a standardized test capable of rapid, high cycle impact fatigue made it necessary to design and fabricate custom test equipment. The test apparatus developed here uses an electrically driven ram that impacts a stationary disk shaped specimen which is clamped in a rigid framework. A dynamic load cell capable of measuring an impact load of up to 22.25 kN is attached to the moving ram and the 12.7 mm diameter ball indenter is attached to the load cell [10]. The resulting out-of-plane impact information is recorded using computer data acquisition at a sampling rate of 45 kHz. The number of impacts, number of impact pulses recorded, peak impact load and the shape of the impact pulse are recorded for further analysis. The test apparatus was designed to generate impact pulses comparable to impact events resulting from drop weight test procedures; however, 1 million impacts can be generated in a 24 hour period. The specimens were impacted at a fixed load for a predetermined number of cycles. After each set of cycles is introduced the specimen is removed from the impact fatigue machine and is transferred to the millimeter wave test apparatus. Millimeter wave measurements were recorded and the specimen was once again mounted in the impact fatigue tester and the test cycle repeated. These cycles of impact fatigue damage and millimeter wave measurement were continued until significant visible damage could be observed and the lifetime history damage indicates an increase in compliance.

A one-sided reflection type measurement system at 34.8 GHz using an open-ended rectangular waveguide sensor was utilized to produce the images presented here [10]. The millimeter wave apparatus was similar to a single coupler reflectometer. Once the millimeter wave frequency and waveguide standoff distance were optimized the system gave excellent images of the damage region. Fig. 16a shows a typical millimeter wave surface map of the central region of an 8-ply composite disk after 3000 impact cycles at a nominal load of 0.70 kN. The primary damage region can be readily observed near the center of the map. It is seen that the region of damage is not circular as might be expected in an isotropic specimen, but actually shows accelerated damage propagation along the fiber bundles. The regularly repeating vertical features on the surface map correspond to the fiber bundles in the composite. Thus, this central zone of the millimeter wave damage map shows, by changing intensity of reflected signal related to changing density, the presence of delamination damage [10].

The same 8-ply glass fiber reinforced disk is shown, after 4000 cycles, in Fig. 16b. In this case the central damage zone has grown noticeably and increased damage is apparent across the map. Visual investigation of the specimen shows significant damage growth between 3000 and

4000 cycles, with concentric rings of cracking and the development of a damage cone by 4000 cycles. These visual observations match well with the results of the scanning millimeter wave NDI [10].

To obtain a preliminary indication of the sensitivity of scanning millimeter wave NDI to low damage levels, a 4-ply disk was impacted at a lower load of 0.53 kN for only 500 cycles. No visible delamination damage or interply cracking was noticeable; however, as seen in Fig. 16c, the scanning millimeter wave technique clearly shows a signal at the warp/weave crossovers of the fiberglass fabric. This millimeter wave damage map seems to be indicative of the presence of either damage induced debond initiation or at least some form of porosity at these positions in the weave. More detailed investigation will be necessary to quantify this feature and determine the form of microstructural inhomogeneity that results in this millimeter wave signal [10].

The results from this preliminary investigation indicate that millimeter wave NDI techniques can yield information related to the initiation and growth of damage in fiber reinforced composite materials. The maps of the changing dielectric constant show that damage is initiating near the point of indentation and growing radially outward as visually observed. The increasing severity of damage and the enlargening of the damage zone are seen in the millimeter wave maps of Figs. 16a-b as sequential results are obtained. It is interesting to realize from this preliminary data that the millimeter wave data indicates the initiation of damage prior to visual recognition. In addition, in each test set the region of damage indicated by the millimeter wave technique seems larger than that visually observed. While this may be related to the waveguide size and the averaging of damaged and undamaged regions at the boundary of the waveguide, the indication is that some level of damage is being discerned by millimeter wave NDI which is not visible, [10].

References [12-34], which give information about microwave imaging in general and several of its specific aspects, are provided for the interested reader.

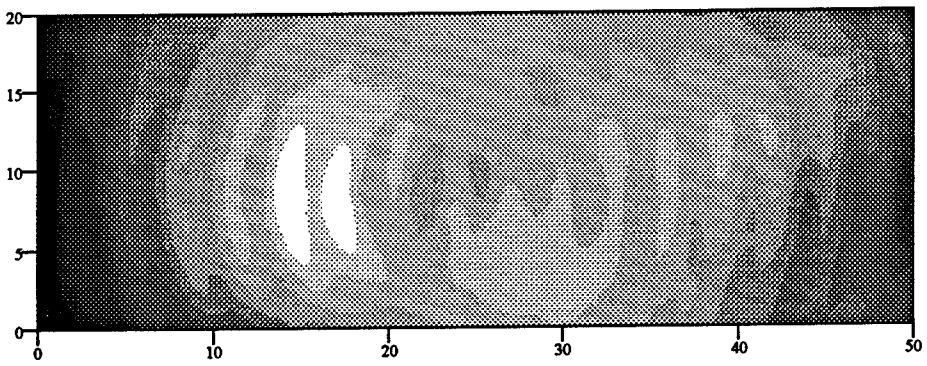

Fig. 16a: Scanning millimeter wave surface map showing damage after 3000 impact cycles, [10].

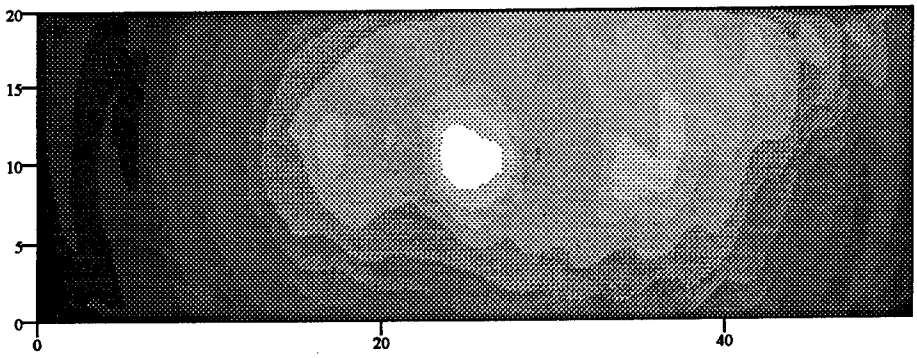

Fig. 16b: Scanning millimeter wave surface map showing damage after 4000 impact cycles, [10].

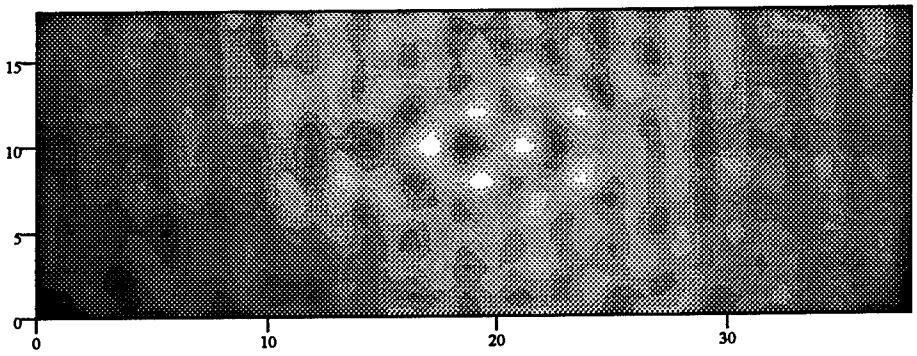

Fig. 16c: Scanning millimeter wave surface map showing damage after 500 impact cycles, [10].

SUMMARY

The ability of microwaves to penetrate inside dielectric materials makes microwave NDT&E techniques very suitable for interrogating structures made of thick glass reinforced polymer composites. Experimental results obtained from scanning several thick composite samples with voids and embedded defects were presented. Images of these composites were created using a measured voltage which is related to the phase or magnitude of the effective reflection coefficient at the aperture of the rectangular waveguide sensor. The defects were detected and located without any signal processing at relatively low microwave frequencies. The influence of the standoff distance on the detection sensitivity was shown to be significant. Hence, a fundamentally sound understanding of the interaction of microwaves with stratified dielectric composites is very important in order to increase measurement sensitivity to the parameters of interest. To enhance the contrast (detection) in the image, without operating at very high frequencies, the standoff distance can be varied. In the case of the detection of flat bottom holes, microwaves produced significantly better results compared to some other NDE methods and the presence of a large area masking disbond did not interfere with the microwave measurements which were tuned to detect the holes. Generally, detection of many different types of defects (including disbonds) are also possible with microwave techniques. The results indicate the potential of utilizing microwave techniques in the on-line inspection of thick composite structures.

Microwave nondestructive testing techniques were utilized to inspect thick sandwich composites consisting of fiberglass epoxy laminates, foam and honeycomb constituents. Several different defects were embedded in these samples during their production. Each technique relies on the measurement of the reflected microwave energy from the composite samples using an open-ended rectangular waveguide as the inspection probe. The experiments were conducted at different frequencies and standoff distances based on the results of measurement parameter optimization conducted for each separate defect. The results of these measurements (presented in image formats) provide impressive detailed information about each defect such as the raised edges associated with the manufacturing of the delaminations, the shape of the indentations caused by the impact fatigue defects and surface skin fiber bundle orientations. As expected, higher frequencies provided better *spatial/lateral* resolutions. The importance of optimizations as it pertains to successful defect detection and characterization was demonstrated both experimentally and theoretically. The results of this study clearly

demonstrate the potential of microwaves as nondestructive tools for inspecting thick composite sandwich structures.

Preliminary investigations of the initiation and propagation of damage in reinforced composite materials have been performed using the combination of impact fatigue testing and millimeter wave imaging. The results are extremely promising as the millimeter wave images closely match the growing damage noted visually by an increased opacity of the glass fiber reinforced epoxy test specimens. Prior to the initiation of visible damage the scanning millimeter wave technique was able to detect a small region, at the point of impact, which showed changing dielectric properties and was clearly related to the morphology of the specific composite specimen. While this technique has yet to be calibrated to generate quantitative information as to the details of the degree of damage, the form and the depth, it is already apparent that the technique is capable of detecting extremely low levels of damage and has great potential for investigations of damage initiation and growth.

REFERENCES

[1] Otto, G.P., and W.C. Chew, "Microwave Inverse Scattering - Local Shape Function Imaging for Improved Resolution of Strong Scatteres," IEEE Trans. on Microwave Theory and Tech., vol. MTT-42, no. 1, pp. 137-141, Jan. 1994.

[2] Qaddoumi, N., and R. Zoughi, "Microwave Scattering Characteristics of Defective Dielectric Cylinders," To appear in the NDT&E International, 1995.

[3] Bahr, A.J., "Nondestructive Evaluation of Ceramics," IEEE Trans. on Microwave Theory and Tech., vol. MTT-26, pp. 676-683, 1978.

[4] Gopalsami, S. Bakhtiari, S. Dieckman, P. Raptis and J. Lepper, "Millimeter-Wave Imaging for Nondestructive Evaluation of Materials," Materials Evaluation, vol. 52, no. 3, March, 1994.

[5] Bakhtiari, S, N. Gopalsami and P. Raptis, "Characterization of Delamination and Disbonding in Stratified Dielectric Composites by Millimeter Wave Imaging," To appear in the Materials Evaluation, 1995.

[6] d'Ambrosio, G., R. Messa, M. Migliore, A. Cilibetro and C. Sabatino, "Microwave Defect Detection on Low-Loss Composites," Materials Evaluation, vol. 51, no. 2, pp. 285-289, Feb. 1993.

[7] Zoughi, R., G. Cone and P. Nowak, "Microwave Nondestructive Detection of Rebars in Concrete Slabs," Materials Evaluation, vol. 49, no. 11, pp. 1385-1388, Nov. 1991.

[8] Qaddoumi, N., S. Ganchev, G. Carriveau and R. Zoughi, "Microwave Imaging of Thick Composites with Defects," To appear in the Materials Evaluation, 1995.

[9] Ganchev, S., R. Unser, N. Qaddoumi and G. Carriveau, "Microwave Nondestructive Evaluation of Thick Sandwich Composites," To appear in the Materials Evaluation, 1995.

[10] Radford, D., B. Barber, S. Ganchev and R. Zoughi, "Millimeter Wave Nondestructive Evaluation of Glass Fiber/Epoxy Composites Subjected to Impact Fatigue," Proceedings of SPIE Symposium, Advanced Microwave and Millimeter Wave Detectors Conference, vol. 2275, pp. 21-26, San Diego, CA, July 24-29, 1994.

[11] Carriveau, G., "Benchmarking of the State-of-the-Art in Nondestructive Testing/Evaluation for Applicability in the Composite Armored Vehicle (CAV) Advanced Technology Demonstrator (ATD) Program," NTIAC Report 7304-104:GWC-D172.17, 1994.

[12] Anderson, A.P., and S.J. Mawani, "A 'Microwave Eye' Can Be Almost Human," Proc. 6th European Microwave Conference (EuMC'76), pp. 105-111, Sept. 1976.

[13] Baribaud, M. and M.K. Nguen, "Maximum Entropy Image Reconstruction from Microwave Scattered Field Distribution," Proc. 18th European Microwave Conference (EuMC'88), pp. 891-896, Sept. 1988.

[14] Bolomey, J.C., L. Jofre and G. Peronnet, "On the Possible Use of Microwave Active Imaging for Remote Thermal Sensing," IEEE Trans Microwave Theory Tech., vol. MTT-31, no. 9, pp. 777-781, Sept. 1983.

[15] Broquetas, A., M. Ferrando, J.M. Rius. L. Jofre, E. de los Reyes, A. Cardama, A. Elias, and J. Ibanez, "Temperature and Permittivity Measurements Using a Cylindrical Microwave Imaging System," Proc. 17th European Microwave Conference (EuMC'87), pp. 892-895, Sept. 1987.

[16] Caorsi, S., G.L. Gragnani and M. Pastarino, "A Numerical Approach to Microwave Imaging," Proc. 18th European Microwave Conference (EuMC'88), pp. 897-902, Sept. 1988.

[17] Chaloupka, H., "Imaging of Objects in a Halfspace with Unknown Permittivity," Electronics Letters, vol. 20, no. 13, pp. 570-572, June 1984.

[18] Chu, T.H., and K.Y. Lee, "Wideband Microwave Diffraction Tomography under Born Approximation," IEEE AP-S Int. Symp. Digest, pp. 1042-1045, June 1987.

[19] Edrich, J., "Centimeter- and Millimeter-Wave Thermography - A Survey of Tumor Detection," J. Microwave Power, vol. 14, no. 2, pp. 95-104, June 1979.

[20] Ermert, H., G. Fuller and D. Hiller, "Microwave Computerized Tomography," Proc. 11th European Microwave Conference (EuMC'81), pp. 421-426, Sept. 1981.

[21] Junkin, G., and A.P. Anderson, "Limitations of Microwave Holographic Synthetic Aperture Imaging over a Lossy Half-Space," IEE Proc., vol. 135, Pt. F, no. 4, pp. 321-329, Aug. 1988.

[22] Mensa, D.L., S. Halevy and G. Wade, "Coherent Doppler Tomography for Microwave Imaging," Proc. IEEE, vol. 71, no. 2, pp. 254-261, Feb. 1983.

[23] Michiguchi, Y., K. Hiramoto, M. NIshi, T. Ootaka and M. Okada, "Advanced subsurface Radar System for Imaging Buried Pipes," IEEE Trans. Geosci. Remote Sensing, vol. GE-26, no. 6. pp 733-740, Nov. 1988.

[24] Orme, R.D., and A.P. Anderson, "High Resolution Microwave Holographic Technique," IEE Proc. vol. 120, no. 4, pp. 401-406, Apr. 1973.

[25] Paoloni, F.J., "Implementation of Microwave Diffraction Tomography for Measurement of Dielectric Constant Distribution," IEE Proc., vol. 134, Pt. H, no. 1, pp. 25-29, Feb. 1987.

[26] Paoloni, F.J., and M.J. Duffy, "Microwave Imaging with Digital Reconstructions," J. Electrical and Electronics Eng. (Australia), vol. 4, no.1, pp. 54-59, March 1984.

[27] Perronet,G., C. Pichot, J.C. Bolomey, L. Jofre, A. Izadnegahdar, C. Szeles, Y. Michel, J.L. Guerquin-Kern and M. Gautherie, "A Microwave Diffraction Tomography System for Biological Applications," Proc. 13th European Microwave Conference (EuMC'83), pp. 529-533, Sept. 1981.

[28] Pichot, C., L. Jofre, G. Peronnet and J.C. Bolomey, "Active Microwave Imaging of Inhomogeneous Bodies," IEEE Trans. Antennas Propagat., vol. AP-33, no. 4, pp. 416-425, April 1985.

[29] Richards, P.J., and A.P. Anderson, "Microwave Images of Sub-Surface Utilities in an Urban Environment," Proc. 8th European Microwave Conference (EuMC'78), pp. 33-37, Sept. 1978.

[30] Rius, J.M., M. Ferrando, L. Jofre, E. de los Reyes, A. Elias and A. Broquetas, "Microwave Tomography:An Algorithm for Cylindrical Geometries," Electronic Letters, vol. 23, no. 11, pp. 564-565, May 1987.

[31] Schulz, K.I., and D.L. Jaggard, "Novel Microwave Projection Imaging for Determination of Internal Structure," Electronic Letters, vol. 23, no. 6, pp. 267-269, March 1987.

[32] Solymar, L., "On the Theory and Application of Volume Holograms," Proc. 7th European Microwave Conference (EuMC'77), pp. 175-176, Sept. 1977.

[33] Tricoles, G., and N.H. Farhat, "Microwave Holography: Applications and Techniques," Proc. IEEE, vol. 65, no. 1, pp. 108-121, Jan. 1977.

[34] Ganchev, S., G. Carriveau and N. Qaddoumi, "Microwave Detection of Defects in Glass Reinforced Polymer Composites," Proceedings of SPIE Symposium, Advanced Microwave and Millimeter Wave Detectors Conference, vol. 2275, pp. 21-26, San Diego, CA, July 11-20, 1994.

CHAPTER 6

CONCLUDING REMARKS AND THE FUTURE OF MICROWAVE NDT&E

The primary objective of this report has been to introduce the reader to microwave and millimeter wave NDT&E methods. Clearly, it is impossible to cover the details of these methods and their applications in their entireties in a relatively short report such as this. In addition, to include the results of all of the investigations that may fall under the category of microwave and millimeter wave NDE is also not been possible. However, the authors have attempted to include as many possible references which may be useful to the reader. The detailed research results presented in this report have been the results of the most recent research activities in these areas. Therefore, the collaborative works of the authors have figured significantly in this report.

From the relatively brief collection of research results presented here, it is clear that microwave and millimeter wave NDE is here to stay. The diverse realm of applications coupled with the specific features outlined in Chapter 1 give credence to this claim. Additionally, the following reasons are believed to significantly impact the future growth, applications, utility and the general acceptance of microwave NDE methods :

- The limitations associated with the more established NDE methods require a fresh look into the applicability of other so-called less established techniques of which microwave methods are the top of this list. Thus, microwave NDE applications are no longer just a passing interest in the minds of those in the NDE community, particularly the practitioners of NDE.

- The advent and increasing use of dielectric composite structures will contribute to more wide spread use of microwave NDE techniques more than any other factor. This is an area which microwave and millimeter wave NDE will impact significantly.

- The issue of curing and cure state, which is a basic concern in composite production, will be addressed by microwave NDE methods more vigorously in the near future. Application of these techniques to monitoring the state of cure in a variety of materials will be a major contribution of microwave methods.

- Those interested in finding alternative solutions to the problem of detecting and evaluating impact damage in dielectric and graphite epoxy composites will significantly benefit from the applications of microwave NDE methods.

- The novelty of these techniques compared to the more established NDE methods will serve as a starting point leading to more prominence.

- Recent applications of microwave methods, the development of testing prototypes and laboratory prototypes have demonstrated that some myths about the cost, design complexity, resolution, operator unfriendliness, radiation hazard and the need for extensive signal processing are unfounded. The more these myths are shown to be untrue, the more doors will be opened for microwave NDE applications.

- Recent renewed vigor on the part of several investigators in research and development of microwave NDE methods and systems will keep their applications on the *current* NDE scene.

- The funding issue should also be addressed here. The so-called standard NDE methods have enjoyed many years of sustained funding to bring them to the level they are at now. Furthermore, there have been, by far, many more investigators who have contributed to the advancement of these standard techniques over the years. The same cannot be said for microwave and millimeter wave methods. Neither has there been a sustained and substantial level of funding, nor have there been many investigators working in these areas. Both of these are changing and these methods have experienced, compared to the decades, an increase in the level of activities and funding. However, it must be noted that this overall increase is no where near the level to bring microwave NDE methods to the current levels of the more established NDE. Considering all of this, we believe that in the past few years some significant improvements have been made.

- Industrial funding for microwave inspection system developments may also increase in the next few years. The

Europeans have been more willing to invest in funds and efforts in this area and are already reaping its benefits.

- One of the most important factors that has kept microwave methods in the back pages of NDE applications is the lack, and in some cases the nonexistence, of available off-the-shelf microwave testing systems. However, this is changing and we envision more rapid changes in the near future. There are several reasons for this including the increased expansion of solid state technology into higher frequencies which provides for smaller and more cost effective microwave sources and components.

- As microwave NDE methods become more and more prominent, there will need to be some standardization of these methods. The American Society for Nondestructive Testing (ASNT), could be very instrumental in this aspect.

- *Sensor fusion* will bring microwave sensors along side of other sensors.

- Since peace has broken out, many organizations previously working on military projects must redirect their efforts and must find new markets for their products and expertise. Many of these organizations are very familiar with microwave technology (radars, etc.). Hence, there may be increased commercial and industrial activities toward microwave NDE by these organizations.

The authors hope that, if nothing else, this report has addressed some of the more important practical issues associated with microwave and millimeter wave NDE. Future will show whether or not the above predictions will take place. Nevertheless, looking back to the last few years, one has every reason to be optimistic and enthusiastic about the future of microwave NDE.